Metabolic Regulation of Circadian Timekeeping

Priya Crosby

St Catharine's College, University of Cambridge

March 2017

This dissertation is submitted for the degree of Doctor of Philosophy

MRC Laboratory of Molecular Biology

Declaration

This dissertation is the result of my own work and includes nothing that is the outcome of work done in collaboration except as specified in the text. It is not substantially the same as any that I have submitted, or, is being concurrently submitted for a degree or diploma or other qualification at the University of Cambridge or any other University or similar. I further state that no substantial part of my dissertation has already been submitted, or, is being concurrently submitted for any such degree, diploma or other qualification at the University of Cambridge or any other University or similar institution. It does not exceed the prescribed word limit for the Biology Degree Committee.

Table of Contents

List of Figures and Tables

Introduction

Chapter 3

Chapter 4

Chapter 5

“Time is an illusion. Lunchtime doubly so.”

Douglas Adams, The Hitchhiker’s Guide to the Galaxy

Acknowledgements

First and foremost, I would like to thank my supervisor John O'Neill for taking what must have been a gamble in choosing me as his first PhD student. His enthusiasm, support, advice and debate have been of the utmost value. I could not have asked for anyone better to guide me through these years of my education.

Thanks must also go to members of the O'Neill lab for all their assistance, particularly Ned Hoyle and Marrit Putker, whose no-nonsense style I have come to appreciate. Although I may not seem to accept it, your advice is almost always correct and I am all the better for it.

I am constantly reminded of how fortunate I am to have been able to complete my studies with access to the incredible facilities and supportive atmospheres of both the Laboratory of Molecular Biology and the University of Cambridge. I would like to thank all within both communities who make them such fantastic places to work. In addition, I would like to thank Michael Hastings and Christian Frezza for acting as my second supervisors.

Thanks also go to Ryan Hamnett for all of his discussion, support, and for always lending a listening ear.

I would also like to thank members of the University sporting community, the swimming, athletics and rowing squads and coaches, for providing me with some life-changing experiences and opportunities which have been so much part of my time at Cambridge, as well as some truly exceptional friends. Particular mention must go to the CUWBC Lightweights, for demonstrating that with hard work and passion, we are endlessly capable.

Finally, I would like to thank my parents, Richard and Maya Crosby, for their unerring support and encouragement.

Abbreviations

2ME	2-Mercaptoethanol
3-Br-pyr	3-Bromopyruvate
Aao	α-amanatin oleate
ALLIGATOR	Bioluminescence incubator
AM	Air Medium
CHX	Cycloheximide
CK1	Casein Kinase 1
cps	Counts per second
CT	Circadian Time
DHEA	Dehydroepiandrosterone
DPI	Diphenyleneiodonium
DMEM	Dulbecco's Modified Eagle Medium
EGF	Epidermal Growth Factor
EMP	Embden–Meyerhof– Parnas
FGF	Fibroblast Growth Factor
FH	Fumarate Hydratase
GSK3	Glycogen synthase kinase 3
G6PDH	Glucose-6-Phosphate dehydrogenase
GAPDH	Glyceraldehyde 3-phosphate dehydrogenase
GOX	Glucose oxidase
GPI	Glucose-6-Phosphate isomerase
HPA	Hypothalamic-pituitary-adrenal
IBMX	3-isobutyl-1-methylxanthine
ID	Internal Diameter
IGF-1	Insulin-like Growth Factor 1
KA	Koningic Acid
LECA	Last Eukaryotic Common Ancestor
LMB	Leptomycin B
LUCA	Last Universal Common Ancestor
NADH	Nicotinamide adenine dinucleotide
NADPH	Nicotinamide adenine dinucleotide phosphate

PAM	Perfusion Air Medium
PBS	Phosphate-buffered saline
PDMS	Polydimethylsiloxane
PI3K	Phosphatidylinositol-4,5-bisphosphate 3-kinase
PPP	Pentose Phosphate Pathway
PGD	6-Phosphogluconate dehydrogenase
PVN	Paraventricular nucleus
qPCR	Quantitative Polymerase Chain Reaction
RF	Restricted feeding
RLU	Relative light units
ROS	Reactive Oxygen Species
SCN	Suprachiasmatic nucleus
TCA	Tricarboxylic acid
TIM	Timeless
TTFL	Transcription and Translation feedback loop
TTX	Tetrodotoxin

Thesis summary

Circadian rhythms are self-sustained endogenous biological oscillations with a period of approximately 24 hours. These rhythms are observed widely across kingdoms and at all levels of biological scale. Recent work has shown there to be circadian variation in metabolism, both at the organismal and cellular level. It has also been posited that rhythmic production of metabolites might be essential for maintenance of circadian rhythmicity within cells, even in the absence of nascent transcription. The first portion of this thesis investigates the contribution of primary carbohydrate metabolism to cellular timekeeping, with particular emphasis on the pentose phosphate pathway. I also describe and validate a new ^{13}C labelling technique for accurate determination of the relative flux through early primary metabolic pathways. This is accompanied by the development and optimisation of a microfluidic system for long-term perfused tissue culture, which allows for longitudinal study of metabolic flux within the same population of cells with simultaneous recording of clock gene activity. This perfused system provides several advantages over static tissue culture.

The second portion considers the effects of the metabolic hormone insulin on circadian rhythmicity, both at the level of the cell and of the whole organism. It shows that administration of insulin is sufficient to shift the phase of circadian gene expression and elicits induction of clock protein PER2. Strikingly, manipulation of insulin signalling is sufficient to determine all the essential parameters of the cellular clock (phase, period and amplitude) in a dose-dependent but glucose independent fashion. Using pharmacological and genetic approaches, a molecular explanation for this effect is determined. This data suggests that insulin is a primary determinant of rhythms in peripheral tissues and is most likely a major signal for circadian entrainment to feeding in mammals, for which I now propose a mechanistic basis.

Chapter 1: Introduction

1.0.1 Circadian rhythms

The term ‘circadian rhythm’ (derived from the Latin “circa”, meaning “around” and “*diēs" meaning “a day”*) refers to an endogenous biological oscillation with a period of ~24 hours. This confers the ability to anticipate, and resonate with the day/night cycle and has been evolutionarily selected for over the 1.5 billion years since the emergence of eukaryotes, such that the majority of plant, fungi and animal species possess intrinsic circadian timekeeping (Bell-Pedersen et al. 2005). In mammals, circadian rhythms are manifest in the temporal organization of behavioral, physiological, cellular and subcellular processes, influencing phenomena as varied as sleep/wake cycles (Lazar et al. 2015), glucose homeostasis (Rudic et al. 2004), innate immunity (Gibbs et al. 2011) and cell division (Matsuo et al. 2003).

Recent investigations have found that an estimated third of protein-coding genes in the mouse genome undergo daily oscillations in one or more tissues (Zhang et al. 2014). Because these endogenous oscillations interact with myriad biological systems, circadian disruption has significant impacts upon human health and diseased states. For example, the chronic circadian dysregulation experienced by long-term shift workers (around 15% of the workforce in developed nations) is associated with an increased susceptibility to cardiovascular disease, type II diabetes, and various forms of cancer (Pan et al. 2011; Haus & Smolensky 2013). Conversely, circadian disruption is an early symptom of a number of neurodegenerative disorders (Mattis & Sehgal 2016).

The earliest recorded observation of a circadian process comes from the writings of Androsthenes of Thasos, who noted diurnal leaf movements in the tamarind tree in the 4th century B.C.E., whilst the first record of a truly endogenous circadian observation occurred some two millennia later, when Jean-Jacques d'Ortous de Mairan noted that 24 hour rhythms in the movement of leaves of the plant *Mimosa pudica* persisted in constant darkness (De Mairan 1729).

1.0.2 Defining a circadian rhythm

The exact definition of a true circadian rhythm was outlined by Colin Pittendrigh at the Cold Spring Harbor Symposia on Quantitative Biology in 1960 (Pittendrigh 1960). This states that a rhythm can be described as circadian in nature if it:

1. Has a free-running period of approximately 24 hours. This must be the period in constant conditions and in the absence of environmental cues.
2. Is capable of entraining to appropriate external cues. Entrainment is the process of resetting the phase of the oscillation in response to environmental stimuli, known as zeitgebers (from the German “time-givers”).
3. Is temperature compensated. Unlike the majority of reactions, the Q_{10} of a circadian rhythm is always approximately 1 (0.8-1.2), allowing it to retain the same period across a range of temperatures.

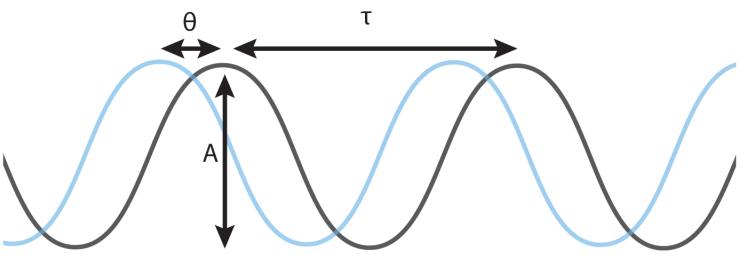

Figure 1.1

Schematic defining the features of a periodic wave

Schematic defining the features of a periodic wave. τ denotes period, A is amplitude and θ phase angle.

The primary features of a circadian rhythm are, as for almost all periodic oscillations, the period (τ, defined as the distance between two equivalent points on the oscillation), the amplitude (A, defined as the distance from the peak to the trough of the oscillation) and the phase or phase-shift (θ, defined as the distance or angle from zero phase) (Figure 1.1). Shifts in phase can be described as either type 0, meaning that the oscillation resets to the same phase regardless of the phase at which it is perturbed or type 1, where the phase at which the oscillation was perturbed influences phase to which the rhythm resets.

It is most likely that rhythms with these properties have been evolutionarily selected for as they confer increased fitness. In the cyanobacterium *Synechococcus elongatus,* a prokaryote, cells with a functioning circadian clock out-compete mutant strains under normal light-dark cycles (Woelfle et al. 2004). In mammals, animals in which behavioural timekeeping has been disrupted show greatly increased mortality in the wild, with the result that few survive to

go on to produce offspring (DeCoursey et al. 2000). The hypothesis is that intrinsic circadian rhythmicity confers an advantage by allowing organisms to predict the timing of external events, be they nutrient availability, predators, prey or DNA damage due to light; this last being proposed to have initially driven the selection for circadian rhythmicity (Pittendrigh 1993).

1.0.3 Molecular Circadian Mechanisms

The first circadian mutant was described by Ronald Konopka and Seymour Benzer in *Drosophila melanogaster* and was mapped to the X-linked *Period* gene (Konopka & Benzer 1971). Subsequent work across a number of organisms led to the identification of other genes that are essential for the maintenance of circadian behaviour.

At the same time, lesion studies identified the suprachiasmatic nucleus (SCN) of the hypothalamus as being essential for generation of circadian rhythms in mammalian behavior (Rusak 1979), as well as levels of many circulating hormones and possibly rhythms in body temperature (Ishida et al. 2005; Refinetti & Menaker 1991). This nucleus of approximately 20,000 cells is often referred to as the “master clock” in mammals, due to its role in the appropriate synchronization of circadian rhythmicity throughout the animal, particularly with regards to entraining to lighting cues. *Ex vivo* study of the SCN informs us that the singular robustness of timekeeping in the SCN is attributable partly to its particular neuronal circuitry and partly to a cell-autonomous circadian rhythm sustained within every neuron of the SCN (Takahashi 1993; Welsh et al. 1995).

Later work has extended this second observation, showing that almost all mammalian cells are capable of exhibiting a cell autonomous circadian rhythm (Balsalobre et al. 1998; Yoo et al. 2004).

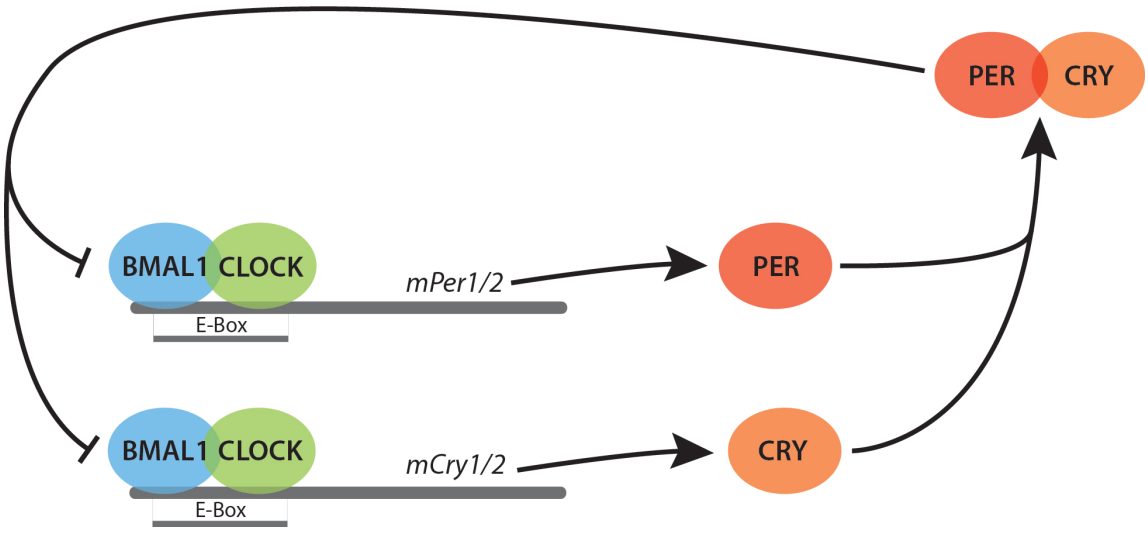

Figure 1.2

Schematic describing the core mammalian TTFL

The core mammalian TTFL consists of a delayed negative feedback loop of CRY, PER, BMAL1 and CLOCK proteins.

The mechanistic model for how this rhythm is maintained in mammals consists of a transcriptional/translational feedback loop (TTFL, Figure 1.2). Briefly, transcriptional activators circadian locomotor output cycles kaput (CLOCK) and BMAL1 positively regulate *Per1,2,3 and Cry1,2* though action at their respective E-box-containing promoter regions. This group of genes are commonly referred to as “clock genes”. The PER and CRY proteins dimerise in the cytosol and form a complex which then translocates to the nucleus, where it interacts with CLOCK and BMAL to repress *Per* and *Cry* transcription, and the transcription of other “clock-controlled genes” in a tissue-specific fashion. The PER and CRY

proteins are then slowly degraded over time, thus allowing the cycle to begin again (Figure 1.2). There are also a number other feedback loops interlinked with this central CLOCK-BMAL1/PER-CRY loop. In particular, retinoic acid orphan receptor-α (ROR-α) and nuclear receptor REV-ERBα/β, which are also direct transcriptional targets of BMAL1 and CLOCK, in turn inhibit the transcription of *Bmal1*, thereby resulting in an oscillation in BMAL1 which is in antiphase to the oscillation of PER and CRY (Partch et al. 2014; Koike et al. 2013).

This TTFL model for maintenance of circadian timekeeping is mimicked across kingdoms. In the bread mold *Neurospora crassa*, the first organism in which a TTFL mechanism was elucidated, the Frequency (FRQ) protein regulates its own transcription (Aronson et al. 1994). *Drosophila,* in turn, possess a mechanism that is highly reminiscent of that observed in mammals. Here, CLOCK and CYCLE (orthologous to CLOCK and BMAL1 in mammals) drive transcription of PER and TIM, which repress their own transcription (Tataroglu & Emery 2015). In *Arabidopsis*, the central loop consists of transcriptional activators CCA1 and LHY, which are morning-expressed, whilst PRR9, PRR7, PRR5 and TOC1 are expressed sequentially and act successively throughout the afternoon and evening to repress CCA1 and LHY transcription and their own transcription. In the evening, TOC1 represses all of the previously expressed proteins (Nohales & Kay 2016).

What is striking about all of these TTFL mechanisms for timekeeping in

eukaryotes is that, although all conform to the same basic principle of a delayed negative feedback loop, the identity of the genes and proteins concerned differs greatly between organisms, with very little clear homology across kingdoms or even phyla (Tei et al. 1997; Sun et al. 1997). This makes the dissection of any core timekeeping mechanism difficult, and has led some to argue for the convergent evolution of eukaryotic circadian timing mechanisms (Rosbash 2009).

An issue not often highlighted when discussing the TTFL model of circadian timekeeping is that of periodicity. Neither transcription nor translation proceed at rates closely comparable to a circadian timescale; indeed, the initial model proposed by Hardin and colleagues could quite plausibly have a period of around 4 hours (Hardin et al. 1990; Johnson 2010). Whilst large bodies of work attempt to address this issue, through the addition of accessory loops (Guillaumond et al. 2005), essential phosphorylation events (Mahesh et al. 2014) and other post-transcriptional regulation (Chen et al. 2013), all of which vary between phyla, it is still difficult to conceive of a 24 hour rhythm constructed from these events, particularly one that is relatively insensitive to temperature.

This argument has led some in the field to posit the existence of an additional post-transcriptional timekeeping mechanism within the cell, functionally comparable to the circadian oscillator in cyanobacteria (Johnson 2010; Lakin-Thomas 2000). Here, the clock mechanism is entirely post-transcriptional,

consisting of the proteins KaiA, B and C. This oscillator can be reconstituted *in vitro* and revolves around the rhythmic phosphorylation of KaiC and the subsequent formation of complexes between the Kai proteins, facilitated by the hydrolysis of ATP. The kinetics of this reaction are such that the periodicity of the oscillation is around 24 hours across a range of temperatures. (Nakajima et al. 2005). This post-translational oscillator is coupled to a TTFL, which acts as a slave oscillator to the Kai loop (Qin et al. 2010).

It is proposed that the existence of such a post-transcriptional oscillator might provide increased robustness against events such as changes in metabolic rate and cell division, through which circadian timekeeping is conserved (Nagoshi et al. 2004), than an oscillation based on transcription and translation, which would likely be perturbed by the change in gene dosage following S-phase. For those wishing to test this hypothesis in eukaryotes, it is therefore of interest to consider a number of post-translational circadian events, particularly those that are more broadly conserved in clock function that those proteins involved in the canonical TTFL models.

1.0.4 Conservation of circadian molecular features

Despite the apparent differences in canonical TTFL mechanisms between different organisms, the functional contribution of a small number of post-translational mechanisms to circadian timekeeping do appear to be conserved across phyla. For example, the *tau* mutation (the first mammalian circadian mutant described (Ralph & Menaker 1988)) is not situated in any of the core

canonical clock genes but is in fact a point mutation in the enzyme casein kinase 1ε (CK1ε). This results in a shortening of the circadian period of both whole animal behavior and also the cellular molecular rhythm (Maywood et al. 2014). Other work suggests that the CK1δ isoform also plays a role in the maintenance of cellular timekeeping (Meng et al. 2010). In both cases, it is proposed that CK1 can form complexes with PER and CRY and so phosphorylate PER proteins, promoting their nuclear translocation and degradation (Meng et al. 2008). Gain-of-function mutations (such as $CK1\varepsilon^{tau}$) or loss of function through genetic knock-out or pharmacological inhibition, results in shortening or lengthening of circadian period respectively. However, the effect of casein kinase on circadian rhythmicity is not restricted to mammals, and despite not having conserved targets across phyla, manipulation of CK activity shows effects on cellular timekeeping across a large number of model organisms (van Ooijen, Hindle, et al. 2013; van Ooijen, Martin, et al. 2013; Lin et al. 2002; Yang et al. 2003).

A second example of a general regulator of circadian period is glycogen synthase kinase 3β (GSK3β). A proline-directed serine-threonine kinase, GSK-3β has been proposed to phosphorylate mammalian CRY2, targeting it for degradation (Kurabayashi et al. 2010), whilst phosphorylation of REV-ERBα by GSK-3β increases its stability (Sahar et al. 2010). It has been identified that both pharmacological inhibition and siRNA-mediated knock-down of GSK-3β results in a shortening of circadian period in mammalian cell culture (Hirota et al. 2008; Yin et al. 2006). In contrast, in *Drosophila*, it is over expression of

GSK-3 ortholog *shaggy* that results in a shortening of behavioral period, probably as a result of phosphorylation of TIMELESS and PER (Martinek et al. 2001). As with CK1, manipulation of GSK-3 activity has a clear effect on circadian effect across a number of phyla (O'Neill et al. 2011; Tataroğlu et al. 2012).

These and similar observations of circadian period effects as a result of modulation of post-translational mechanisms, even across organisms with highly non-homologous TTFL components, lends credence to the idea that, despite their apparent dissimilarity, there are some common underlying features across eukaryotic timekeeping networks. As such, it is postulated that the varied eukaryotic timekeeping mechanisms might represent the result of a divergent process of evolution from the biological oscillation in an early eukaryotic ancestor.

The realization that circadian timekeeping is not just a phenomenon observed at the level of the whole organism, but is a fundamental autonomous feature of every individual cell, is one of the most significant advances made in the field in recent times. As a result of this, there has been increasing interest in the circadian rhythmicity of many processes at the cellular level. The previously described TTFL is certainly the most documented example of a cell autonomous circadian rhythm. However, there are an increasing number of cases where cell autonomous rhythms appear to occur in the absence of direct input from the canonical TTFL clockwork. For example, one of the earliest

observations concerning cellular metabolic rhythms was the realization that uptake of the 2-deoxyglucose – a glucose analogue which is capable of being taken up by classical glucose transporter – is rhythmic with a period of around 24 hours in both the SCN and peripheral cells (Cassone et al. 1988). This rhythm is observed even in the absence of TTFL activity (Paulose et al. 2012).

The idea that rhythmic TTFL expression is not essential for circadian activity is supported by the observation that in the arrhythmic tim^{01} fly, expression of the *tim* transgene can be sufficient to restore behavioral rhythms, without restoring rhythmicity in the levels of *tim* mRNA. The same also applies for constitutive *Per* expression in its null line (Yang & Sehgal 2001). This indicates that rhythmic transcription and translation of the canonical clock genes, the central theme of the TTFL model, may not be absolutely required for cellular rhythmicity. Instead, it may be the case that these proteins are merely required to be present within a certain range for clear rhythmic outputs to be observed.

1.0.5 Peroxiredoxins as a circadian marker

Peroxiredoxins (Prx) are a family of highly abundant cellular proteins that play a major role in the reduction of endogenously produced peroxides: it is estimated that over 99% of cytosolic and 90% of mitochondrial peroxides react with Prx proteins (Winterbourn 2008; Adimora et al. 2010). Reaction of peroxides with a cysteine residue in the Prx active site results in the formation of disulphide-linked dimer of Prx. The oxidised protein is then ultimately reduced by NADPH, mostly through the thioredoxin system, although some specific Prx reductases

exist (Takeda et al. 2004). In some cases, this final recycling step is avoided and instead a second (and even a third) peroxide can react with the protein, converting it to Cys-$SO_{2/3}$. This second reaction has been has been reported to be around 1000 times slower than the disulphide formation step (Perkins et al. 2015) and the rate of this so-called “hyperoxidation” appears to increase almost linearly with an increase in peroxide concentration. All Prx proteins appear to be capable of undergoing this hyperoxidation step, although some are more sensitive to it than others (Cox et al. 2009).

Screening of mouse hepatic proteins has previously shown that Prx6 is rhythmically translated in mouse liver and in addition, has an anti-phasic rhythm in post- translational modification (Reddy et al. 2006). This was subsequently found to be the case for other members of the Prx family (O’Neill & Reddy 2011; Edgar et al. 2012). Use of a polyclonal antibody for the $SO_{2/3}$ modification showed that this rhythm in post-translational modification of the Prx active site is observed across a broad spectrum of circadian model organisms. Furthermore, this rhythm persists in classical circadian mutants, but the free-running period of the oscillation is clearly perturbed compared to WT controls (O’Neill et al. 2011). In addition, circadian rhythmicity in the abundance of hyperoxidised Prx persists in isolated erythrocytes (O’Neill and Reddy, 2011). This last observation is of particular interest, as mature mammalian erythrocytes are enucleate and therefore lack the capacity to maintain the canonical circadian TTFL. This rhythm in erythrocytes conforms to the technical definition of a circadian rhythm, in that the 24-hr rhythm in post-translational

modification is also temperature compensated and capable of entraining to appropriate external cues. Observations in the marine algae *Ostreococcus tauri* under transcriptional inhibition display similar trends (O'Neill et al. 2011). As such, rhythms in the hyperoxidation Prx proteins act as a rhythmic marker even in the absence of the TTFL.

A rhythm in the abundance of hyperoxidised Prx is the result of three possible events: rhythmic oxidation of Prx, rhythmic reduction of Prx or rhythmic degradation of hyperoxidised Prx (or a combination of these three). As cellular metabolism is the primary source of both ROS and cellular reducing equivalents, particularly NADPH and H_2O_2, we must consider whether potential drivers of this rhythm lie within the pathways of primary metabolism.

1.1 Metabolism

1.1.1 Conserved pathways of primary metabolism in eukaryotes

Primary metabolism – the set of reactions by which substances are both broken down and synthesised in order to provide energy and essential cellular building-blocks – represents one of the defining features of a living organism, and the enzymes that catalyse these reactions are amongst the oldest and most conserved of their kind (Keller et al. 2014). Consequently, the metabolic pathways to which these enzymes contribute are exceptionally similar, with the core pathways involved in carbohydrate, lipid and amino-acid metabolism (Figure 1.3) widely represented across all three phylogenetic domains. For this reason, it is generally accepted that all of these pathways were almost certainly

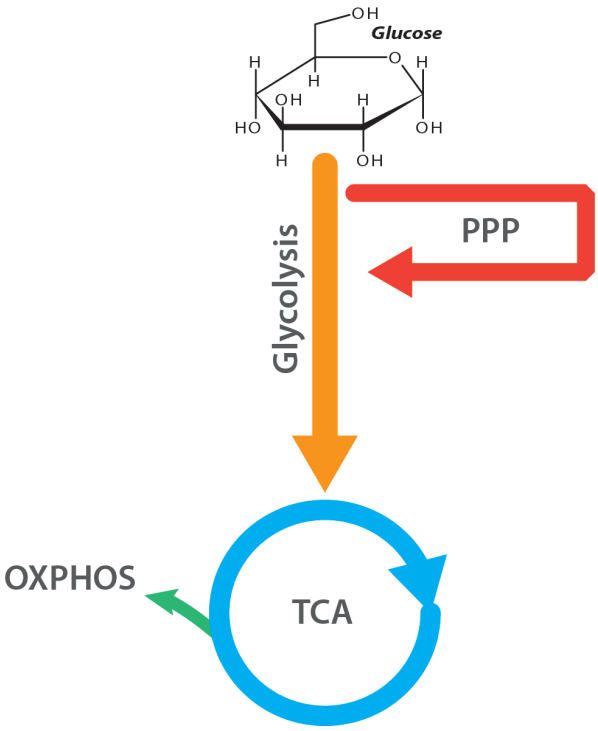

Figure 1.3
Schematic overview of carbohydrate metabolism.

present in some form in the Last Universal Common Ancestor (LUCA) and also, following further spatial compartmentalization of these processes, in the Last Eukaryotic Common Ancestor (LECA) (Margulis et al. 2006). These are further described below.

1.1.2 Glycolysis

Glycolysis refers to the sequence of ten enzymatic reactions that convert glucose to pyruvate. A number of pathways fall under the name glycolysis, the most common of which is the *Embdeb-Meyerhof-Parnas* (EMP) pathway. Glycolysis does not directly require oxygen and is therefore a major pathway for carbohydrate metabolism in both aerobic and anaerobic organisms. The process can be considered as two main stages: an initial investment stage, where two molecules of ATP are consumed in the process of converting each 6 carbon glucose molecule

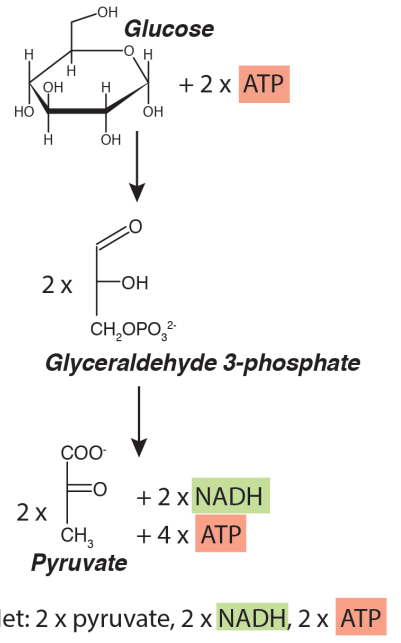

Figure 1.4
Schematic equation of glycolysis

to two 3 carbon glyceraldehyde 3-phosphate molecules and a subsequent "pay-off phase", where each glyceraldehyde-3 phosphate molecule is further converted to pyruvate, producing two molecules of NADH and four molecules of ATP (Alberts et al. 2002). Thus, as a net total, glycolysis produces 2 molecules of NADH and 2 molecules of ATP for every molecule of glucose that passes through the pathway (Figure 1.4).

1.1.3 Pentose Phosphate Pathway (PPP)

Also known as the hexose monophosphate shunt, the PPP runs in parallel with the early steps of glycolysis. Again, this pathway is divided in to two main stages. The first, known as the "oxidative" phase, converts 6-carbon glucose 6-phosphate to 5- carbon ribulose 5-phosphate, producing two molecules of NADPH and releasing one molecule of CO_2 for every glucose molecule. This stage of the pathway is particularly critical for cells that are sensitive to oxidative damage by peroxides, as the NADPH produced here is used for the formation of reduced glutathione and the reduction of other cellular disulphides, as well as many biosynthetic reactions such as fatty acid synthesis. The second – known as the non-oxidative phase – coverts ribulose 5-phosphate to either glyceraldehyde 3-phosphate or fructose 6-phosphate (Alberts et al. 2002). Crucially, this stage of the pathway also produces ribose 5-phosphate as an intermediate, which is required for the synthesis of nucleotides and nucleic acids. In total, the stoichiometry of the PPP is such that for every three glucose 6-phosphate molecules that enter the pathway, two molecules of fructose 6-phosphate, one molecule of glyceraldehyde 3- phosphate and 6 molecules of

NADPH are produced (Figure 1.5).

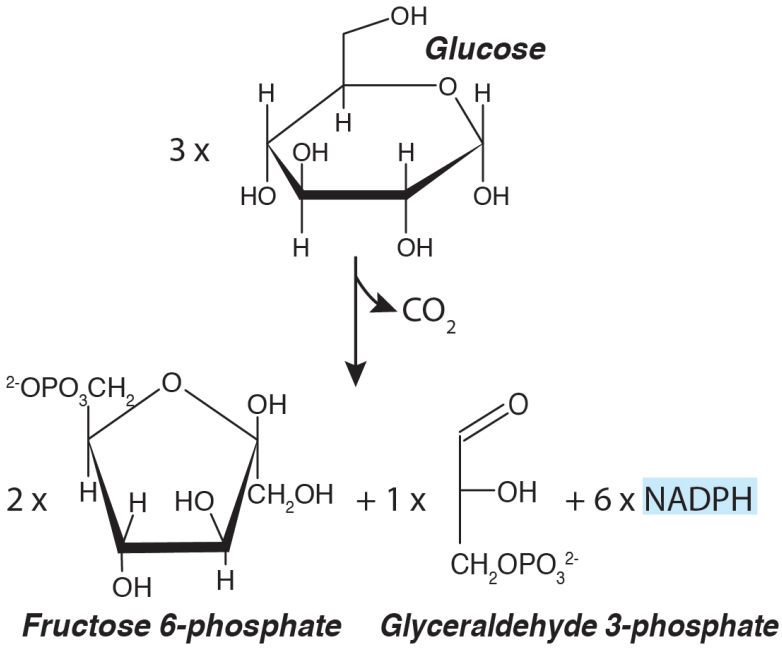

Figure 1.5

Schematic equation of the Pentose Phosphate Pathway

1.1.4 The Tricarboxylic Acid Cycle (TCA)

The tricarboxylic acid cycle (also known as the Krebs cycle or the citric acid cycle) is often considered to be the unifying pathway of metabolism in eukaryotes. Compartmentalised within mitochondria, the TCA cycle oxidises intermediates derived from carbohydrates, lipids and amino acids, whilst also providing intermediates for a large number of anabolic processes, including gluconeogenesis, lipogenesis and amino acid metabolism. Briefly, the TCA cycle oxidises acetyl- CoA, which is either formed from pyruvate by pyruvate dehydrogenase or is obtained directly from β-oxidation of fatty acids, to two molecules of CO_2. As the name suggests, this is achieved through a cyclical process where the two acetyl groups of acetyl CoA are donated to oxaloacetate to form 6 carbon citrate. Two of the carbons that formed the original

oxaloacetate back-bone are lost sequentially in the cycle as CO_2, the carbons that were originally donated from acetyl CoA are formed in to a new oxaloacetate back-bone and the cycle begins again (Alberts et al. 2002). The energy released following the loss of the two carbon molecules is stored in the form of GTP, NADH and $FADH_2$, with a final stoichiometry of one GTP, three NADH and one $FADH_2$ per molecule of acetyl CoA (Figure 1.6).

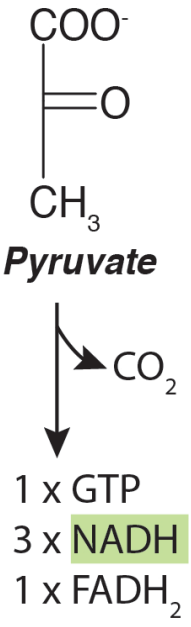

Figure 1.6 ***Schematic equation of the TCA cycle*.**

1.1.5 Oxidative Phosphorylation

Oxidative phosphorylation is the process by which the electron donors generated through the citric acid cycle – namely NADH and $FADH_2$ – are made to donate their electrons in order to provide energy for the synthesis of ATP within mitochondria. This is brought about through a series of redox reactions, which are catalysed by a sequence of four protein complexes situated within the inner mitochondrial membrane and which have the collective name of the "electron transport chain". The energy produced from the flow of electrons through this chain is used to drive protons across the inner mitochondrial membrane, thereby creating an electrochemical H^+ gradient. This gradient is then relieved as protons are able to flow back in to the inner mitochondrial space through ATP synthase, a large multi-unit transporter also situated within the inner mitochondrial membrane. The energy from the dissipation of this gradient is used to synthesise ATP (Alberts et al. 2002). This is, however, by no means a perfectly efficient process, and it is important to

note that electron leakage across the mitochondrial membrane is the major source of intracellular source of reactive oxygen species (ROS) (Han et al. 2001).

1.1.6 Beta-oxidation

Beta-oxidation is the process by which fatty acids are formed from the circulating ester triacylglycerol and subsequently oxidised to form acetyl CoA for further oxidation in the citric acid cycle. Initially, triacylglycerol is broken down in the cytosol to form 3 molecules of palmitate and one of glycerol. The palmitate is then converted to palmityol CoA – consuming ATP to AMP in the process. This is then transported in to the mitochondria, where it is progressively oxidised and cleaved to form 8 molecules of acetyl CoA per molecule of palmitate, producing seven NADH and seven $FADH_2$ in the process. The acetyl CoA then enters the TCA cycle (Alberts et al. 2002).

What is hopefully is clear when considering all of these metabolic pathways is that they all produce or utilise the reducing equivalents NADH and NADPH as co-factors and that all catabolic processes ultimately result in a degree of ROS generation. Metabolism is therefore the primary source of both reducing and oxidising agents within the cell. As such, primary metabolism is a key modulator of cellular redox state and control of metabolism therefore plays a major role in maintenance of redox homeostasis.

1.2 Circadian metabolism

1.2.1 Circadian metabolism in the whole animal

When considering metabolism, in addition to the pathways of primary cellular metabolism described above, it is also important to consider metabolism at the level of the whole organism, including systems such as digestion and associated hormonal and neuronal signaling. There is a long history of observation of clear links between circadian timekeeping and metabolism at the level of physiology. For example, it has been well documented that animals that display a significant disruption in timekeeping, such as the arrhythmic *bma1l*$^{-/-}$ and *cry1*$^{-/-}$*cry2*$^{-/-}$ mice, show a strong metabolic phenotype, with increased propensity to diabetic and obesity-related disorders (Barclay et al. 2013; Marcheva et al. 2010). *Bmal*$^{-/-}$ mice also exhibit profound hyperglycemia (Lee et al. 2011).

A distinct feature of timekeeping in whole mammals is the role of the suprachiasmatic nucleus (SCN) of the hypothalamus. *In vivo*, the SCN has neuronal projections from the SCN to the paraventricular nucleus of the hypothalamus (PVN). This gives the SCN the capacity to influence endocrine regulation both humourally through the hypothalamic-pituitary-adrenal (HPA) axis and also neuronally via projections from the PVN to the autonomic nervous system (Kalsbeek et al. 2012). As levels of many adrenal hormones known to regulate cellular metabolism, particularly glucocorticoids, are rhythmically expressed (Oster et al. 2006), it is therefore entirely plausible to propose that the SCN might regulate rhythmic metabolism in this manner. This is idea is

supported by the observation that ablation of the SCN or adrenalectomy leads to a loss of rhythmicity in levels of these hormones (Ishida et al. 2005).

The process of sleep is also a major regulator of changes in metabolism at the level of the whole organism – primarily as a result of the fact that the sleep wake cycle is intrinsically linked to cycles in energy intake. As the SCN is the principal effector of the circadian drive to sleep, it is often considered to influence metabolic rhythms via sleep patterns, in addition to direct regulation as previously described.

There is also a large body of work demonstrating that time of feeding and the associated whole animal metabolism pathways are capable of influencing the phase of circadian behaviour. Mammals normally feed during their active phase, which is generally driven by signals from the light-entrained SCN. In these cases, animals are active according to their diurnal or nocturnal preference, and behavioural and gene expression cycles reflect this. However, if animals are subjected to restricted feeding (RF) protocols, where food is only available at certain times throughout the circadian day, it is possible to uncouple SCN signals from circadian oscillations in the rest of the organism. It has thus been shown that food consumption only during the normally inactive phase can result in a phase shift in the rhythmic expression of clock genes and metabolic activity in peripheral tissues, as well as a shift in body temperature and activity rhythms (Saini et al. 2013). As such, the mammalian circadian clock, both at cellular and the behavioral level, is entrained by time of feeding.

It is of note that, unlike in peripheral tissues, this shift in circadian molecular expression in response to feeding is not observed in the SCN (Damiola et al. 2000), nor is the SCN, nor even a functioning TTFL required for the effect on behaviour or the molecular clock to be observed (Storch & Weitz 2009). This suggests that, although the SCN generally synchronizes such processes in the periphery, it is not the sole determinant. Indeed, it appears that the influence of the SCN on behaviour can be overridden by time of feeding and associated metabolism, as nocturnal mice with food availability restricted only to the light phase will shift their behavioural rhythms towards diurnality such that they become most active prior to the anticipated timing of food availability (Stokkan et al. 2001). However, the exact mechanism by which timed feeding influences circadian animal behaviour is not currently well understood. Perhaps influenced by the SCN, which acts as a central cite for co-ordination of light inputs, many have proposed that entrainment to feeding must require a central locus – referred to as the "Food Entrainable Oscillator" (FEO), although no anatomical site for such a locus has been identified, despite great endeavor towards this end (Stephan 2002; Davidson et al. 2003; Mistlberger 2006) .

Similar observations are made in the *Drosophila* fat body, which serves an analogous function to the mammalian liver. Here tissue-specific expression of a dominant negative CLOCK, an essential gene in the *Drosophila* TTFL, only in the fat body, results in either dampening or loss of transcriptional rhythms in a large number of metabolically active genes across all tissues, despite the fact that clock gene expression cycles of the central clock in the brain remain

functional (Xu et al. 2011).

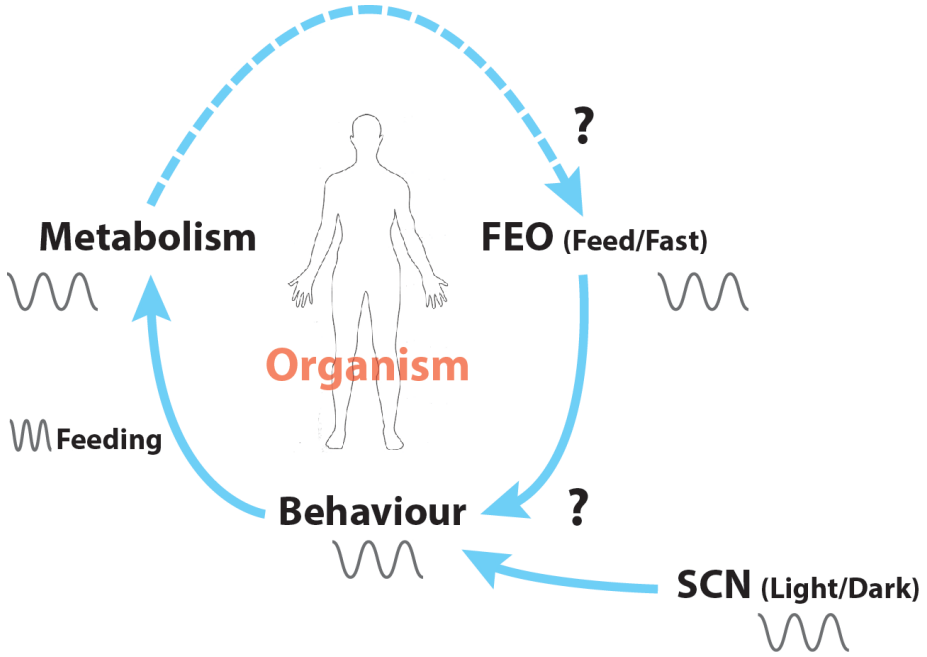

Figure 1.7 Behavioural regulation by the SCN and feeding
Diagram outlining the current knowledge of circadian behavioural regulation by the SCN and feeding. Unknown elements are indicated as '?'.

These observations suggest that gross metabolism might well be capable of influencing circadian rhythmicity, as well being influenced by circadian rhythmicity at the level of the whole organism (Fig 1.7).

1.2.2 Circadian cellular metabolism

The interplay between circadian timekeeping and metabolism, in the form of primary metabolism, is also clearly demonstrated at the cellular level. For example, cells derived from the arrhythmic *Bmal1*$^{-/-}$ mouse show increased levels of oxidative stress (Musiek et al. 2013), potentially as a result of mitochondrial dysfunction (Jacobi et al. 2015).

Recent work from Peek et al. has shown there to be a self-sustained 24 hour rhythm in both cellular β-oxidation and, offset in phase by around 4 hours, in glucose oxidation (Peek et al. 2013). Both of these being primarily mitochondrial metabolic activities, we can thus envisage that there might be a rhythm in other mitochondrial activities. Meanwhile, Altman et al. have demonstrated a rhythm in glucose utilization in U2OS cells (Altman et al. 2015). Most strikingly here, manipulations that suppressed expression of clock proteins also suppressed the rhythm in glucose uptake.

Given the diurnal difference in the metabolic demands of an organism, the temporal segregation of antagonistic metabolic processes – such as glycogenesis and glycogenolysis – makes intuitive sense. Such temporal segregation is observed in a wide number of circadian model organisms and at all levels of biological scale, from transcription of relevant proteins at the cellular level to rhythms of whole organism gross metabolism (Tu & McKnight 2006; Fustin et al. 2012). This has led to the general belief that circadian variation in metabolism is a result of the rhythmic regulation of metabolic enzymes driven by the canonical circadian TTFL (Gerhart-Hines & Lazar 2015).

1.2.3 The interplay between circadian timekeeping and metabolism

The current prevailing paradigm for how metabolism is rhythmically regulated is that the genes, or a subset of genes, involved in certain metabolic pathways possess a promoter element that is under circadian control *via* the binding of

one of the canonical “clock genes” (Harmer et al. 2000; Shinohara et al. 1998). This idea is not without support. It is most certainly the case that many genes do exhibit circadian rhythms in transcription as a result of this kind of control. Work from Zhang et al. suggest that over a third of protein coding genes had observable rhythms in transcription in at least one mouse tissue, but that exactly which transcripts oscillated was highly tissue specific (Zhang et al. 2014). However, genes that coded for proteins with known metabolic functions are generally over-represented across tissues.

In addition to rhythmic transcription of crucial metabolic genes, there is also a growing understanding that there exists the potential for circadian regulation at the level of translation. Through the use of ribosomal profiling experiments, Jang et al. show that not only is there significant circadian regulation at the translational level, but that it can be observed both in addition to rhythms in transcription and in the absence of transcriptional oscillations. Again, there appears to be an enrichment of genes associated with metabolism amongst those genes that show oscillations in ribosomal association (Jang et al. 2015). Recent work has shown that canonical clock gene *bmal1* is able to act as a translational regulator, in addition to its well- documented transcriptional role (Lipton et al. 2015), which indicates at least one mechanism by which such circadian regulation of translation might be facilitated.

Regardless of whether transcription or translation of a metabolic enzyme is rhythmic, the current prevailing explanation for circadian rhythmicity in

metabolism is that abundance of certain enzymes that form nodal points in these pathways is rhythmically regulated by TTFL components. A number of examples for this kind of regulation exist. For example, Glyceraldehyde-3-phosphate has been proposed to be regulated by the TTFL in *Neurospora* (Shinohara et al. 1998).

It must be noted, however that even in the absence of rhythmic protein production, rhythmic metabolic flux is still both entirely plausible and has been reported. Work by Paulose et al. observed there to be a rhythm in both glucose uptake and glucose transporter expression in mouse embryonic stem cells prior to the development of rhythmic clock gene expression (Paulose et al. 2012), suggesting that the rhythmic transcription and translation of these proteins is not necessarily required for occurrence of cellular rhythms. This resonates with the previously described observations that rhythms in Prx hyperoxidation persist in enucleate cells and in the absence of nascent transcription or translation (O'Neill & Reddy 2011; O'Neill et al. 2011).The combined observations that firstly, rhythmic transcription and translation is not essential for rhythmic activity, secondly, that rhythmic Prx hyperoxidation continues in the absence of any nascent transcription and thirdly, that metabolism, the primary source of intracellular peroxides and reducing equivalents, also exhibits circadian rhythmicity in a number of pathways has led some to posit an alternative hypothesis with regards to the nature of the link between circadian rhythmicity and metabolism. This postulates that some of the pathways of metabolism might constituent an essential, evolutionarily conserved component

of cellular timekeeping (Haydon et al. 2013; Asher & Schibler 2011). Such a post-transcriptional circadian mechanism has been proposed to be analogous to the Kai oscillator in cyanobacteria, acting as the dominant oscillator within the cell, providing the essential 24 hour periodicity of the circadian rhythm with the TTFL acting as a slave oscillation providing a functional output in the form of protein expression, but not as a competent circadian oscillator in its own right (Johnson 2010) (Fig 1.8). Some preliminary work suggests that the hypothesis that cellular metabolism might contribute to such an oscillator is not implausible (Rey et al. 2012).

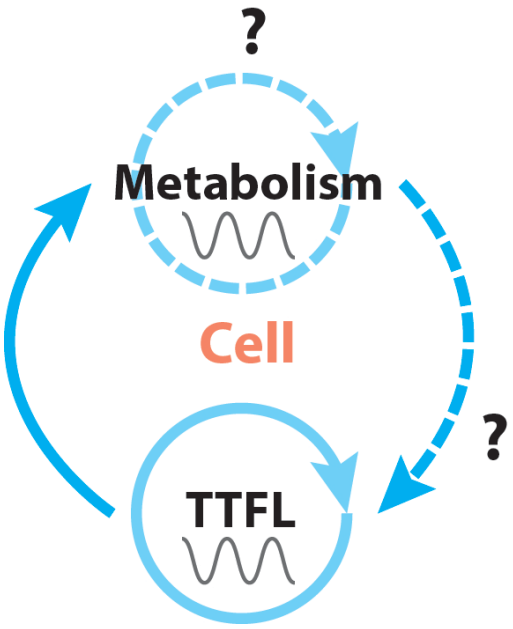

Figure 1.8 ***Reciprocal regulation between primary metabolism and the TTFL***
Diagram outlining potential reciprocal regulation between primary metabolism and the TTFL. Unknown elements are indicated as '?'.

In this thesis, I investigate the complex relationships between metabolism and circadian rhythmicity and attempt to elucidate the nature of the relationship between these two processes. The first results chapter describes the development of a new technique to assist in study of metabolism in a circadian context. The second chapter carries out this investigation at the intracellular level, considering the contribution of primary metabolism to cellular circadian

rhythms. The final chapter considers metabolism at the intercellular level, investigating how feeding and associated changes in metabolism in the whole organism can influence circadian timekeeping.

Chapter 2: Materials and Methods

2.0 Common solutions

Common stock solutions were obtained from the media kitchen of the MRC Laboratory of Molecular Biology. These included LB (Luria-Bertani) media, PBS (phosphate buffer saline), 0.1 M EDTA (Ethylenediaminetetraacetic acid), trypsin, 1 M $MgCl_2$, 1 M Tris-HCl pH 7.4, S.O.B. (Super Optimal Broth), glycerol, 1 M $CaCl_2$, penicillin/streptomycin, Millipore water and antibiotic-supplemented LB and TYE agar plates.

2.1 Materials

2.1.1 Materials

All materials were obtained from Sigma-Aldrich unless otherwise stated. MHY 1485 was a kind gift from Madeleine Lancaster (MRC Laboratory of Molecular Biology).

2.1.2 Cell Lines

U2OS and NIH 3T3 cells were obtained from ATCC. PER2::LUC fibroblasts were derived in-house. $FH1^{-/-}$ embryonic kidney cells and pFH controls were a kind gift from Christian Frezza (MRC Cancer Unit, Cambridge).

2.1.3 Plasmids

Plasmids for the expression luciferase reporters of clock gene transcription contained promoters for Bmal1 or Per2 (originally cloned by Hiroki Ueda, RIKEN Quantitative Biology Centre), subcloned in pGL4.20 (Promega).

2.1.4 Antisera

Antisera were obtained from the following sources and used at the following dilutions:

Anti-6-phosphogluconate dehydrogenase (ab129199) – abcam – 1:2000

Anti-b-actin (SC-47778) – Santa Cruz – 1:5000

Anti-Bmal1 was a gift from the Hastings lab (MRC Laboratory of Molecular Biology) - 1: 2000

Anti-Cry1 was a gift from the Lamia lab (The Scripps Research Institute) - 1:2000

Anti-Cry2 was a gift from the Lamia lab – 1:2000

Anti-GAPDH (G99545) – Sigma 1:5000

Anti-Glucose 6-phosphate dehydrogenase (ab66340) – abcam – 1:2000

Anti-Myc-tag – in house – 1:500

Anti-PER1 was a gift from the Hastings lab – 1:2000

Anti-PER2 was a gift from the Lamia lab – 1:2000

Anti-Phosphoglucose isomerase (ab993) – abcam – 1:2000

Anti-Tubulin – in-house – 1:5000

Anti-rabbit IgG conjugated to HRP– Sigma – 1:5000

Anti-mouse secondary IgG conjugated to HRP– Sigma – 1:5000

Anti-guinea pig IgG conjugated to HRP (sc2438) – Santa Cruz – 1:5000

2.1.5 NS21

Serum replacement NS21 was made in-house as described in Chen et al. 2008. Unless otherwise specified, the composition of this supplement when diluted in cell culture media was as in the table below:

Component	Concentration (μM)
Bovine Albumin	37
Catalase	0.010
Glutathione	3.2
Insulin	0.6
Superoxide dismutase	0.077
Holo-transferrin	0.062
T3 (triiodo-L-thyronine)	0.0026
L-Carnitine	12
Ethanolamine	16
D(+)-Galactose	83
Putrescine	183
Sodium Selenite	0.083
Corticosterone	0.058
Linoleic Acid	3.5
Linolenic Acid	3.5
Lipoic Acid	0.2
Progesterone	0.02
Retinol acetate	0.2
Retinol, all trans	0.3

D,L-alpha-Tocopherol	2.3
D,L-alpha-Tocopherol acetate	2.1

2.2 Tissue and Cell Culture

2.2.1 Animal Methods

All experiments were licenced under 1986 Home Office Animal Procedures Act (UK) and carried out in accordance with local animal welfare committee guidelines. PERIOD2::LUCIFERASE (PER2::LUC) mice were originally supplied by Joe Takahashi (University of Texas Southwestern; Yoo et al. 2004) and subsequently bred locally.

2.2.2 Organotypic Slices

For organotypic slice culture, brains and other tissues were removed from pups (9-10 day old) and adult mice, respectively, and sectioned to 300µm slices using a McIlwain “Tissue Chopper”. Areas of interest were further microdissected and cultured on a Millipore membrane insert at 37°C as previously described (House et al., 1998). For bioluminescent recording, SCN slices were transferred in to 1.2ml serum-free, HEPES buffered “air medium” (Hasting et al., 2005), with 100µm firefly luciferin (Biosynth), supplemented with 6% corticosterone and insulin-free NS21 (made in-house, as for Chen et al. 2008). Other tissues were cultured and recorded in DMEM, with 5.5mM glucose, 1% glutamax, 2% corticosterone and insulin-free NS21 and 1mM firefly luciferase. Slices were placed in a 35mm polystyrene petri dish and

sealed with circular 44mm No. 1 coverslips (Thermo Fisher) and vacuum grease before recording. SCN slices were taken and cultured by Ryan Hamnett.

2.2.3 Isolation of primary fibroblasts and immortalisation

Isolation

Lung tissue was isolated from recently euthanized mice and immediately placed in ice-cold PBS and transferred to a tissue culture hood. Here the tissue was further dissected to approximately 1mm^3 sections. The dissected tissue was then transferred in to 10ml DMEM/F12 medium (Gibco) containing Liberase (0.14 Wunsch unit/ml) and 1x penicillin/streptomycin and stirred slowly for 60 minutes at 37°C. 30ml DMEM/F12 containing 15% Hyclone™ Fetalclone™ III and 1x penicillin/streptomycin was then added to the existing tissue media and centrifuged at 524xg for 5 minutes. The supernatant was removed and the cell pellet resuspended and centrifuged a time a total of three times. Following this, the resultant pellet was resuspended in 10ml DMEM/F12 containing 15% Hyclone™ Fetalclone™ III (GE Healthcare), 1x penicillin/streptomycin and 1x Mycozap™ plus-PR (Lonza), transferred to a 10cm dish and incubated at 37°C, 5% CO_2, 3% O_2 for two weeks, with media changed every 3-5 days. After two weeks, cells were then split and continued to be cultured at 37°C, 5% CO_2, 3% O_2.

Immortalisation

For production of immortalised lines, cells underwent serial passage at 37°C, 5% CO_2, 20% O_2. After around 15 passages, the doubling time of the cells

decreased and cells continued to be split 1:1 until approximately 20 passages, when the rate of doubling was seen to increase again to approximately 48 hours. At this stage, cells were considered immortalised.

2.2.4 Primary Dissociated Neuron Cultures

Primary cortical neuron cultures were obtained from PER2::LUC mice at birth (P0). Cortical tissue was dissected in a solution of EBSS without Mg^{2+} and Ca^{2+} (Invitrogen), 100mM HEPES and Penicillin/Streptomycin. Cells were then digested using enzymes and buffers provided in the MACS Neural Tissue Dissociation Kit – Postnatal Neurons (Miltenyl Biotec), following the manufacturers instructions. Briefly, this is a follows: cells were incubated at 37°C for 15 minutes with 650 µl enzyme mix 1 per pup. Cells were then titurated x6 using a fire-polished glass pipette. Cells were then incubated for a further 10 minutes at 37°C with 10µl enzyme mix 2 per pup. An additional 5µl enzyme mix 2 was added per pup and cells were titurated again. The entire mixture was then passed through a 50µm filter (Partec) and EBSS + 0.5% BSA (3.33ml per pup) was added immediately before centrifugation for 5 minutes at 300xg. Cells were resuspended in MEM, 20mM glucose, 1mM NaPyruvate, 25mM HEPES, 1x N2 (ThermoFisher), 10% horse Serum and penicillin-streptomycin to a density of $2x10^6$ cells per ml and 250µl per well was seeded in PEI Borate-coated 24 well plates. Plates were left for 12 hours and then an additional 250µl Neurobasal A Medium, supplemented with 2% B27, 1% glutamax and PenStrep was added per well. Cells subsequently underwent a half media change every week for 3 weeks before

experimentation. Prior to experimentation, cells were changed in to insulin-free media containing luciferin by serial half media change, subjected to temperature cycles and placed in an ALLIGATOR (Cairn Research).

2.2.5 Cell Culture – maintenance of lines

Cells were maintained in 75cm^2 flasks (Falcon) in 10ml DMEM (Thermo Fisher) supplemented with 10% serum and Penicillin/Streptomycin. PER2::LUC immortalised fibroblasts and NIH 3T3s were maintained in Hyclone™ FetalClone™ III bovine fetal serum (GE Healthcare) whilst Hyclone™ FetalClone™ II bovine fetal serum (GE Healthcare) was used to maintain U2OS and FH1$^{-/-}$ and pFH lines. Cells were passaged when the monolayer reached 90% confluence. This was achieved by washing cells in warm PBS and then treating with 2.5ml trypsin in EDTA for 5 minutes at 37°C, or until most cells had detached. 250µl of cells in EDTA and trypsin was then added to a new flask with 10ml complete medium and the flask incubated at 37°C.

2.2.6 Cell culture - experimental

Unless otherwise stated, cells were grown to confluence (passage no. <50) in either 35mm dishes, 24-well plates or 96-well plates in DMEM (GIBCO) supplemented with 10% serum and penicillin/streptomycin. Cultures were kept for up to 4 weeks with media refreshed every 5-7 days. Before the start of recording, unless otherwise described, cells were subjected to temperature entrainment cycles of 12hrs at 32°C followed by 12hrs at 37°C for a minimum

of 48 hours. Cells were then changed to “Air Media” (Hastings et al. 2005) or stated variations of this medium, and dishes sealed using either vacuum grease and circular 44mm No. 1 coverslips (Thermo Fisher) or gas-impermeable PCR Adhesive film (Thermo Fisher). Cells were then transferred to a Lumicycle®32 luminometer (Actimetrics), an ALLIGATOR (Cairn Research) or a Luminescence microplate reader (Bertold).

2.2.7 Perfusion cell culture

For experiments carried out under perfused media conditions, cells were seeded and grown to confluence in a fluidics slide (μ-Slide I 0.6 Luer, Ibidi) in DMEM (Gibco) supplemented with 10% serum and penicillin-streptomycin. Cultures were incubated for 1-2 weeks, with DMEM media refreshed every 5-7 days. Cells were also subjected to temperature entrainment cycles during this time, as previously described. Before the start of recording, cells were changed to low-glucose DMEM (Sigma, D5921) supplemented with 1% glutamax, penicillin-streptomycin, 0.1mM luciferin and, unless otherwise stated, 2% serum and 2% B27. Cells were then perfused with the same media, driven by syringe pump (NE-1600) at a flow rate of 50µl/hr for the duration of the experiment. Syringes and slides were connected using 1mm I.D. ETFE tubing (GE Healthcare), elbow, male and female luer fittings (Ibidi). Tubing was sterilised prior to use with 70% ethanol. Recording was performed using a bioluminescence incubator (Cairn Research). Boli were applied using three-way luer fittings (Cole-Parmer) to produce a diversion of flow, with no

change in flow rate or detectable flow disturbance. Further details of this method and its optimisation can be found in chapter 2.

2.2.8 Experimental cell handling

Air Medium

Unless otherwise stated, bioluminescence experiments were carried out using "Air Medium" (Hastings et al. 2005). The composition of 500ml of "Air Medium" stock is:

DMEM (powder, D5030)	4.15g
$NaHCO_3$	0.175g
Glucose	2.25g
1M HEPES	5ml
Penicillin/Streptomycin	5ml
Millipore Water	up to 500ml

Stock was then adjusted to pH 7.4 at ambient temperature and sterile filtered.

Prior to recording, a working stock was made. 50ml of "Working Air Medium", unless otherwise stated, consists of:

Air Medium Stock	45ml
Foetal Bovine Serum (Hyclone™ Fetalclone™)	5ml
B27/NS21 (Life Technologies/in house)	1ml

Firefly luciferin (Biosynth AG)	1mM
GlutaMAX™ (Thermo Fisher)	500µl

Working stock was sterile filtered and osmolarity adjusted to 350mOsm/L before use.

Addition of pharmacological agents

For addition of pharmacological agents during an experiment, maintaining cells at 37°C was crucial. This was achieved by placing dishes directly onto an isothermal pad for the duration of the treatment. When cells were to be treated with multiple drugs, cells were placed in 37°C incubators and given 5-30 minutes to equilibrate (as appropriate) before a second drug was applied.

2.3 Molecular Biology

2.3.1 Isolation of DNA for bacterial enzymes

To obtain genomic DNA for bacterial pentose phosphate pathway enzymes, pelleted k12 E. coli was resuspended in 350µl 10 mM Tris-HCl, pH 8.0, with 0.1 M NaCl, 1 mM EDTA, and 5% TRITON X. 25µl 10mg/ml lysozyme in 10 mM Tris-HCl, pH 8.0 was added, the mixture vortexed and incubated at 37°C for 30 minutes. The mixture was then boiled for 40 seconds, before centrifuging at maximum speed in a bench-top centrifuge for 5 minutes and the pellet discarded. The resulting supernatent was then used as the starting material for PCR. Here, PCR tubes were each filled with 5µl Q5 reaction buffer (New England BioLabs), 0.5µl 10mM dNTPs, 1.25µl forward primer,

1.25µl reverse primer, 0.5µl genomic DNA, 0.25µl High-Fidelity DNA Polymerase (New England BioLabs) and 16.25µl nuclease-free water. Samples were then subjected to 30 seconds at 98°C, followed by 35 cycles of 98°C for 10 seconds, a variable annealing temperature for 30 seconds (Tm determined using NEB Tm calculator, New England BioLabs) and 72°C for 20 seconds. Sampled were then cleaned up using the QIAquick PCR purification kit (Qiagen) as per manufacturers intructions. Following PCR, samples were run on a 0.8% agarose E-Gel® DNA gel (Thermo Fisher) using an E-Gel® iBase™ (Thermo Fisher) to confirm fragment size.

Primer sequences used were:

PGI Forward – TTCTGTGACTGGCGCTACAA

PGI Reverse – ACCGCGCCACGCUUUAUAGCG

GND Forward – TAGCTGAAGACGGTGAACCA

GND Reverse – ATCCAGCCATTCGGTATGGAA

ZWF Forward – TAAGTACCGGGTTAGTTAAC

ZWF Reverse - CTCAAACTCATTCCAGGAACG

2.3.2 Colony PCR

Colony PCR was performed by PCR using Q5® High-Fidelity DNA Polymerase (New England BioLabs). Wells of a 96-well PCR plate were each filled with 5µl Q5 reaction buffer, 0.5µl 10mM dNTPs, 1.25µl forward primer, 1.25µl reverse primer, 0.25µl High-Fidelity DNA Polymerase and 16.75µl nuclease-free water and stored on ice. Single colonies were selected using a

sterile toothpick, which was subsequently dipped directly in to the PCR reaction mixture before being stored in LB at 4°C. Once all colonies had been selected, the plate was subjected to 10 minutes at 98°C, followed by 35 cycles of 98°C for 10 seconds, 55-65°C for 30 seconds (dependent on predicted annealing temperature) and 72°C for 20 seconds. Following PCR, samples were run on a 0.8% agarose E-Gel® DNA gel (Thermo Fisher) using an E-Gel® iBase™ (Thermo Fisher) to identify those samples containing fragments of the appropriate size.

2.3.3 Production of stable over-expression lines

For generation of stable overexpression lines, recently immortalised PER2::LUC fibroblasts were transfected with the Tet repressor plasmid pcDNA6/TR© (Thermo Fisher) and Tet operon vector plasmid pcDNA™4/TO/*myc*-His A (Thermo Fisher).

Cloning

The plasmids were propagated using One Shot® TOP10 chemically competent E. coli (Thermo Fisher), as per the manufacturers recommended protocol. In short, per transformation, 50µl of E. coli was thawed on ice, 1µg of the plasmid DNA added, mixed by gently agitating the vial and then returned to ice for 30 minutes Vials were then placed in a 42°C water bath for 45 seconds before returning to ice. 250µl of pre-warmed S.O.B was added to the vial, before cells were place in a 37°C shaking incubator for 1 hour at 225rpm. 100µl of this mix was then spread on an LB agar plate containing

100µg/ml ampicillin an incubated at 37°C overnight. The following day, 3 distinct colonies per plasmid were selected and grown up overnight in 6ml LB containing 100µg/ml ampicillin in a 37°C shaking incubator at 225rpm. Samples were then centrifuged at 1000rpm for 5 minutes and the supernatant discarded. Plasmid DNA was then prepared using the QIAprep spin miniprep kit (Qiagen), as recommended by the manufacturer. DNA was stored at -20°C until required.

The pcDNA™4/TO/*myc*-His A plasmid was further processed to act as a vector for the overexpression of bacterial isoforms of pentose phosphate pathway enzymes, which were isolated as described above. Following elution, DNA underwent restriction digest using BamHI-HF® and HindIII-HF® (New England BioLabs) for 60 minutes at 37°C. The digest was then cleaned-up using QIAquick PCR purification kit (Qiagen) as per the manufacturer's instructions. The digested production was then ligated to the appropriate insert using T4 Ligase (New England BioLabs), with 50ng of the digested vector, 37.5ng of the insert and 2µl of ligase, made up to 20µl with nuclease-free water. The reaction mixture was left at room temperature for 10 minutes, before being heat-inactivated by heating to 65°C for 10 minutes. The ligation reaction was then chilled on ice before being transformed into One Shot® TOP10 chemically competent E. coli (Thermo Fisher) as described above and plated on to LB agar plates containing 100µg/ml ampicillin. The next day, 3 colonies of each insert were selected, grown up overnight in liquid LB and the plasmid DNA isolated using the QIAprep spin miniprep kit (Qiagen), as

described above. Samples of each insert were sent for Sanger sequencing using the CMV forward and BGH reverse primers, which flank the multiple cloning site, to confirm sequence identity. Due to contamination of the ligation reaction, the pcDNA™4/TO/*myc*-His C plasmid containing the bacterial isoform of phosphoglucose isomerase was selected using colony PCR prior to sequencing, as described above.

Primers used for sequencing were:

CMV Forward Primer – CGCAAATGGGCGGTAGGCGTGT

BGH Reverse Primer – TAGAAGGCACAGTCGAGG

Transfection

Cells were transfected with the pcDNA6/TR© plasmid using a forward transfection method to produce a line stably expressing the tet-repressor. Briefly, cells were seeded in 100µl complete medium a 24-well plate, such that they reached 70% confluencey after 24 hours. Transfection medium was made up to consist of 2µg pcDNA6/TR© and 6µl FuGENE® transfection reagent (Promega), made up to 100µl with Opti-MEM® (Thermo Fisher). 24µl of this medium was added to each well. Cell were incubated for 24 hours at 37°C for 24 hours before undergoing a full media change to complete medium. Cells were subsequently selected for stable expression of pcDNA6/TR© using 3µg/ml blastcidin, media changed every 3-5 days. Once appropriate sequences had been obtained for all inserts, these were transfected in to PER2::LUC lung fibroblasts which stably expressed the

pcDNA6/TR© Tet repressor using FuGENE® transfection reagent (Promega) as described above. Cells were selected in complete media containing both 3µg/ml blasticidin and 250µg/ml Zeocin™ (Invitrogen). Once selection was complete, cells were maintained in complete media containing 3µg/ml blasticidin and 250µg/ml Zeocin™ (Invitrogen) until experimentation.

2.3.4 Gel Electrophoresis and Western Blotting

Protein Preparation

To prepare protein for western blotting, cells were removed from the 37°C incubator and placed on ice. Cell culture media was removed and the cells washed with ice-cold PBS. Cells were then lysed on ice in lysis buffer containing 50mM Tris-HCl (pH 7.5), 1% TritonX100, 1.5mM $MgCl_2$, 5mM EDTA and 100mM NaCl in the presence of ptrotease and phosphatase inhibitors for 10 minutes. Lysate was then transferred to an ice-cold microcenrifuge tube and centrifuged at max in a bench-top centrifuge for 5 minutes. The supernatant was removed and added to 1/3 volume SDS sample buffer containing 4% BME (β-mercaptoethanol). The sample was then warmed at 70°C for 10 minutes.

Gel Electrophoresis and Western Blotting

NuPAGE Novex 4–12% Bis-Tris gradient gels (Life Technologies) were run using the manufacturer's protocol with a reducing MES-SDS buffer system at 200V for 35 minutes. Protein transfer to nitrocellulose membrane for blotting was performed using the iBlot system (Life Technologies), with a standard

(P0, 9 min) protocol. The nitrocellulose membrane was washed briefly in water, and then blocked for 1hr in blocking buffer (0.5% BSA/non-fat dried milk (Marvel) in Tris buffered saline with 0.05% Tween-20 (TBST)). Membranes were then incubated with antibody diluted in blocking buffer overnight at 4°C. The following day, membranes were washed for 3 x 10 minutes in TBST and then incubated with 1:5,000 HRP-conjugated secondary antibody (Sigma-Aldrich) for 60 min. 3 x 10 minute washes in TBST were then performed before performing chemiluminescence detection using Immobilon reagent (Millipore). Membranes that were probed with antibodies multiple times were washed in 0.2% sodium azide for 15 minutes before being blocked and probed with primary antibody as before.

2.3.5 Quantitative PCR for mRNA

For qPCR, cells were grown to confluence in 35mm dishes, subjected to temperature cycles and changed in to “Air Media” as previously described for bioluminescence recording. At an appropriate time point, cells were harvested in 350µl RLT buffer and RNA was extracted with the RNAeasy mini kit (Qiagen) using the recommended protocol. On column DNase digestion was performed. cDNA was generated from these samples using the iScript cDNA synthesis kit (BioRad) using a total RNA quantity of 100-500ng per sample. RNA quantity was kept consistent across all samples within a given experiment. 20µl reactions were processed using a Veriti™ thermal cycler (ThermoFisher) for 5 minutes at 25°C, 20 minutes at 46°C, 1 minute at 95°C and then held at 4°C. The generated cDNA was then diluted with 80µl

nuclease-free water to give a total sample volume to 100µl. 10µl of each of these samples was then pooled to give the highest concentration standard. This standard was then serially diluted 1:5 in nuclease-free water to produce a total of 6 standards. Experimental samples were then further diluted 1:10 in order to ensure that samples lay within the range of the standard curve. qPCR was carried out using a Prime Pro 48 machine (Techne) and KAPA SYBR Fast qPCR reagents (KAPA Biosystems). Each sample well had a total volume of 12.5µl, consisting of 6.5µl KAPA SYBER master mix, 0.5µl forward primer, 0.5µl reverse primer, 2.25µl nuclease-free water and 2.5µl cDNA. Plates were sealed, vortexed and centrifuged briefly before placing in the Prime Pro 48. Plates were initially heated to 95°C for 2 minutes, before cycling between 5 seconds at 95°C and 30 seconds at an empirically determined annealing temperature (see below) for 40 cycles. A melt curve was then determined by heating to 95°C for 15 seconds, 55°C for 15 seconds before returning to 95°C for a further 15 seconds. Data was analysed using the Prime Pro Study software, using the determined thresholds. Wells with unexpected melting curves were excluded at this stage. All remaining samples were then compared to the standard curve in order to determine relative mRNA quantity. All quantities were subsequently normalised to RNS18 quantity.

Sequences and annealing temperatures for all primers used were as follows:

PER1 Forward – CACCACTGCCGATCTAAAGC

PER1 Reverse – TCGAGGGGAGAATACTGGGA - 59°C

PER2 Forward – CCTACAGCATGGAGCAGGTTG A

PER2 Reverse – TTCCCAGAAACCAGGGACACA - 58°C

RNS18 Forward – CGCCGCTAGAGGTGAAATTC

RNS18 Reverse – TTGGCAAATGCTTTCGCTC - 58°C

2.3.6 Isolation of cellular fractions

In order to obtain separate nuclear and cytoplasmic fractions, confluent cells in 60mm dishes were scraped in 1ml ice-cold PBS, transferred to an ice-cold 1.5ml microcentrifuge tube and centrifuged at 200xg at 4°C for 5 minutes. The supernatant was discarded and the resulting pellet resuspended in 50 µl Gentle Lysis Buffer (0.5% NP40, 0.14M NaCl, 10mM Tris-HCl (pH 8.0), 1.5mM $MgCl_2$ and 10mM EDTA) and incubated on ice for 5 minutes. Samples were then centrifuged for 5 minutes at 410 x g and the supernatant removed and set aside. The pellet was then resuspended in a further 50µl gentle lysis buffer and centrifuged for a further 5 minutes at 410 x g. The supernatant taken here was added to the previously removed supernatant and is the cytoplasmic fraction. The remaining pelleted nuclei were resuspended in 50µl gentle lysis buffer. Fractions were then processed using the RNAeasy mini kit (Qiagen) as per manufacturers instructions.

2.3.7 qPCR primer design and optimisation

Primers for qPCR were designed using Primer3 (Untergasser et al. 2012) to be 20bp in length and to flank regions of approximately 150bp within the mRNA of interest. Preference was given to primer pairs that spanned an exon

junction. Specificity of primer pairs was confirmed by checking primers against appropriate libraries in the NCBI Basic Local Alignment Search Tool (BLAST®). Primers were synthesised in a desalted form by Sigma Aldrich. Optimised annealing temperatures were determined empirically by making up multiple wells as for qPCR with cDNA known to contain the mRNA of interest. Wells were then subjected to temperature cycles as for qPCR, with a gradient of annealing temperatures around the predicted annealing temperature (NEB Tm Calculator, New England Biosciences) in 2°C steps. Following PCR, samples were run on a 0.8% agarose E-Gel® DNA gel (Thermo Fisher) using an E-Gel® iBase™ (Thermo Fisher). The annealing temperature that produced the highest quantity of single product was chosen as the annealing temperature for qPCR.

2.3.8 qPCR for miRNA

In order to perform qPCR for miRNA, cells were harvested in 350µl RLT as for mRNA and miRNA isolated using an RNAeasy miRNA isolation kit (Qiagen) as per the manufacturers protocol. On column DNase digestion was not performed. cDNA was generated using the miScript II RT kit (Qiagen). A total reaction volume of 20µl consisted of 4µl HiSpec Buffer, 2µl miScript nucleics mix, 2µl reverse transcriptase mix and 500ng RNA, made up to volume with nuclease-free water. Samples were the incubated at 37°C for 60 mins, followed by 5 minutes at 95°C. Samples were then kept on ice whilst they were made up to a volume of 100µl with nuclease-free water. Pooled standards and further dilution of samples was performed as for qPCR for

mRNA. qPCR was performed using the miScript SYBR green PCR kit. Wells consisted of 5µl QuantiTect SYBR green PCR master mix, 1µl miScript Universal primer, 1µl Primer Assay, 1ng cDNA, made up to 10µl with nuclease-free water. The plate was then sealed, vortexed and centrifuged briefly before placing in the Prime Pro 48 qPCR machine. Wells were then subjected to 15 minutes at 95°C, followed by 40 cycles of 15 seconds 94°C, 30 seconds at 55°C and 30 seconds at 70°C. A melting step was also performed as above. Results were analysed and outliers excluded using the Prime Pro Study software, as above. All values were then normalised to RNU6 and SNORD6.

2.3.9 Transient knockdown of mRNAs

Knockdown of mRNA was performed using the appropriate ON-TARGETplus siRNA SMARTpool (Dharmacon). Cells were transfected using HiPerFect transfection reagent (Qiagen) in a fast-forward transfection protocol in 24-well plates. Briefly, each well of a 24-well plate was filled with 100µl Opti-MEM®, supplemented with 5nM microRNA inhibitor and 3µl HiPerFect transfection reagent. Cells in 500µl complete medium were then seeded in to these wells at a density of $3x10^6$ cells per well and plates incubated for 20 hours at 37°C. Medium was then changed and cells were maintained in temperature cycles for 72 hours before changing to experimental conditions.

2.3.10 Transient knockdown of miRNAs

Knockdown of miRNAs was performed using miRCURY LNA™ microRNA Inhibitors and miRCURY LNA™ microRNA Power Inhibitors (Exiqon). Cells were transfected using HiPerFect transfection reagent (Qiagen) using a fast-forward transfection protocol, as described above. Cells were subjected to temperature cycles for 48 hours before being changed in to experimental conditions as previously described.

2.3.11 Polyribosome Fractionation

To obtain polysome fractions, cells were grown to confluence in a 125cm^2 flask. Immediately prior to harvesting, cells were incubated with 100µg/ml cycloheximide for 5 minutes at 37°C. Cells were then placed on ice and washed twice with 10ml ice-cold PBS containing 100µg/ml cycloheximide. Cells were then scraped in 5ml ice-cold PBS with 100µg/ml cycloheximide and centrifuged at 200 x g at 4°C for 5 minutes. The resultant pellet was resuspended in 425µl hypotonic buffer (5mM Tris-HCl, 2.5mM $MgCl_2$, 1.5mM KCl, 1x protease inhibitor cocktail (Roche)). 5 µl 10 mg/ml CHX, 1 µl of 1 M DTT and 100 units of RNAse inhibitor (ThermoFisher) were added and the mixture vortexed for 5 seconds. Triton X-100 and sodium deoxycholate were added to total 0.5% of each and vortexed again for 5 seconds. The lysate was then centrifuged at 16,000 x g at 4°C for 7 minutes and the pellet discarded. The remaining supernatant was made up 750µl using RNA-free water and added to 750µl Trizol. 500µl of sample was then loaded on to pre-poured sucrose gradients (5-50% sucrose in H_2O with 200 mM HEPES, 1 M KCl, 50

mM $MgCl_2$, 100µg/ml cycloheximide, 1x protease inhibitor cocktail and100 units/ml RNase inhibitor). The gradients were then ultracentrifuged at 222,228 x g for 2 hr at 4 °C using SW41Ti rotor in 'low brake' mode. Following centrifugation, the samples were separated in to 10x 1ml fractions using a fraction collector with simultaneous detection of UV absorbance at 254 nm.

2.3.12 $NADP^+$:NADPH ratio

Assays to determine $NADP^+$:NADPH ratio were performed using the $NADP^+$/NADPH-Glo(TM) Assay (Promega) as per manufacturer's instructions. 250 μM diamide was used as a positive control.

2.4 Bioluminescent Recording

2.4.1 Photon Multiplier Tube (PMT) recording set up

Recordings of cells or SCN slices within 35mm dishes were made using the LumiCycle® 32 (Actimetrics). Here, 4 photomultiplier tubes are used to record from 32 dishes, with each recording from 8 individual dishes. Recordings were made in 108 second bins every 15 minutes. Conditions were maintained at constant 37°C and ambient by housing the LumiCycle® 32 within a light-tight incubator which was not humidified.

2.4.2 EMCCD Camera Recording

Recordings of any dish or plate size were made using an ALLIGATOR (Cairn Research). Here, a New Brunswick Galaxy 170R (Eppendorf) was adapted with a top camera port. Both Hamamatsu ImagEM and Andor iXon Ultra

EMCCD digital cameras were used. Imaging time ranged between 10 minutes and 1 hour as required.

2.4.3 Luminescence Microplate Reader

Recordings from cells in 96-well plates were made using CentroPRO LB 962 Microplate Luminometer. Recording time was 37.5 seconds per well per hour. Cells were maintained at constant 37°C by housing the plate reader within a light-tight incubator which was not humidified.

2.5 Data Analysis

2.5.1 Circadian analyses

Bioluminescent traces of cells were fitted with damped cosine waves using the following equation:

$$y = (mx) + C + amplitude*exp(-k*x)*cos(((2*pi*(x-phase))/period))$$

where y is the signal, x the corresponding time, amplitude is the height of the peak of the waveform above the trend line, k is the decay constant (such that 1/k is the half-life), phase is the shift in x relative to a cosine wave and the period is the time taken for a complete cycle to occur (Hirota et al. 2008).

This enables an estimation of period, amplitude and phase to be made, with goodness-of-fit determined using R^2 values.

Bioluminescent signal is given as relative light units (RLU) or counts per second (cps) as appropriate.

SCN analysis was performed using BioDare (Zielinski et al. 2011).

2.5.2 Statistics

Data is presented as mean +/- SEM, and statistical significance of mean differences determined using student's t-test or ANOVA as appropriate. Statistical analyses were performed using Graphpad Prism. P values are reported using the following symbolic representation: ns = $p>0.05$, * = $p\leq0.05$, ** = $p\leq0.01$, *** = $p\leq0.001$, **** = $p\leq0.0001$.

Chapter 3: Development of a system for perfused cell culture

3.0.1 Cell culture for circadian experimentation

The methodology for maintaining cell cultures *ex vivo* or *in vitro*, commonly known as tissue or cell culture, has been in use for a little over a century (Harrison 1912) and has become an extremely widely used laboratory technique, as it confers a number of advantages over work *in vivo*. Firstly, it limits the need to use live animals, thereby reducing the time and financial costs associated with maintaining an animal colony. Secondly, cells have a far faster generation time than animals, allowing for vastly increased throughput of study. Thirdly, use of cells in culture can allow for the closer study of certain processes in isolation, without the conflicting humoural or neuronal cues and associated variability that occur within a living animal. Instead, it is possible to control the extracellular environment, through the use of well-defined media conditions and constant temperature.

However, *in vitro* culture does possess limitations. For example, cells are constantly metabolising components of the extracellular media. As in tissue culture, unlike *in* vivo, there is no means of clearing and replacing these media components, media composition will change over time. This means that cells no longer experience truly constant extracellular conditions if maintained in culture media for prolonged lengths of time. As a large number of media components, by their very nature, are essential for the maintenance of cellular health and viability, it is quite possible that changes in their levels in

the extracellular media could impact upon experimental results achieved under these conditions.

This is of particular relevance when wishing to investigate circadian timekeeping *in* vitro. As media change is associated with resetting of the cellular molecular clock, cells for circadian experimentation are maintained in the same media for weeks at a time. This means that changes in the extracellular environment of these cells have the potential to be highly significant. This problem can potentially be solved through use of techniques that allow for clearance and renewal of cellular media in a physiological manner. One candidate for this technique is microfluidic culture.

3.0.2 Microfluidics

Microfluidics is concerned with the movement of small volumes of a fluid within a contained, often artificially manufactured, space. In the context of experimental cell biology, microfluidic systems can be used as cell culture technique. The use of such systems has grown steadily over the almost two decades since the methodology was first described for tissue culture (Tilles et al. 2001), and has been employed in applications as wide ranging as toxicity assays, migration assays and organoid culture. However, it is still by no means a common cell culture method. This is possibly due in part to the relative novelty of the technique compared to traditional cell culture methods, but also possibly due to the myriad challenges faced when attempting to design new microfluidic devices and experiments, such as appropriate cell

adhesion, mechanics of flow and maintenance of cell viability (Halldorsson et al. 2015).

When well implemented, microfluidic techniques provide a number of advantages over traditional cell culture models. It is possible to more closely mimic the *in vivo* cellular microenvironment in such systems, as they allow for removal and renewal of extracellular media components. This comes hand-in-hand with the capacity to produce chemical gradients and also the possibility of perfused cell culture. Perfusion of cells in culture is of particular interest, as it allows for downstream analysis of extra cellular media (Croushore et al. 2012), as well as real-time analysis of the cellular response to the environment and environmental changes without the confounding factors associated with media change (Ges & Baudenbacher 2010; Grossmann et al. 2011).

3.0.3 The advantage of perfused circadian cellular experimentation

To date, there have been relatively few published reports of perfused cell culture in a circadian context (Lee et al. 2013; Teng et al. 2013). Indeed, there are no commonly used microfluidic systems that have been demonstrated to be able to sustain viable cells culture under perfused flow for the time periods necessary for circadian experimentation. However, it is clear that development of a reliable perfused system for circadian experimentation would be of great utility to the field for a number of reasons. Firstly, it allows for observation of circadian behaviour of cells and tissues under truly constant

conditions, as the constant removal and renewal of extracellular media is such that the extracellular environment remains constant, thereby removing the variability this produces. In addition, such maintenance of a constant extracellular environment is appreciably more physiologically relevant than standard tissue culture methods, as it mimics the maintenance of the *milieu intérieur* found in vivo.

The second major advantage of a perfused cell culture system for circadian assays is the ability to take repeat measurements from the same population. As further outlined for the metabolomics assay in the next chapter, a number of experimental techniques require sampling of extracellular media. Within a traditional static tissue culture model, sampling of any great media volume is effectively an end-point procedure, due to the disturbance caused to a cell population or tissue by changes in the extracellular environment. As such changes in the extracellular media are sufficient to influence the subsequent phase of the circadian oscillation in cells (Balsalobre et al. 1998), it would in inappropriate to repeatedly sample the same static population for circadian experiments. The solution generally used for this is to have multiple, identically treated populations running in parallel and to sample a number of these at each time point. However, using different dishes does introduce increased variance, which can be sufficient to obscure more subtle longitudinal trends. A perfused tissue culture technique removes this source of technical error, as samples of media can be taken repeatedly from the same population of cells simply by collecting media at from the system outflow.

3.0.4 Challenges

There are number of obstacles to overcome when designing a new microfluidic cell culture system, including some that are specific to the development of a system for study of circadian phenomena. First and foremost, a system for circadian perfused culture must be capable of sustaining a cell population under perfused flow for much longer periods of time than most existing systems: weeks as opposed to the hours currently used for migration or growth assays.

Secondly, as rhythmic activity in cells and tissues can be reset by relatively small changes in extracellular temperature (Buhr et al. 2010), serum (Balsalobre et al. 1998), or glucose (Hirota et al. 2002), to name but three, the conditions within a perfused circadian cell culture system must remain almost entirely constant for the duration of the experiment.

These challenges are in addition to the considerations that must be made when building any microfluidic system for biological use, such as rate of flow, fluid dynamics of the system, cell type, media composition and growth surface.

In this chapter, I discuss the development and optimisation of such a microfluidic system for constantly perfused circadian assays, highlighting both the challenges of constructing such a system, as well some of the many advantages of the functioning technique. I also demonstrate the difference in

experimental result that can be observed when studying cells under perfusion compared with static conditions.

3.1 Results

3.1.1 Experimental approach

A number of factors require optimisation when designing a new microfluidic system, such as flow rate, media composition and cell adhesion surface (Halldorsson et al. 2015). However, as this system has a comparatively low throughput, with a capacity to run a maximum of 9-12 independent chambers at any one time, it is not feasible to test all factors at once. Instead, the system was optimised iteratively, testing only one or two factors at once. Details of the various set-ups tested are given in the table below, with further information about the optimisation of each component given in further detail in the subsequent chapters.

Cell type	Reporter	Chamber	Flow rate, µl/hr	Glucose, g/L	Serum, %	B27, %	Viability	Rhythmicity	Notes
U2OS	Per2:LUC	Kirstall	200	5	10	2	--	--	Cells died within 70 hours
U2OS	Per2:LUC	Kirstall	200	1	10	2	+	--	
U2OS	Per2:LUC	Kirstall	200	1	7	2	--	--	
U2OS	Per2:LUC	Kirstall	200	1	5	2	--	--	
U2OS	Per2:LUC	Kirstall	200	1	2	2	+	+	Rhythmicity not always seen
U2OS	Per2:LUC	Kirstall, no coverslip	200	1	2	2	--	--	Cells dead with 12 hours
U2OS	Per2:LUC	Kirstall	200	1	2	1	+	+	No improvement with low B27
3T3	Bmal1:LUC	Ibidi, 0.2	50	1	2	2	--	--	Channel too shallow
3T3	Bmal1:LUC	Ibidi, 0.4	50	1	2	2	++	--	Lack of rhythms may have been due to inconsistent flow rate
3T3	Bmal1:LUC	Ibidi, 0.6	100	1	2	2	++	+	No improvement with higher flow rate
3T3	Bmal1:LUC	Ibidi, 0.6	50	1	2	2	++	+	
3T3	Bmal1:LUC	Ibidi, 0.6, in series	50	1	2	2	++	+	Use of buffer slide greatly reduces noise
Immortalised Fibroblast	PER2::LUC	Ibidi, 0.6, in series	50	1	2	2	++	++	

Table 3.1

Summary of perfusion conditions tested

Summary table of perfusion conditions tested. Due to low throughput, systems were tested iteratively. Cell viability and rhythmicity were scored by observation as lacking (-), poor (--), fair (+) or good (++).

3.1.2 Initial perfusion setup

As a starting point for the development of a perfused cell culture system, a Quasi Vivo® 500 (Kirstall) system was selected. This system consists of a number of cylindrical polydimethylsiloxane (PDMS) chambers connected with tygon tubing (Figure 3.1A). The inflow tubing has an internal diameter (I.D.) of 1/6", whilst the outflow tubing has an ID of 3/32". The total chamber volume is 2ml. Media was driven through the system using an NE-1600 syringe pump (Figure 3.1B). U2OS cells expressing the Bmal1:LUC reporter were made up to a 200,000 cells/ml suspension in DMEM supplemented with 10% serum and 200μl of this was seeded on to a poly-L-lysine coated coverslip placed at the base of the PDMS chamber. Cells were left at room temperature for 1 hour. A further 500μl supplemented DMEM was added to the chamber, which was then incubated under temperature cycles until required. For bioluminescent recording, chambers were connected to a syringe and pre-warmed air media flushed through the system. The syringe was then connected to a syringe pump and media driven across the cells at a constant flow rate. Cell chambers were maintained at 37°C, at atmospheric CO_2 and O_2 for the duration of the experiment.

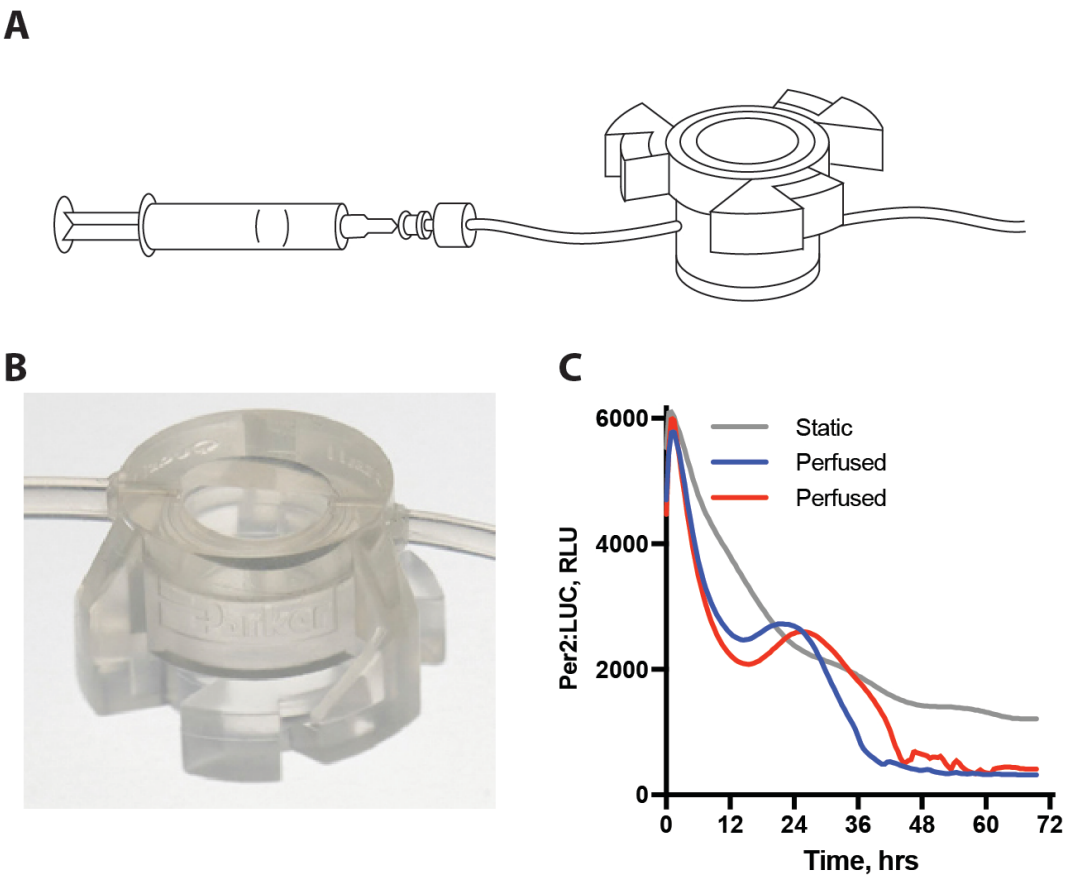

Figure 3.1

Initial perfusion setup

A Schematic diagram of the Quasi Vivo® 500 system. **B** Image of a Quasi Vivo® 500 chamber (image: Kirkstall). **C** Per2:LUC bioluminescence from initial perfusion conditions. Per2:LUC U2OS cells were perfused at 200*µ*l/hr with complete air medium containing 10% HY2 serum (n=2, all replicates shown).

3.1.3 Media composition determines cell survival under perfusion

For initial perfusion experiments, cells were grown to confluence on a poly-L-lysine-coated coverslip and subjected to temperature cycles in PDMS chambers as described above. Cells were perfused with a standard “air medium” (AM) formulation (Hastings et al. 2005). This consists of a stock

solution of Dulbecco's Modified Eagle's Medium (DMEM, Sigma D5030), supplemented with:

- 5 g/L glucose
- 0.35 g/L sodium bicarbonate
- 0.01 M HEPES
- Penicillin/streptomycin (25 mg/L each)

This stock solution was adjusted to pH 7.4 at room temperature. Prior to experimentation, this stock solution was further supplemented with:

- 10 % serum (HyClone™ FetalClone™ II or III as appropriate)
- 2 % B-27® supplement
- 1 % Glutamax
- 1 mM Luciferin

This working solution was then adjusted to an osmolarity of 350mOsm.

As Figure 3.1C shows, perfusion with AM was not comparable with the static control condition. Furthermore, those cells under perfusion ceased to produce a light signal substantially above background at around 48 hours and upon examining the cells under a light microscope after 72 hours, the vast majority of the cell population was dead. The cell monolayer in the static condition remained both alive and intact. This was indicative that the act of perfusion was the cause of cell death, rather than the unusual cell culture conditions.

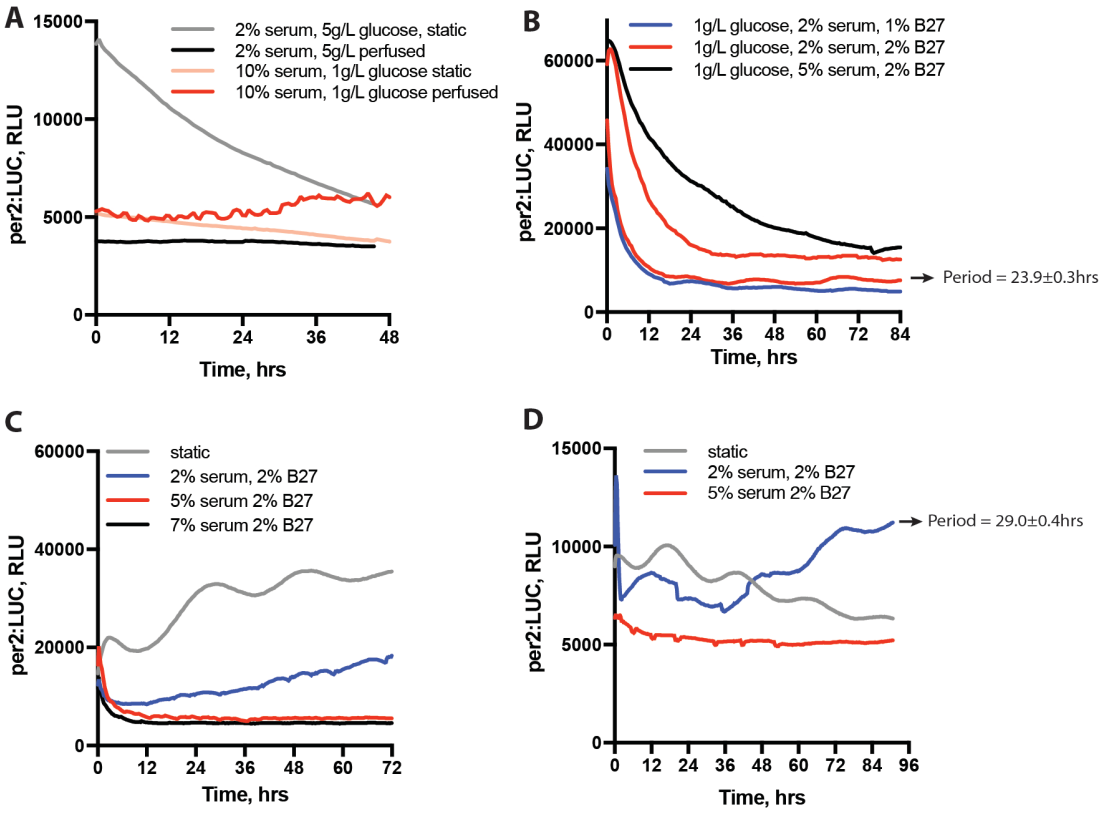

Figure 3.2

Low glucose and serum aid cell survival under perfusion

A Bioluminescence from Per2:LUC U2OS cells under perfusion with either reduced glucose (1g/L vs 5g/L) or reduced serum (2% vs 10%). Flow rate was 200*µ*l/hr (n=2, representative). **B, C, D** Bioluminescence from Per2:LUC U2OS cells all in media containing 1g/L (5.4mM) glucose, with 2, 5 or 7% serum and 1 or 2 % B27. Flow rate was 200*µ*l/hr. Those perfused chambers that showed measurable circadian rhythmicity in bioluminescence have period indicated. Static chambers contain 5% serum (n≥2, representative).

High levels of both glucose and serum are reported to have adverse effects on cellular viability (Risso et al. 2001; Rajah et al. 1999), as well as acute changes in these factors having the capacity to reset the cellular circadian oscillation (Balsalobre et al. 1998; Hirota et al. 2002). It was thus hypothesised that the continual renewal of glucose and serum that occurs

under perfusion might be responsible for the high level of cell death in this condition. To test this, the experiment was repeated with the same setup, but with either the glucose concentration reduced to 1g/L or the serum proportion reduced to 2% (Figure 3.2A). Under these conditions, cells perfused with low glucose media showed increased survival, whilst those that were maintained in high glucose continued to show a high level of cell death, regardless of the level of serum available, suggesting that the high level of glucose was the primary cause of apoptosis in this circumstance. However, reducing the serum concentration in addition to the glucose concentration did allow for observation of cellular rhythmicity over 3 days under perfusion in some, although not all, chambers (Figure 3.2B,D), a feature not observed at higher serum levels. It is plausible that this is a result of continual resetting of the cellular circadian oscillation at higher serum concentrations. Reducing the concentration of cell culture supplement B-27®, a product that was initially designed as a serum-replacement, did not result in a clear improvement in cell survival or circadian gene expression.

These changes to the medium used for perfusion result in a formulation much closer to the original formation of Dulbecco's Modified Eagle's Medium (Dulbecco & Freeman 1959). Furthermore, the glucose concentration in this lower glucose media (5.4mM) lies well within the normal range for mammalian blood sugar levels, making this a much more physiologically relevant condition, as it more closely represent the milieu intérieur that cells experience *in vivo*. However, despite these changes, the ability to observe

rhythms in reporter gene expression in perfusion was highly inconsistent, for reasons discussed later in this chapter (Figure 3.2C,D).

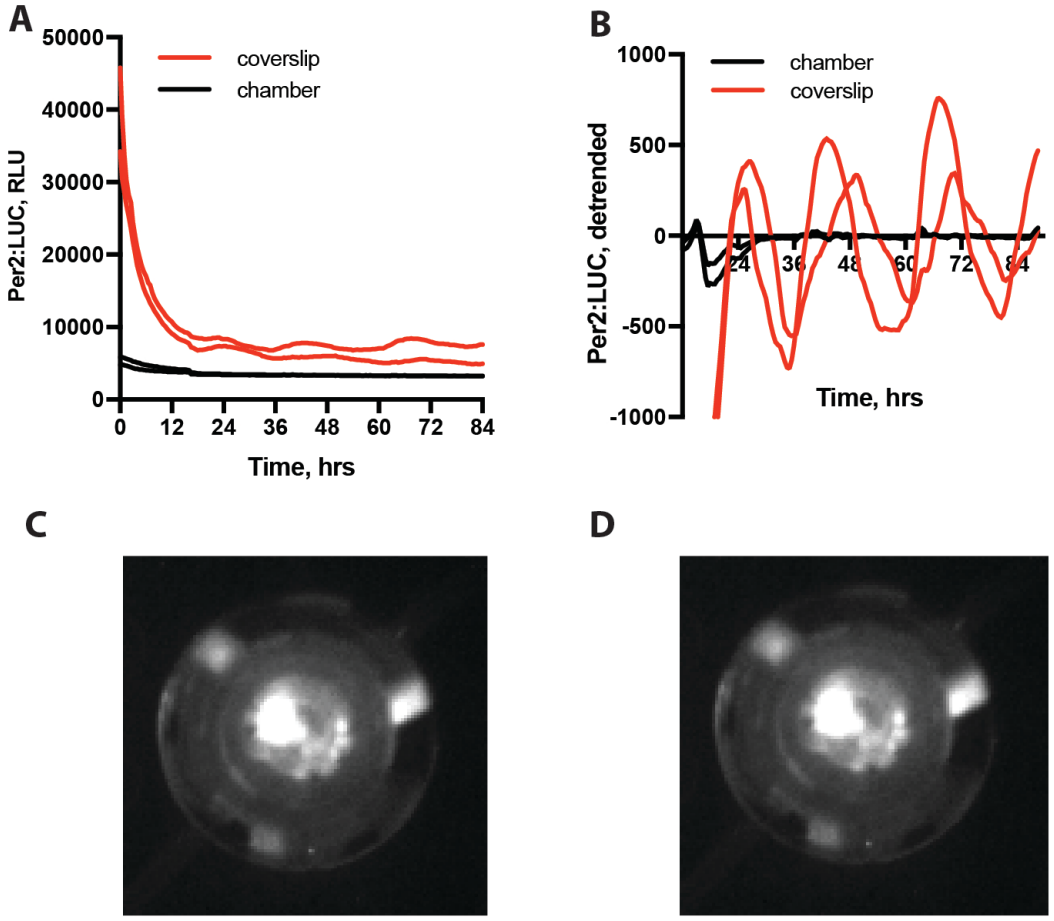

Figure 3.3

Cell viability on PDMS and poly-l-lysine

A Bioluminescence from perfused Per2:LUC U2OS cells grown either directly on to PDMS or on poly-l-lysine coated glass coverslips. Media conditions were 2% serum, 2% B27, 1g/L glucose. Flow rate was 200µl/hr. **B** 24-hour de-trended (n=3, representative). **C,D** Representative images demonstrating uneven bioluminescence due to cell death on coverslips in kirkstall chambers.

3.1.4 Cell culture surface influences robustness under perfusion

A large proportion of microfluidic cell culture devices are made from polydimethylsiloxane (PDMS). This form of silicone is particularly popular as a result of the ease with which it can used to make microfluidic chambers using a technique known as soft lithography (Halldorsson et al. 2015). It is also transparent and has a low autofluoresence, making it attractive for bioluminescence assays. In addition, the surface is thought to be relatively biocompatible. It was therefore attempted to culture cells directly on the PDMS surface of the Quasi Vivo® chambers, rather than on coverslips (Figure 3.3A). Although cells initially formed a confluent monolayer on this surface, their expression of circadian reporter constructs was low. Furthermore, after several days under perfusion, most cells were no longer viable. In contrast, cells grown in parallel on poly-L-lysine cover slips were still viable and showed far higher basal circadian reporter expression, as well as circadian variation in the expression of these reporters in some chambers.

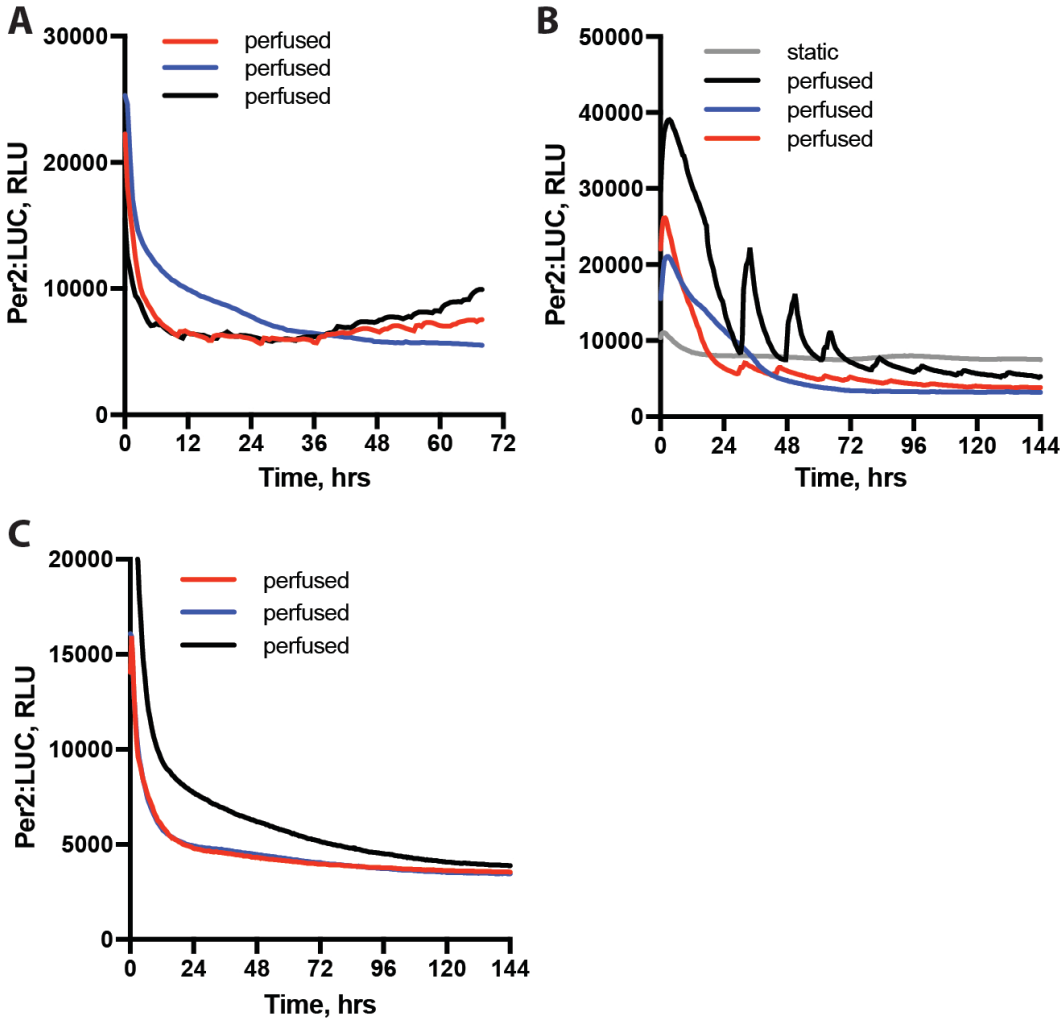

Figure 3.4

Variable rate of flow affects expression of reporter genes

A Bioluminescence from Per2:LUC U2OS cells perfused at 200*µ*l/hr with an NE-1600 syringe pump (n=3, all replicates shown). **B** Bioluminescence from Per2:LUC U2OS cells perfused at 200*µ*l/hr with a Harvard PHD ULTRA™ syringe pump (n=6, representative). **C** Bioluminesence from Per2:LUC U2OS cells perfused at 200*µ*l/hr with a NE-1600 syringe pump following drive-screw lubrication (n=3, all replicates shown). All cells were perfused with media containing 1g/L glucose, 2% serum and 2% B27.

3.1.5 Maintenance of constant rate of flow

As outlined in the introduction to this chapter, one crucial feature required for a system for perfused circadian assays is a constant extracellular

environment. In order to obtain this in a system under flow, it is therefore important that the rate of flow of media across the cells remains as constant as possible. If instead, flow rate of media across the cellular monolayer is variable, it is possible that acute changes in the cellular microenvironment might stimulate gene expression that masks or inhibits circadian gene expression under true constant conditions. This was observed to be the case to a greater or lesser extent in a large number of perfused experiments (Figure 3.4A,B), although the effects observed on circadian reporter gene expression were highly variable even within the same experiment.

However, a number of experiments showed the same pattern of acute reporter changes in multiple replicates, although at different amplitudes (Figure 3.4B). This was indicative of a systematic problem with the setup, rather than chamber or tubing specific issues, which would not be expected to show the same timing of effect across more than one chamber. As each cell culture chamber exists independently of any others in the same experiment, the only common element between different chambers is the syringe pump driving the media through the system, which can drive up to six syringes simultaneously. We can therefore assume that systematic fluctuations in flow rate occur primarily as a result of an uneven rate of syringe compression, most likely due to an uneven rate in the turning of the drive-screw. To counteract this, the drive screw was lubricated with a silicone grease (Super Lube®). This eliminated acute changes in gene expression when using the Quasi Vivo® system, although it did not necessarily increase the frequency

with which circadian oscillations in reporter gene expression was observed (Figure 3.4C).

3.1.6 Laminar and equal flow

Another important consideration when designing perfused system is the nature of fluid flow through the system. In order for extracellular conditions to remain as constant as possible, flow through the system, and particularly across the cellular monolayer should be laminar, as the eddies produced by turbulent flow might lead to an uneven extracellular microenvironment. Whether or not flow through a system will be laminar can be predicted by calculation of its Reynold's number, defined as:

$$Re = \frac{Q D_H}{\upsilon A}$$

where Re is the Reynold's number, Q the volumetric flow rate (m^3/s), D_H the hydraulic diameter (m), v the kinematic viscosity (m^2/s) and A the cross sectional area (m^2) of the channel or duct (Stokes 1922). Generally, a Reynold's number of greater than 2000 is indicative of turbulent flow, although there is a transitional range slightly below and slightly above this number. If we assume the kinematic viscosity of cell culture media to be comparable to that of water at 37°C, then the Reynold's number of the tubing of the perfusion system can be calculated using the following values:

$$Q = 2\times10^{-7}, \qquad D_H = 1\times10^{-3}, \qquad \nu = 6.96\times10^{-5}, \qquad A = (5\times10^{-4})^2\pi$$

This gives a Reynold's number of 365.8, well within the range for laminar flow.

This model of flow breaks down when one considers the structure of the Quasi Vivo® chamber, which sits as a cylinder at 90° to the direction of flow, with a diameter of 15mm and a height of 10mm (Fig 3.1). Modelling the flow in and around such a chamber could easily constitute another thesis in its own right, but given it's non-linear shape, it is certain that the flow within such a chamber would not be of an equal rate at all points within the chamber and may well also not be laminar. This may account for some of the uneven areas of cell death observed in a number of perfusion experiments (Fig 3.3C,D). Furthermore if, as proposed in the introduction, one wishes to use such a perfused system to collect media outflow samples that correspond to discrete time intervals, then it is crucial that flow through the chamber occurs at a similar rate at all points, which is not possible with this chamber shape.

In order to solve this problem, the Quasi Vivo® 500 chambers were substituted with Ibidi μ-slide I luer chambers and the tygon tubing used with this system replaces with 1mm I.D ETFE tubing (Figure 3.5A,B). These chambers consist of a 5mm wide, 50mm long channel, are gas permeable and are available in a number of different depths. The inside of the channel is not coated, but the plastic is texturized in order to aid cell adhesion. Given the simple internal shape of these chambers, it is easy to calculate a Reynold's number for these chambers. Depending on depth, Re rages from 65.4 to 196 when the flow rate is 100μl/hr, well within the range for laminar flow.

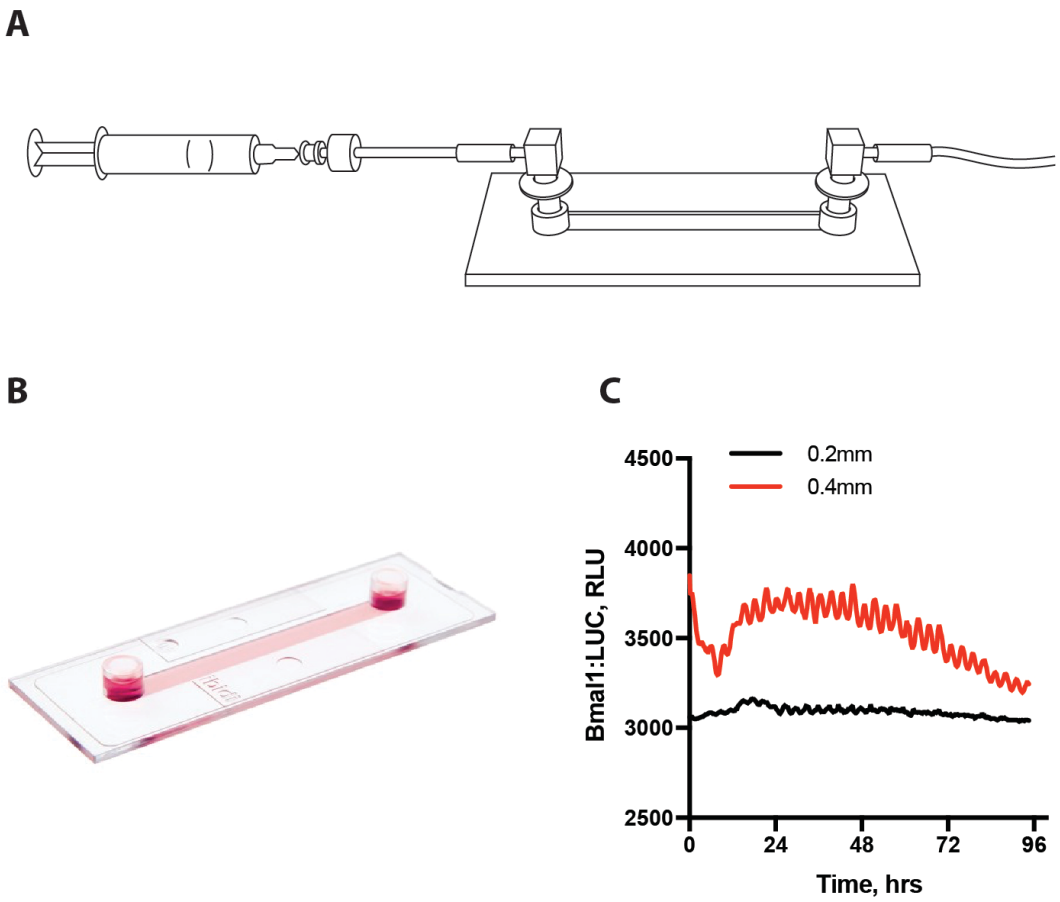

Figure 3.5

Depth of chamber influences cell tolerance of perfusion

A Schematic diagram of the ibidi chamber system .**B** Image of an ibidi *μ*-slide (image: ibidi). **C** Bioluminescence from Bmal1:LUC 3T3 cells seeded in ibidi *μ*-slide I luer channels of 0.2 and 0.4 mm depth (n=3, representative). Media contained 1g/L glucose, 2% serum and 2% B27. Flow rate was 50*μ*l/hr

Upon initial testing with these chambers, it was noted that cell survival and circadian reporter gene expression was much improved in chamber with a depth of 0.4mm or greater when compared to chambers of 0.2mm depth (Figure 3.5C). Given that fibroblasts are generally 10-15*μ*m in diameter, it is possible that seeding cells within these chambers significantly affected or even obstructed flow within the system, with the resulting sheer stress

contributing to greater cell death. As such, chambers with a depth of 0.6mm were chosen as being optimal for this system.

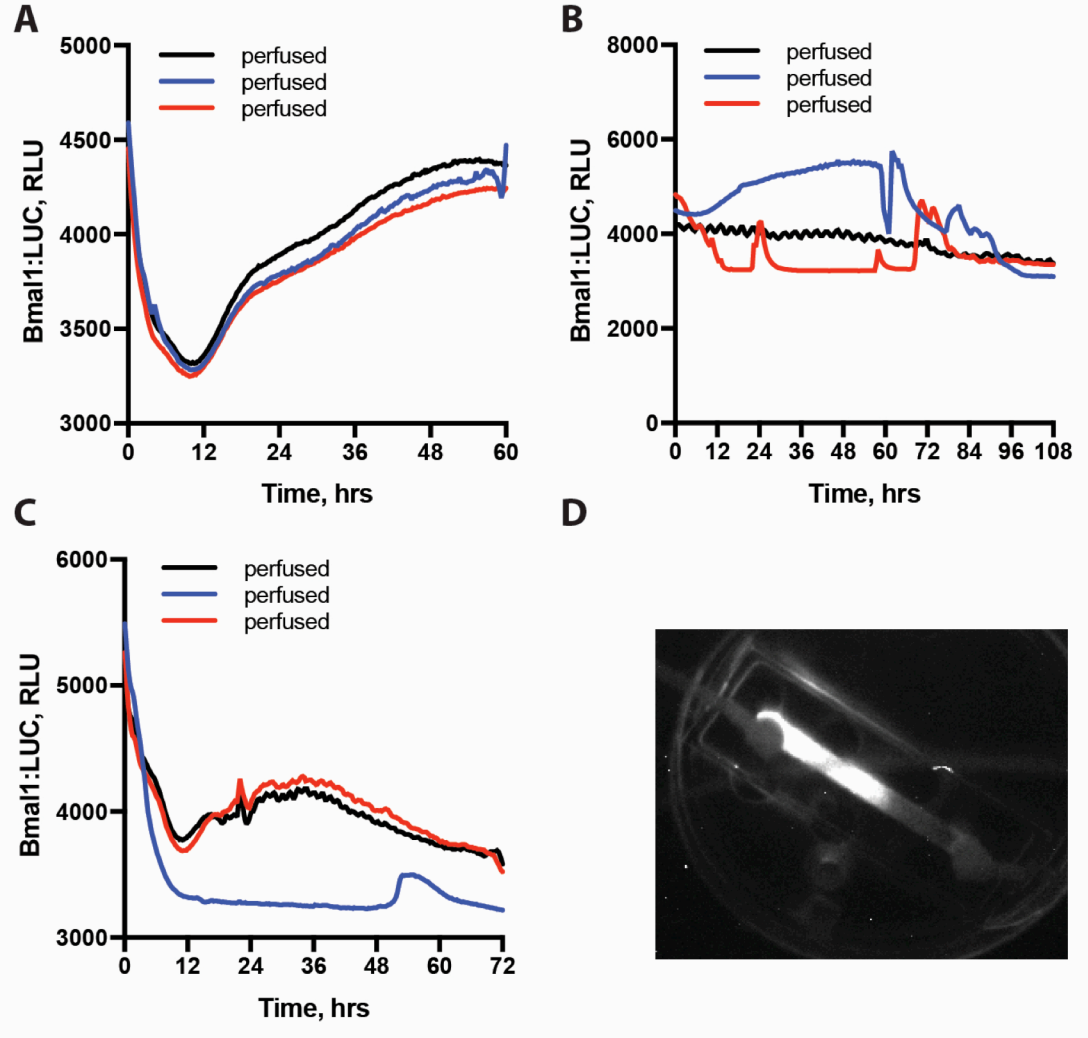

Figure 3.6

Unequilibrated media and bubbles affects reporter expression

A,B,C Bioluminescence from Bmal1:LUC 3T3 cells grown in ibidi *μ*-slide I 0.6 luer channels. Cells were perfused with media containing 1g/L glucose, 2% serum and 2% B27 at 100*μ*l/hr (n=9, all replicates shown). **D** Image showing uneven bioluminescence along the length of an ibidi slide.

3.1.7 Introduction of a gas permeable bubble trap

The use of the *μ*-slide chambers greatly reduced variability in the bioluminescent signal between different chambers within the same

experiment (Figure 3.6A). However, a number of experiments showed acute changes in reporter gene expression. Often, these changes were not comparable between different chambers (Figure 3.6B,C). Unlike the earlier flow rate variability, which was solved through greater lubrication of the syringe pump drive-screw, these changes were suggestive of variations in flow that were specific to each chamber, possibly as a result of individual variations in the chambers or tubing. Close observation of the raw data images of these experiments showed that those chambers that showed acute changes in reporter expression often did so after a bubble of air passed through the chamber. It was also observed that there was some variability in the brightness of cells along the length of the cell culture chamber (Figure 3.6D). As the media within the system has not been previously oxygenated at the same temperature and partial pressures as the incubator in which the cells are contained, it was hypothesised that this difference in brightness might be the result of varying partial pressures of oxygen along the length of the gas-permeable chamber. In order to try to both prevent bubbles from reaching the cell culture chamber and to equilibrate the perfusion media with the temperature and pressures inside the experimental incubator before passing across the cells, a new setup was devised which ran two ibidi μ-slide in series (Figure 3.7A), the idea being that the first slide acts as a gas-permeable bubble trap, to equilibrate media to atmospheric gas concentrations and to prevent bubbles from entering the rest of the perfusion system. Although for most experiments this first chamber does not contain any cells, seeding cells in both chambers and measuring the bioluminescence

produced provides a visual indication of how well this buffering slide works, with cells is the second slide (slide 2) showing dramatically less acute variation in bioluminescence than those cells in slide 1 (Figure 3.7B).

3.1.8 Cell type-specific tolerance of perfusion

All initial perfusion experiments were performed using either U2OS or later, NIH 3T3 cell lines, stably transfected with firefly luciferase under the control of either the *Bmal1* or *Per2* promoter. These lines were selected for the clear circadian rhythmicity they display in expression of these reporters and also for their ability to contact-inhibit, allowing them to remain confluent in culture for the long periods of time required for circadian assays. It is important to remember that the reporters used here are reporters of the transcriptional activity of these genes and are not necessarily reflective of the relative abundance of their associated proteins.

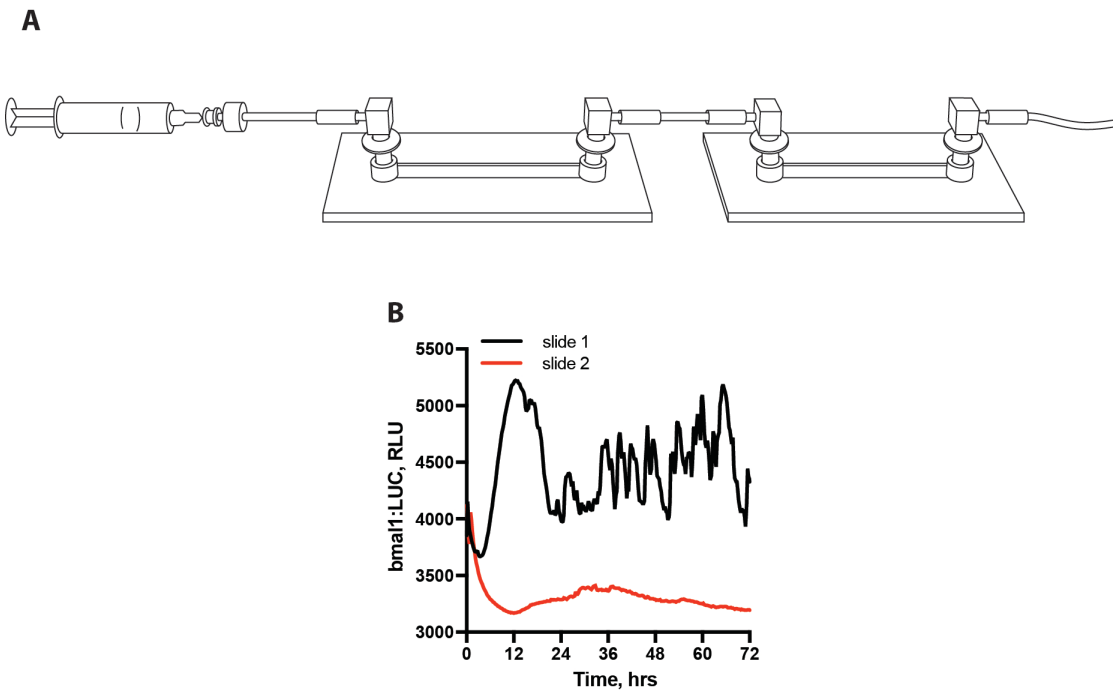

Figure 3.7

Buffer devices can eliminate variable flow rate

A Diagram of the perfusion system with ibidi *μ*-slides connected in series. The first of these slides acts as a buffer slide. **B** Bioluminescence from Bmal1:LUC 3T3 cells in ibidi *μ*-slide I 0.6 luer channels connected in series, as in A. Slide 1 indicates the slide nearest to the syringe (n=4, representative).

In contrast, using cells derived from the PER2::LUC mouse (Yoo et al. 2004), where luciferase is fused directly to the endogenous PER2 protein, it is possible to infer information about the translation and abundance of PER2 protein from the bioluminescent signal given off by these cells. When immortalised fibroblasts derived from the PER2::LUC mouse were cultured under perfusion at a flow rate of 50 *μ*l/hr in the perfusion setup outlined in Figure 3.7A, the oscillations in bioluminescence had an appreciably larger relative amplitude and showed substantially less noise than in the two transcriptional reporter lines (Figure 3.8A, B).

There are two potential reasons as to why observation of rhythmicity under perfusion is appreciably clearer when using cells expressing PER2::LUC. The first is simply that untransformed fibroblasts are more amenable to healthy culture under perfusion, possibly because this more closely reflects environment *in vivo*. In contrast, U2OS and 3T3 cells are transformed lines, which have been grown using traditional cell culture methods for over 100 passages, which may well have been inadvertently selected for survival under static conditions over perfusion.

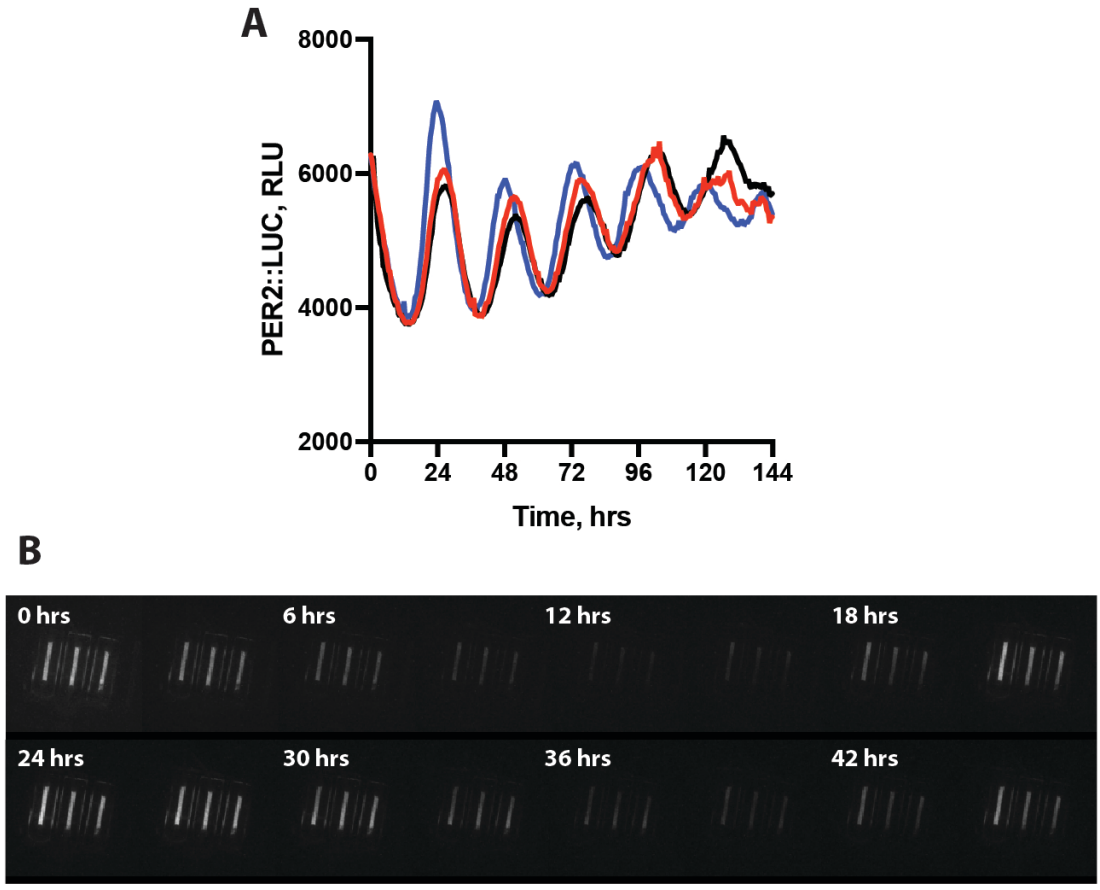

Figure 3.8

Final perfusion setup

A Bioluminescence from immortalised PER2::LUC fibroblasts perfused with media containing 1g/L glucose. 2% serum and 2% B27 at 50 μl/hr (n=3, all replicates shown). Period=24.9±0.8. **B** Series of images of cells under perfusion from A taken over 50 hours showing clear variation in bioluminescence.

Alternatively, it is possible that the nature of the circadian reporter is important in explaining the difference in bioluminescent oscillations observed between the PER2::LUC fibroblasts and the U2OS and 3T3 lines. Anecdotally, it has been noted that smaller changes in the external environment are required perturb reporter expression in cells expressing the transcriptional reporters than in the translational reporter PER2::LUC line. Circadian gene expression is regulated post-transcriptionally by a number of mechanisms (Kojima et al. 2011; Chen et al. 2013), so it may be the case that these extra mechanisms of regulation, not all of which will be capable of regulating expression of the transcriptional reporters but will regulate PER2::LUC, provide increased robustness against acute, non-circadian changes in transcription of these circadian genes. Given that small acute changes in the cellular environment are clearly possible within a perfused cell culture system, it might be that translational reporters are better suited to accurately reporting cellular circadian state under such conditions.

3.1.9 Optimised perfusion conditions

As a result of all of the iterative optimisation steps described above in detail, the final setup for perfused circadian cell culture, and the system used for all further experiments in this chapter, is:

Cell culture media

Stock:

- DMEM (5030)

- 1 g/L glucose
- 3.7 g/L sodium bicarbonate
- Penicillin/streptomycin (25 mg/L each)

Working solution (Perfusion Air Medium, PAM):

- 2 % serum (HyClone™ FetalClone™ III)
- 2 % B-27® supplement
- 1 % Glutamax
- 1 mM Luciferin

Maintained in an incubator at 37°C with atmospheric oxygen and 5% CO_2.

Depending on experimental requirements, it is also possible to use HEPES-buffered stock media. In this case, DMEM is supplemented with only 0.35g/L and with an additional 0.01M HEPES. The incubator used in these conditions must be set to atmospheric CO_2 levels.

Perfusion system

Pump: NE-1600 syringe pump

Tubing: 1 mm I.D. ETFE tubing. Connection to luer fittings with 1 mm I.D silicone tubing

Connectors: All connections were made with luer fittings

Chambers: Ibidi μ-slide I, 0.6

Flow rate was 50 µl/hr.

Experiments were run using immortalised PER2::LUC lung fibroblasts in a specially adapted ALLIGATOR, and imaged using an EMCCD camera.

Technical protocol

Cells are grown to confluence in ibidi µ-slides and synchronised using temperature cycles. Prior to experimentation, all tubing and buffer slides are flushed with 70% ethanol, sterile water and phosphate buffered saline (PBS) and connected up in the experimental configuration. The µ-slides containing cells are then changed in to the experimental media and the tubing flushed through with the same media. The µ-slides containing cells are then connected up with all tubing and the buffer slides and the whole system is flushed with approximately 1 ml of media. The entire system is then transferred to the experimental incubator or ALLIGATOR and the syringe fixed within the syringe pump. The entire system is flushed again with a further 1-2ml of media, ensuring no bubbles remain within the tubing or slides, before the flow rate is set at 50µl/hr and recording initiated.

3.1.10 Comparison of perfused and traditional cell culture methods

As with the development of any new technique, it is of interest to consider how results achieved under perfusion compare against equivalent experimental conditions under static cell culture. Figure 3.9A compares the effect of culturing cells in pyruvate rather than glucose (replicated from Figure

4.6) in either static culture or under perfusion. It is clear that the rapid damping of PER2 expression observed in the static pyruvate condition is not replicated in cells treated with pyruvate under perfusion. Furthermore, analysis of the circadian period of cells under these conditions shows that the ~2 hr increase in period observed in the static pyruvate condition is not replicated in the perfused pyruvate condition, which does not exhibit a period that is significantly different from either of the glucose-treated conditions. It is of note here that the cells under perfused conditions are exposed to a lower absolute concentration of pyruvate than those in static conditions, with the concentration of pyruvate used being equivalent to the amount of glucose used in both conditions. However, it is not possible to discount the possibility that the differing effects observed between the two set-ups is the result of the difference in concentration, rather than the effect of perfusion itself.

Similarly, PF670462 is a well-characterised inhibitor of casein kinase 1 (CK1) and is widely documented to greatly increase the period of the circadian oscillation (Meng et al. 2010). In cells maintained in static culture, 3μM PF670462 increases circadian period to over 60 hours. However, when the same concentration of inhibitor is applied to cells under perfusion, the increase in period is significantly reduced to slightly less than 29 hours (Figure 3.10A,B). Interestingly, this is much closer to the behavioural period observed in when animals are treated with PF670462 *in vivo* (Meng et al. 2010).

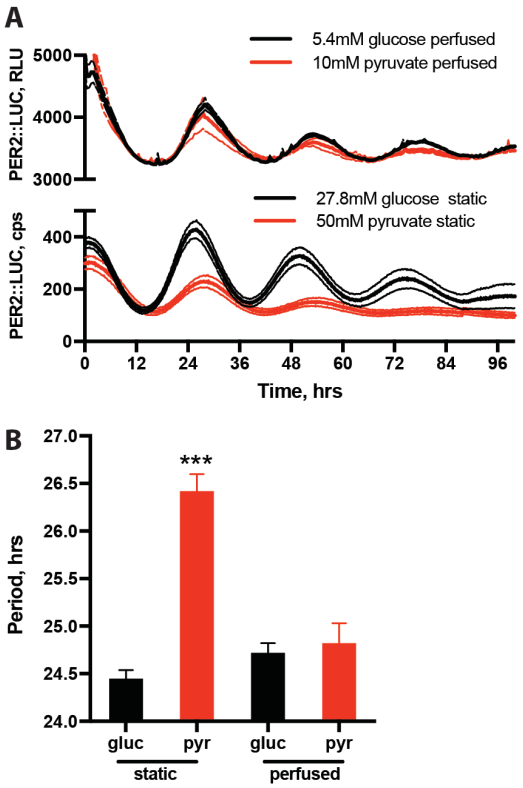

Figure 3.9

Perfusion with pyruvate

A Bioluminescence from PER2::LUC fibroblasts under perfusion and in static conditions with either glucose or an equivalent concentration of pyruvate (n=3, mean±SEM). **B** Analysis of period following fitting to a damped cosine wave (extra-sum-of-squares F test vs a straight line $p<0.0001$,Two-way ANOVA, Tukey's multiple comparisons test).

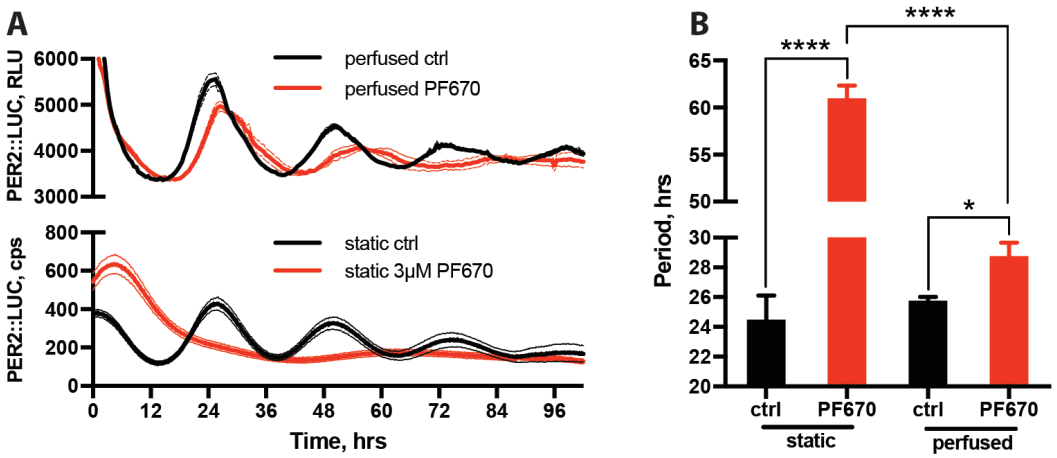

Figure 3.10

Perfusion with ck1δ inhibitors

A Bioluminescence from PER2::LUC fibroblasts under perfusion and in static conditions with 3μM CK1 inhibitor PF670462 (n=3, mean±SEM).

B Analysis of period difference between perfused and static conditions with and without CK1 inhibition (extra-sum-of-squares F test vs a straight line $p<0.0001$, Two-way ANOVA, Holm-Sidak's multiple comparisons test).

3.1.11 Modification of the perfusion system

A basic setup for perfused circadian tissue culture has been described above, but the system possesses a huge amount of flexibility, with potential for many modifications. For example, it is possible to collect the media outflow from the system for further analysis – as in Figure 4.13, either manually or through use of a fraction collector. Alternatively, as shown in Figure 5.5, it is possible to deliver timed boli of treatments to cells under perfusion without disrupting the rate of flow. This allows for observation of the effect of acute perturbations without the confounding effects of serum shock that occur when media is changed in cells in static culture (Balsalobre et al. 1998). This is achieved using a system of luer valves in the tubing prior to the first buffer slide (Figure 3.11A).

3.2 Discussion

In this chapter, I have described the development and utility of a system for perfused cell culture that functions over durations sufficient for circadian measurements. This provides a unique ability to measure multiple parameters from the same cell population over several weeks, with cells maintained in constant conditions.

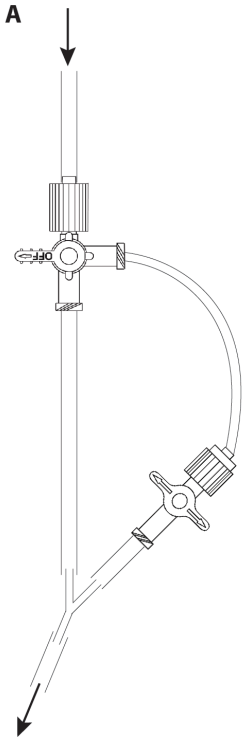

Figure 3.11

Application of timed boli

A Schematic diagram of a luer valve system for applying a single boli of defined length. The length of tubing flanked by the two valves is filled with media containing the drug of interest and bubbles excluded. The valves are then closed and the rest of the system filled and perfusion begun as in the basic protocol. When application of boli is required, luer valves are turned to divert flow only through the drug-

3.2.1 Comparison of perfused and static systems

When comparing data obtained from cells under traditional static conditions to those obtained from identically treated cells under perfusion (Figure 3.9, 3.10), it is striking that clear differences are observed, particularly with regard to the effect of pharmacological manipulations. The exact biological reason for this difference is unclear. On the one hand, it is possible that the smaller volume of the perfusion chambers – 150μl compared with 1ml under static conditions

– which results in a lower ratio of drug per cell in this condition, might lead to differing pharmacokinetics and so a different response between these two conditions. Such a small volume:cell ratio cannot be readily tested in static experiments, due to the metabolism of and excretion into the extracellular media and the associated change in media composition. Alternatively, it is possible that higher concentration of bicarbonate per cell in the perfused condition may affect drug transport in to the cell, which may also influence the pharmacokinetics of any manipulation. Further experiments will be required, however in order to determine the exact factors that give rise to the differences observed between static and perfused cell culture.

3.2.2 Further optimisation

Although entirely functional, countless modifications of the perfused system are possible, allowing for the effects of complex manipulations to be studied. It would be possible, for example, to perfuse with multiple media types, or to apply pharmacological agents acutely through injection port.

For certain applications, it may also be useful to manufacture specific components for the system. In particular, it would be of interest to see if meaningful modifications or improvements could be made on the ibidi μ-slide chamber, possibly using PDMS (Halldorsson et al. 2015; Shrirao et al. 2012). Previous work has placed a variety of biosensors in to these chambers (Luka et al. 2015). Given the circadian oscillations observed in cellular oxygen and glucose consumption in the next chapter, it might well be useful to be capable

of measuring these parameters in cells under perfusion in order to provide an alternative readout for cellular circadian state.

One continuing issue with the system is the relatively low throughput, making assays using this system slow when compared to traditional cell culture methods. To increase throughput, it would be desirable to have multiple independent cell chambers being fed media by the same syringe. However, problems can arise when it comes to splitting a single flow of media into multiple equal streams. This could potentially be overcome by manufacturing a slide where splitting of fluid streams occurs within the slide, rather than prior to the slide. This modification would also have the benefit of making the system much quicker to use, as the most time-consuming part of setting up this system is the sterilisation of the tubing.

3.2.3 Summary

In this chapter, I have described the development and optimisation of a system for perfusion circadian cell culture. This system allows for bioluminescent recording of mammalian cells over at least two weeks under conditions where cells display clear circadian rhythms in clock gene expression. It is also possible to vary the media applied to cells and to apply acute boli without the disruptive effects of media change. Furthermore, this system allows for collection and analysis of the extracellular media outflow form the cells, making the system suitable for a number of metabolomic assays.

Chapter 4: Cellular Metabolism as a Circadian Regulator

4.0.1 Current understanding

Circadian rhythms are a cellular phenomenon found across phylogenetic kingdoms. The model for how cells maintain a daily cycle is commonly proposed to consist of a transcription-translation feedback loop (TTFL). In its simplest form, this model proposes transcription and translation of a certain gene (or genes), with the resulting protein then translocating to the nucleus to inhibit its own transcription. Over time, the protein is degraded, releasing repression at the gene's own promotor, thereby allowing it to be transcribed again and the cycle to restart - the assumption being that this cycle takes approximately 24 hours, although how this critical time-delay is achieved is currently not fully elucidated (Johnson 2010). The resulting cycles in core clock gene expression are thought to drive further cycles in the expression of a number of so-called "clock-controlled" genes. It is the cycling of these genes that is proposed to bring about the vast majority of circadian rhythms in cellular processes. One of these processes, as described at length in the introduction to this thesis, is cellular metabolism, which has been shown to be rhythmic at a number of points, including glucose uptake (Feneberg & Lemmer 2004) and oxidative phosphorylation (Peek et al. 2013).

Although the model of TTFL negative feedback remains consistent across all organisms known to exhibit circadian rhythms, the specific genes and proteins that make up this cycle show very little homology between kingdoms. This has been taken by some as evidence of convergent evolution of circadian

rhythmicity (Rosbash 2009), arguing that the ability to predict external daily events confers such an evolutionary advantage that it is extremely likely to be favoured when it arises.

At odds with this hypothesis, an increasing body of work has shown that it is possible to observe circadian rhythmicity even in the absence of nascent transcription, which is required for the canonical TTFL model (O'Neill et al. 2011; O'Neill & Reddy 2011; Cho et al. 2014). In particular, a number of redox and metabolic pathways continue to exhibit rhythms under these conditions. The most well-known marker of these post-transcriptional oscillations is probably the oxidation state of peroxiredoxin (PRX-$SO_{2/3}$), although rhythms in redox co-factors, such as NADPH, have also been reported. These rhythms have been observed across phylogenetic kingdoms, despite the lack of homology between their canonical TTFL mechanisms (Edgar et al. 2012). This and related observations have fuelled the prior speculation about the existence and nature of an underlying post-transcriptional circadian oscillator that is present in all organisms that display circadian rhythmicity and that was present in the last eukaryotic common ancestor (LECA) (Putker & O'Neill 2016), analogous to the KaiABC oscillator in cyanobacteria. Such an oscillator would potentially be capable of providing answers to problems with the current TTFL model, including the mechanistic explanation for the 24-hour period (Lakin-Thomas 2000). That cellular redox metabolism might be implicated in this seems increasingly probable when one considers that a

number of the core clock genes have ben proposed to be redox sensitive (Yoshii et al. 2014; Schmalen et al. 2014; Rutter et al. 2001).

4.0.2 Challenges

Within cells, the primary determinant of redox state is the relative quantities of oxidising reactive oxygen species (ROS) and reducing equivalents NADH and NADPH. Both of these are produced and utilised during processes of primary cellular metabolism (Ying 2008; Andreyev et al. 2005). As such, many have speculated that any kind of core conserved circadian oscillator that influences cellular redox state might be intimately linked with cellular metabolism. This is supported by the observation that a number of metabolic processes are known to be rhythmic in at least some organisms (Figure 4.1A). To date, work has focussed on steady-state levels of redox co-factors when attempting to determine the metabolic or redox state of the cell. However, it is the rate of flux through the relevant pathways that would have to vary for a cellular

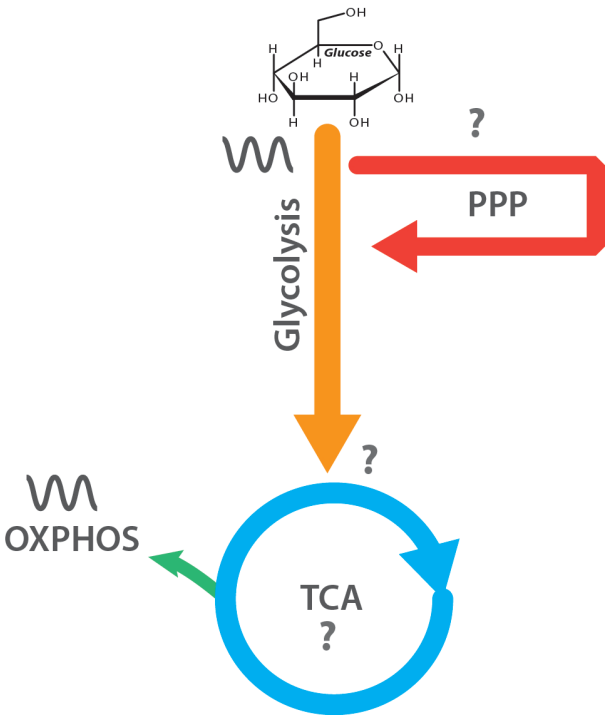

Figure 4.1
Schematic of primary metabolism
A Schematic overview of primary metabolism. Processes previously described to be under circadian control, and those about which rhythmicity is unknown, are indicated as '?'

rhythm in NADH, NADPH or ROS to arise. Therefore, new approaches are required to determine flux through these pathways before this question can be fully addressed.

4.0.3 Hypotheses

Given the previously described debate concerning the presence and nature of a post-transcriptional circadian oscillator, three possible hypotheses for the nature of the relationship between cellular redox/metabolism and cellular timekeeping exist. Firstly, it is possible that there is rhythmic flux through cellular metabolism in such a way that there is rhythmic variation in production of NAD(P)H and/or ROS and this is required for cellular rhythms in clock proteins to persist (this should also persist in the absence of a functioning TTFL). Importantly, this should be capable of determining periodicity. Alternatively, it may be the case that there is rhythmic flux through metabolism, but this is a post-translational clock output and has no bearing on maintenance of a cellular circadian rhythm. Thirdly, there may be rhythmic flux through metabolism, which is both a clock output and input, but is not essential for rhythms to persist.

The aim of this project was to determine which of these hypotheses might account for the previously observed oscillation in cellular redox state and so determine whether such a circadian variation in flux might make up a more evolutionarily conserved circadian oscillator.

4.1 Results

4.1.1 Metabolic pathways are rhythmic in their function

A well known marker of circadian rhythms in cellular redox state is the over- and hyperoxidation of peroxiredoxins, a highly abundant family of antioxidant proteins (Edgar et al. 2012). However, it important to note that oxidation of PRX proteins of itself is not essential for observation of cellular rhythmicity, since when the oxidation of PRX is inhibited in fibroblasts through use of conoidin A, a potent inhibitor of mammalian PRXs (Liu et al. 2010), PER2::LUC rhythmicity continues to be observed (Figure 4.2A,B). As such, it is important to note that PRX oxidation is merely a post-transcriptional marker for timekeeping and is unlikely to be involved cellular timekeeping mechanism itself. Instead, as PRX state oxidation is an indicator of cellular redox state,

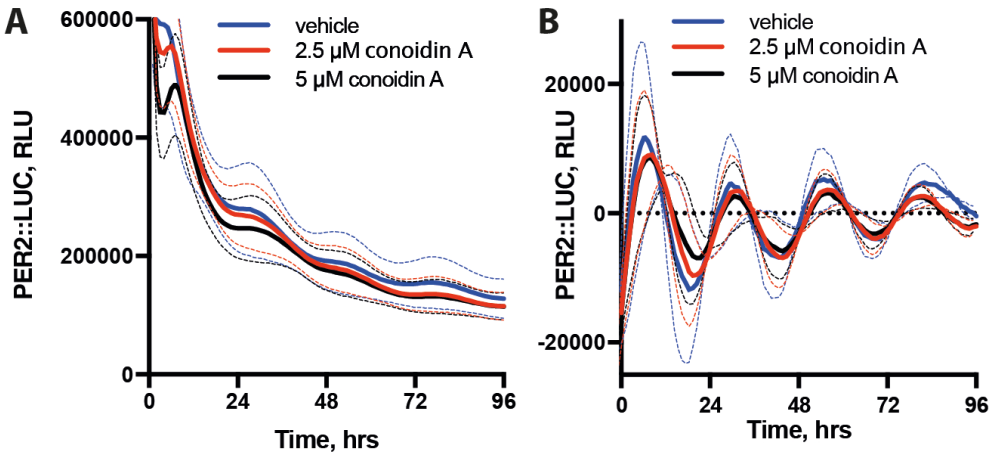

Figure 4.2

PRX2 inhibition does not affect cellular rhythmicity

A Fibroblasts in the presence of PRX inhibitor conoidin A (n=16, mean±SEM). **B** 24 hour moving average detrended data from A more clearly shows that there is no loss of PER2::LUC rhythmicity in the presence of conoidin A.

we postulate that oscillations in the abundance of PRX- $SO_{2/3}$ are associated with an underlying rhythmic regulation of cytosolic redox balance.

It has been previously observed that a number of metabolic pathways display a circadian variation in their function (Peek et al. 2013; Altman et al. 2015; Feneberg & Lemmer 2004). In order to test whether our PER2::LUC fibroblasts also showed cell-autonomous circadian rhythms in metabolism, both maximal and basal respiration and maximal and maximal glycolytic capacity was determined across the circadian cycle though use of a Seahorse respirometer (Figure 4.3). Maximal respiratory capacity was determined following treatment with mitochondrial uncoupler FCCP, whilst maximal glycolytic capacity was measured following treatment with ATP synthase inhibitor oligomycin. Respiratory measurements were determined by measuring the oxygen consumption rate of the cells (OCR), whilst glycolytic capacity is determined using the extracellular acidification rate (ECAR), with the rate of non-glycolytic acidification (determined following glucose starvation) subtracted. From this we see that all four of these parameters show variation across a circadian cycle, peaking at a comparable phase to the peak in PER2 expression recorded from control cultures.

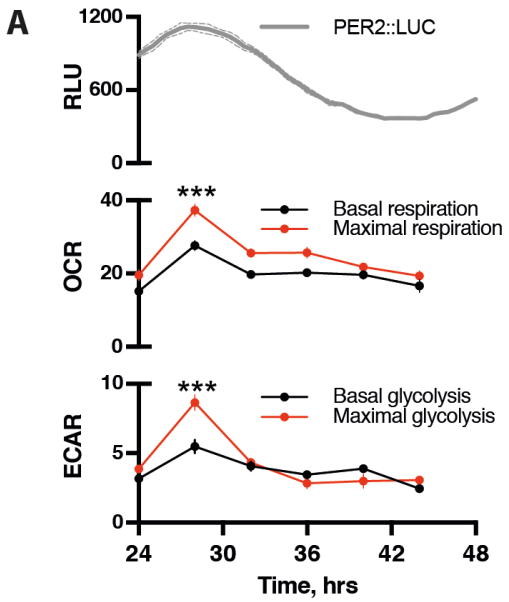

Figure 4.3

Circadian variation in primary metabolism

A Measurement of primary metabolism shows significant variation in basal glycolysis, maximal glycolytic capacity, basal respiration and maximal respiratory capacity across the circadian cycle (n=16, mean±SEM, Tukey's multiple comparisons test). Glycolytic capacity is determined using extracellular acidification rate (ECAR) following the addition of oligomycin, whilst basal and maximal respiration are determined using the oxygen consumption rate (OCR) in the absence of pharmacological agents and in the presence of FCCP respectively. PER2::LUC (n=4, mean±SEM) is shown to indicate related circadian phase.

4.1.2 Glucose metabolism pathways are required for cellular rhythmicity

Having confirmed that cellular metabolism varies across the circadian cycle in our chosen cell line, the next question is whether flux through primary carbohydrate metabolism is required for cellular rhythmicity to be observed. It was noted that cells cultured in varying concentrations of glucose, including in

the absence of extracellular glucose, still exhibited robust circadian rhythms (Figure 4.4A), with minimal changes in period, although an amplitude

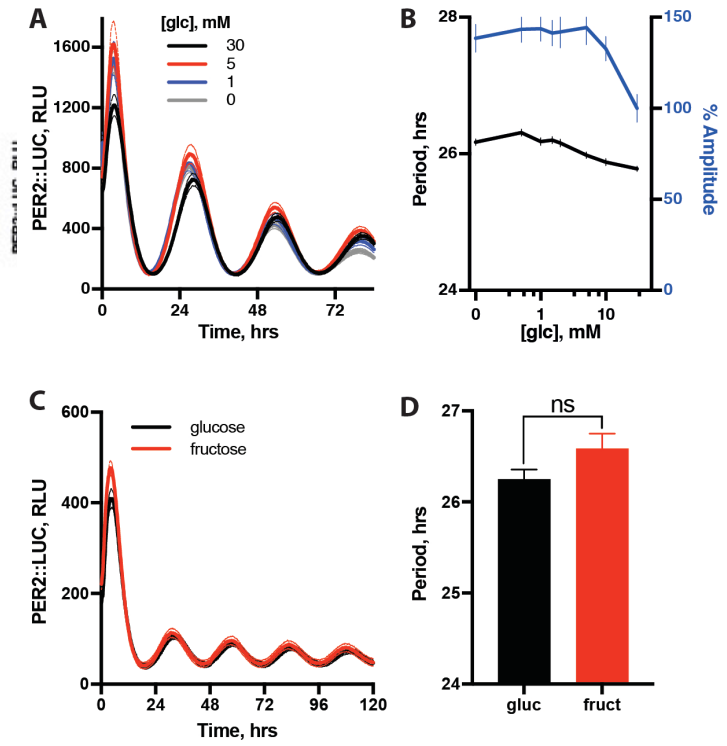

Figure 4.4

Glucose starvation does not abolish PER2::LUC rhythms

A Varying extracellular glucose concentration incrementally from 30mM to 0mM has no major effect on cellular period although **B** there is a slight increase in amplitude observed when glucose concentration is lowered (n=4, mean±SEM). **C** Substitution of glucose in cellular media with fructose has no effect on PER2::LUC rhythmicity (n=4, mean±SEM). **D** Quantification of period from C (Welch's t-test).

decrease was observed in cells cultured in 30mM glucose compared to those culture in 10mM or lower (Figure 4.4B); this observation is somewhat surprising when one considers that the concentration of glucose in the DMEM formulation most commonly used for cell culture is 27.8mM. Similarly, cells cultured in the absence of extracellular glucose

but in the presence of an equivalent concentration of fructose showed no significant difference in circadian gene expression compared to controls (Figure 4.4C,D). These data indicate that extracellular glucose concentration has very little impact upon the cellular clockwork in mouse fibroblasts.

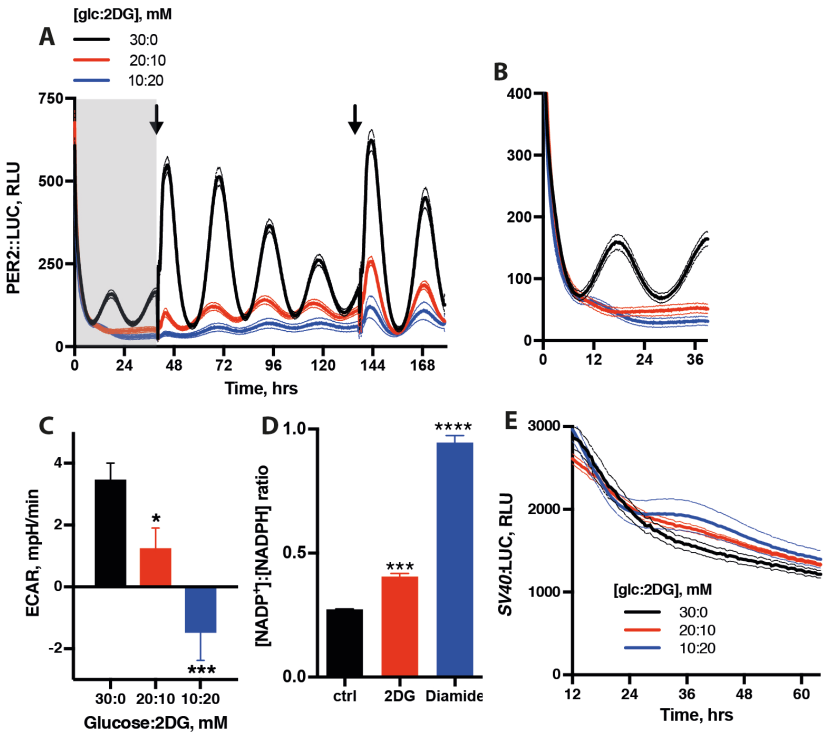

Figure 4.5

Inhibition of early primary carbohydrate metabolism supresses PER2::LUC expression

A,B(inset) Inhibition of both glycolysis and the pentose phosphate pathway with 2-deoxyglucose (2DG) results in loss observable rhythms in PER2::LUC (n=4, mean±SEM, comparison of fits prefers a first order polynomial, $p<0.0001$). 2DG is applied in ratio with glucose, such that the total molarity of the two combined is always 30mM. **C** 2DG applied in this manner is sufficient to significantly reduce glycolytic flux after 24 hours, as measured by ECAR (n=10, mean±SEM, Holm-Sidak's multiple comparisons test). **D** 2DG applied in a 20:10 ratio also increases the $NADP^+$:NADPH ratio within cells, creating a significantly more oxidized intracellular environment (n=4, mean±SEM, Dunnett's multiple comparisons test). **E** Application of 2DG does not reduce *SV40*:LUC signal (n≥4, mean±SEM).

In contrast when, rather than being starved of glucose, cells were cultured in the presence of the anti-metabolite 2-deoxyglucose (2DG), a profound suppression of PER2::LUC rhythmicity was observed, which was reversed following media change in to 2DG-free media, suggesting that this effect was not merely a result of cell death (Figure 4.5A,B). Here, 2DG was applied in ratio with glucose, such that the final concentration of the two combined was always 30mM. Upon transport into the cell via glucose transporters 2DG, like glucose, is phosphorylated by hexokinase (see Figure 3.11 for schematic) to form 2DG-6-P. However, this cannot be further metabolised through either glycolysis or the pentose phosphate pathway, but instead dose-dependently inhibits both pathways (Barban & Schulze 1961). The effect of 2DG on glycolysis was further confirmed by ECAR (Figure 4.5C), whilst $NADP^+$:NADPH assays showed 2DG to increase this ratio, suggesting a more oxidised intracellular environment in the presence of this drug (Figure 4.5D). Furthermore, this effect appears to have some specificity for PER2, as application of 2DG to cells constitutively expressing luciferase under the *SV40* promoter did not show any loss of bioluminescent signal (Figure 4.5E, this control experiment was done with the assistance of Kevin Feeney). This also confirms that ATP levels, which are required for the activity of luciferase, were not greatly reduced by 2DG treatment. From these observations, we can conclude that 2DG acts to supress PER2::LUC expression not through glucose starvation or ATP depletion but through some alternative mechanism.

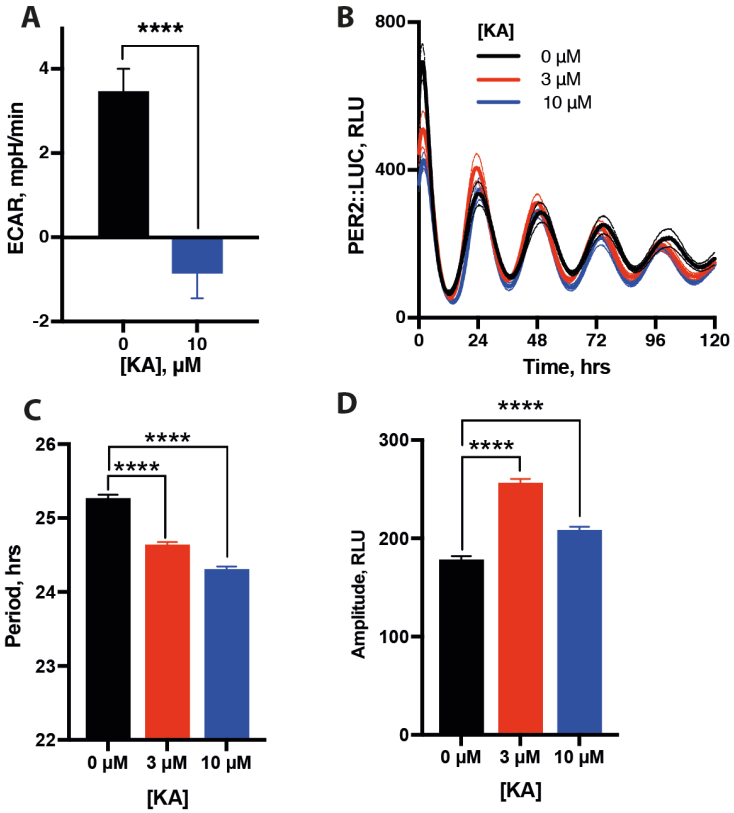

Figure 4.6

Inhibition of glycolysis alone does not abolish PER2::LUC rhythmicity

A 10μM GADPH inhibitor koningic acid (KA) greatly reduces glycolysis rate, as measured by ECAR (n≥5, mean±SEM, Holm-Sidak's multiple comparisons test). **B** Application of KA has minimal effects on PER2::LUC rhythmicity (n=4, mean±SEM) whilst **C** producing a small decrease in period (Dunnett's multiple comparisons test) and **D** a small and inconsistant effect on the amplitude of the PER2::LUC oscillation (Dunnett's multiple comparisons test).

That the effect of glycolytic and PPP inhibition on cellular rhythmicity is so different from the effect of glucose starvation may initially appear counter intuitive. However, as fibroblasts are capable of gluconeogenesis (Sumbilla et al. 1983), autophagy and β-oxidation, it is likely that cells experiencing glucose starvation are still experience some glycolytic and PPP flux.

Meanwhile, 2DG inhibition prevents flux through both glycolysis and the PPP, thereby having a much more profound effect on cellular metabolism and NADPH production and thus producing the observed effects of cellular timekeeping.

4.1.3 Neither glycolysis or the TCA cycle are essential for circadian rhythmicity

As 2DG inhibits the very initial stages of primary carbohydrate metabolism, it is unclear through use of this drug alone as to which aspect of carbohydrate metabolism is required for observation of PER2::LUC rhythmicity. In order to determine which aspect is responsible for this change in PER2 expression, pharmacological inhibitors of each pathway were applied and the effects on PER2::LUC expression recorded. Despite having clear effects on basal glycolysis (Figure 4.6A), GADPH inhibitor koninigic acid had only minimal effects on PER2::LUC expression (Figure 4.6B), showing a decrease in period under 1 hour (Figure 4.6C), which does not increase when KA is applied at higher concentrations (data not shown) and a variable effect on amplitude (Figure 4.6D).

Pyruvate analogue 3-bromopyruvate (3-Br-Pyr), which acts as an inhibitor of entry in to the TCA cycle, whilst significantly reducing cellular respiratory capacity (Figure 4.7A) has no apparent effect on PER2::LUC rhythms (Figure 4.7B). Similarly, mouse embryonic kidney cells that lack fumarate hydratase ($FH1^{-/-}$) and therefore lack a competent TCA cycle (Frezza et al. 2011), still exhibit rhythms in the transcriptional circadian reporter *Bmal1*:LUC (Figure

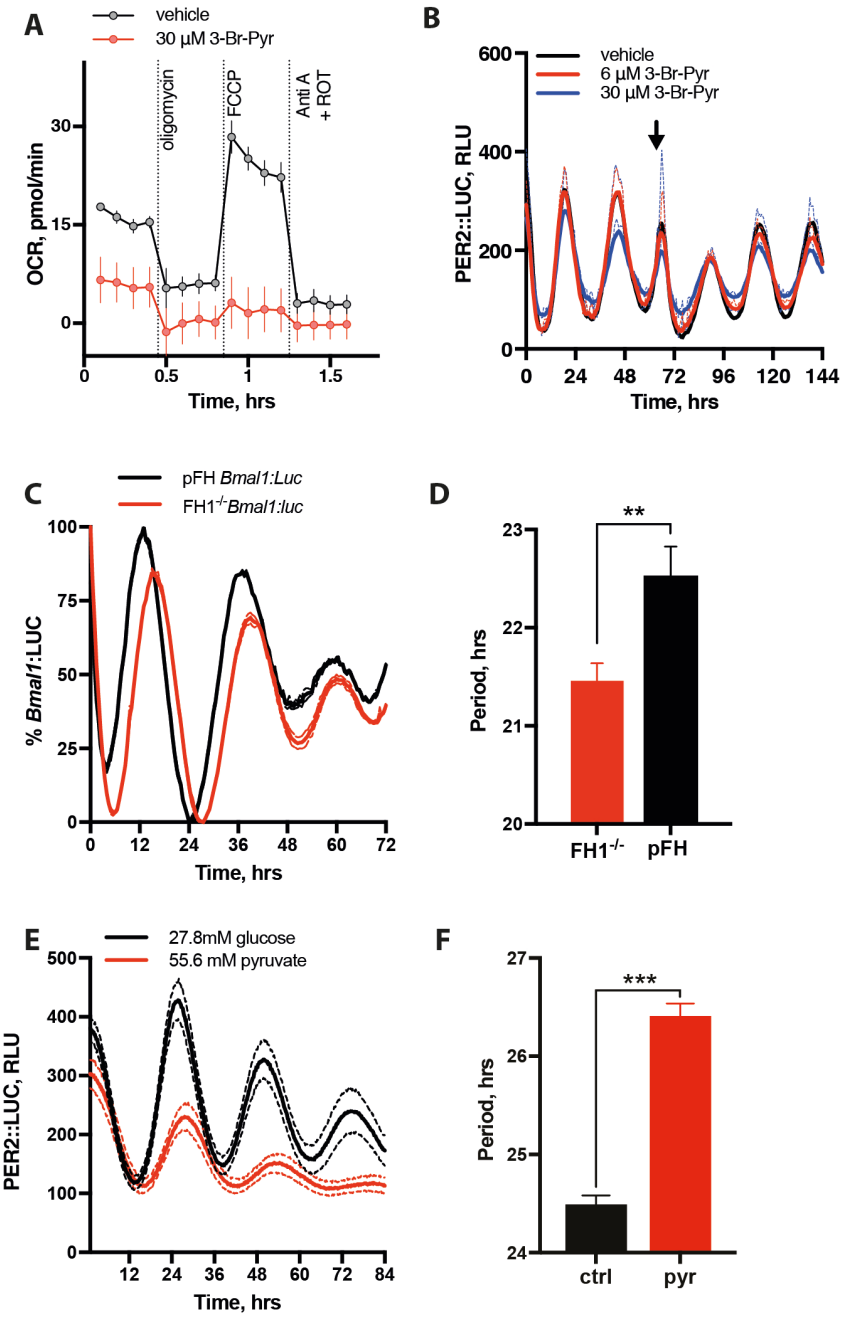

Figure 4.7

TCA cycle inhibition does not mimic the effect of 2-DG

A Pyruvate analogue 3-bromopyruvate (3-Br-Pyr) reduces respiratory capacity at both basal and maximal levels, determined prior to drug addition and following FCCP respectively (n≥5, mean±SEM). **B** 3-Br-Pyr has minimal effects on the cellular oscillation as reported by PER2::LUC. Arrow indicates drug wash-off (n=4, mean±SEM). **C** Mouse kidney cells that lack the enzyme fumarate hydratase (FH) and so a functional TCA cycle still show rhythms in Bmal1:LUC bioluminescence (n=3, mean±SEM).

Continued on next page

D These cells do show a small decrease in period (1.07hrs±0.2, Welch's t-test). **E,F** Replacing glucose in the extracellular media with an equivalent concentration of pyruvate significantly lengthens period in PER2::LUC fibroblasts (n=3, mean±SEM, Welch's t-test). Period change is 1.9hrs±0.2.

4.7C). These rhythms are comparable to cells in which FH1 has been genetically rescued (pFH). It is also noted that cells lacking FH1 show a reduction in cellular period of slightly over 1 hour (Figure 4.7D).

In contrast, cells cultured in the absence of extracellular glucose and instead with an equivalent concentration of pyruvate showed a marked increase in period, accompanied by a decrease in the amplitude of PER2::LUC expression, although this was not as marked as the effects seen with 2DG (Figure 4.7E,F). The discrepancy between these observations we feel can be explained in light of further findings described below.

From these data, it is possible to conclude that, although both glycolysis and the TCA cycle are competent to contribute to cellular timekeeping, they are not essential for the observation of cellular rhythmicity. Certainly, none of the manipulations described above in anyway recapitulate the suppression of circadian gene expression observed with 2DG treatment.

4.1.4 PPP inhibition recapitulates the effects of 2DG

As neither perturbation of glycolysis or the TCA cycle were capable of recapitulating the effects of 2DG, the effects of pentose phosphate pathway (PPP) inhibition alone was investigated. The pentose phosphate pathway runs parallel to glycolysis, taking glucose-6-phosphate and converting it to

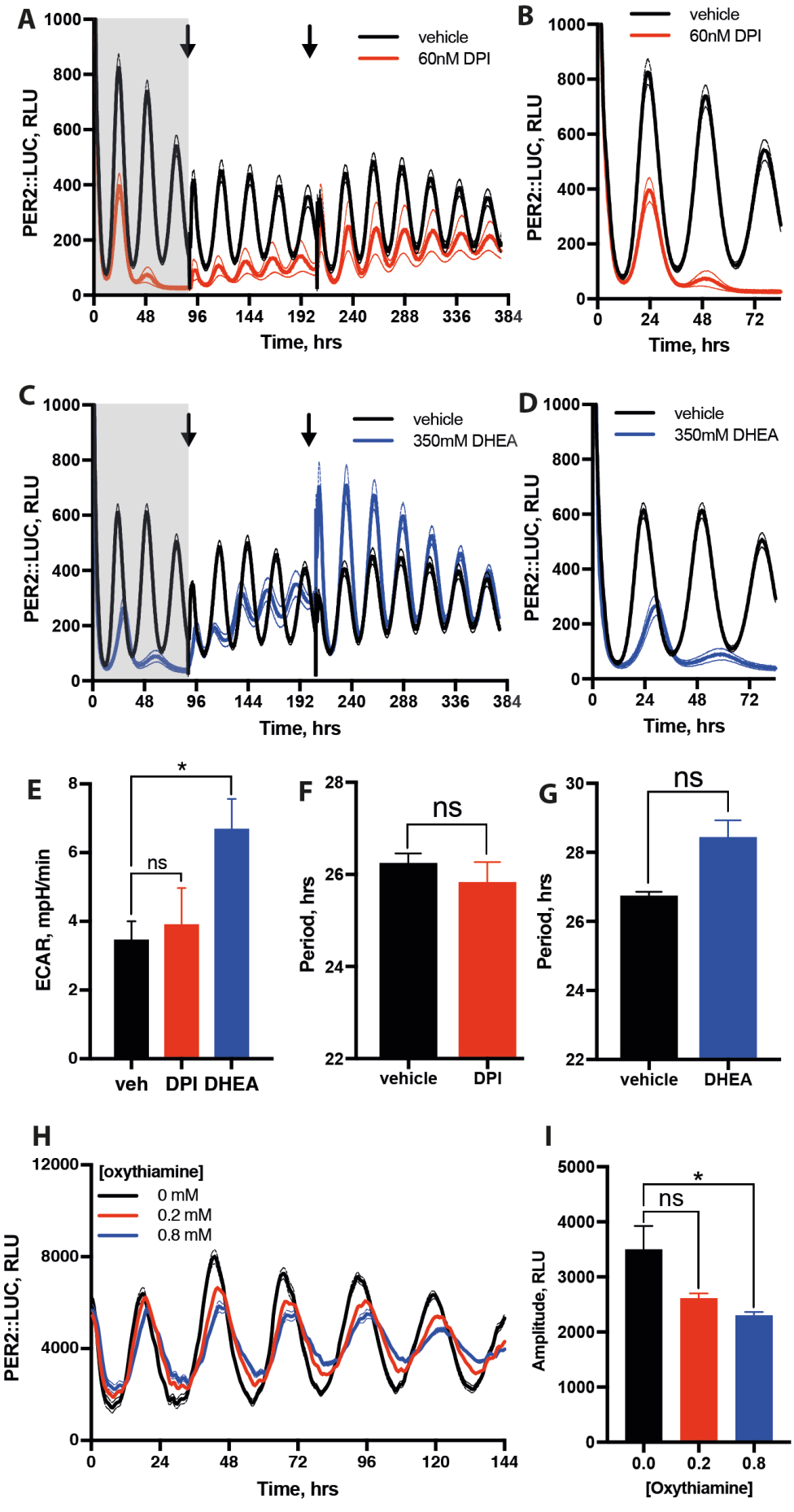
A
PER2::LUC, RLU
Time, hrs
vehicle
60nM DPI
B
PER2::LUC, RLU
Time, hrs
vehicle
60nM DPI
C
PER2::LUC, RLU
Time, hrs
vehicle
350mM DHEA
D
PER2::LUC, RLU
Time, hrs
vehicle
350mM DHEA
E
ECAR, mpH/min
ns
*
veh
DPI
DHEA
F
Period, hrs
ns
vehicle
DPI
G
Period, hrs
ns
vehicle
DHEA
H
PER2::LUC, RLU
[oxythiamine]
0 mM
0.2 mM
0.8 mM
Time, hrs
I
Amplitude, RLU
ns
*
[Oxythiamine]

Figure 4.8

Inhibition of the oxidative PPP phenocopies the effect of 2DG

A,B Application of PPP inhibitor DPI attenuates PER2::LUC rhythmicity, as does **C,D** DHEA (n=4±SEM). **E** Neither of these drugs significantly reduce glycolytic flux as m easured by ECAR; indeed DHEA causes a significant increase in ECAR (n=4±SEM, Dunnett's multiple comparisons test). **F,G** Neither DPI nor DHEA have significant effects on period, measured as the time between peaks (Welch's t-test). **H** Transketolase inhibitor oxythiamine has a small effect on period, (0.56hrs±0.0, n=4, mean±SEM) and **G** produces a small suppression of PER2::LUC amplitude (Dunnett's multiple comparisons test). Oxythiamine treatment was performed by Kevin Feeney.

pentoses, including ribose-5-phosphate, in what is known as the oxidative stage (see Figure 4.11 for schematic). This step also generates 2 NADPH molecules per glucose-6-phosphate molecule. Those pentose sugars may be utilised for nucleotide synthesis, but otherwise are subjected to a number of rearrangements during the non-oxidative phase of the pentose phosphate pathway, and are ultimately returned to the glycolytic pathway as either fructose-6-phosphate or as glyceraldehyde-3-phosphate. Both flavoprotein inhibitor Diphenyleneiodonium (DPI) and steroid and non-competitive glucose-6-phosphate dehydrogenase inhibitor Dehydroepiandrosterone (DHEA) act as inhibitors of the oxidative stage of the PPP (Riganti et al. 2004; Drummond et al. 2011),whilst producing no significant reduction in glycolytic function (Figure 4.8E). When applied to PER2::LUC fibroblasts, both drugs produced a rapid dampening of PER2::LUC expression which was rescued with successive wash-off (Figure 4.8A,B,C,D). This is reminiscent of the effects seen on PER2 in the presence of 2DG. It is also noteworthy here that although both drugs act to rapidly decrease the amplitude of the PER2::LUC oscillation, the period of

the oscillation is not significantly affected (Figure 4.8E,F), although we did note a phase shift following application of DHEA .

In contrast, when the non-oxidative portion of the PPP was inhibited, in this case with oxythiamine, a competitive inhibitor of transketolase (Boros et al. 1998), no large suppression of PER2 expression is observed (Figure 4.8G, this experiment was performed by Kevin Feeney). There is a small dose-dependent decrease in the amplitude of PER2 expression (Figure 4.8H). A small period increase was also observed with oxythiamine, but as this was at most approximately 30 minutes, it was not considered biologically relevent.

This suggests that PER2::LUC expression is particularly sensitive to inhibition of the oxidative PPP over the non-oxidative PPP, glycolysis and the TCA. Since application of oxidative PPP inhibitors results in a particularly large decrease in the NAD^+:NADH ratio (Figure 4.13D), is plausible that the effect of both DPI and DHEA on cellular rhythmicity is the result of major changes in the cellular redox state following from greatly reduced PPP flux (Figure 4.13B).

4.1.5 Genetic knockdown and over-expression of PPP enzymes

In order to confirm the observations made following pharmacological perturbation, siRNA knockdown was performed in PER2::LUC fibroblasts against four major glycolytic and PPP enzymes, namely glucose 6-phosphate dehydrogenase (G6PDH) and phosphoglucose isomerase (GPI), the entry

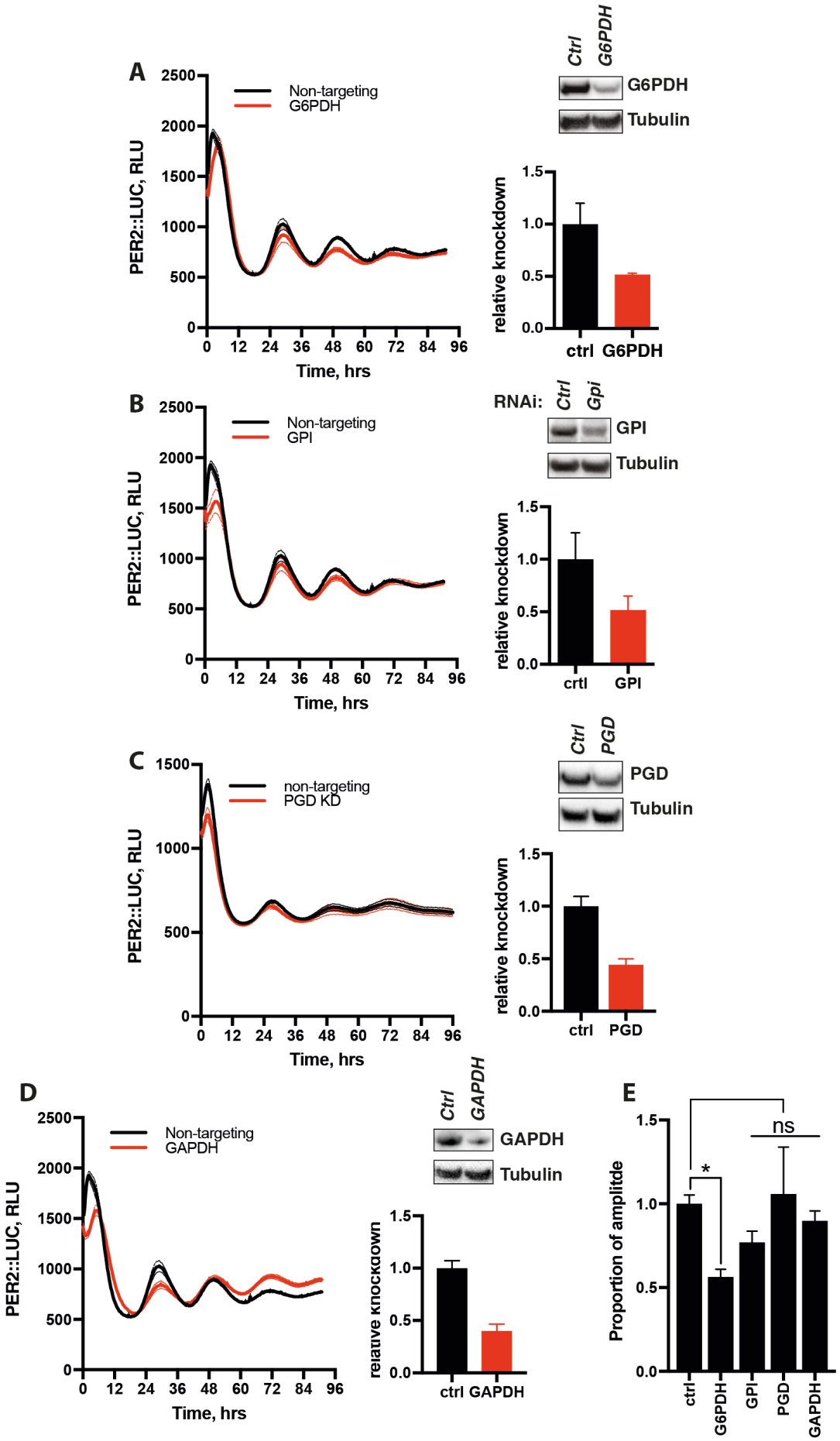
A
Non-targeting
G6PDH
PER2::LUC, RLU
Time, hrs
Ctrl
G6PDH
G6PDH
Tubulin
relative knockdown
ctrl G6PDH
B
Non-targeting
GPI
PER2::LUC, RLU
Time, hrs
RNAi:
Ctrl
Gpi
GPI
Tubulin
relative knockdown
crtl GPI
C
non-targeting
PGD KD
PER2::LUC, RLU
Time, hrs
Ctrl
PGD
PGD
Tubulin
relative knockdown
ctrl PGD
D
Non-targeting
GAPDH
PER2::LUC, RLU
Time, hrs
Ctrl
GAPDH
GAPDH
Tubulin
relative knockdown
ctrl GAPDH
E
Proportion of amplitde
ns
*
ctrl
G6PDH
GPI
PGD
GAPDH

Figure 4.9

siRNA knockdown of PPP enzymes

A siRNA knockdown of glucose 6-phosphate dehydrogenase (G6PDH, 48±11%), **B** phosphoglucose isomerase (PGI, 48±16%), **C** 6-phosphogluconate dehydrogenase (PGD, 56±11%) or glyceraldehyde 3-phosphate dehydrogenase (GAPDH, 60±6%) **D** had small and variable effects on cellular period (n≥3, mean±SEM). Knockdown quantified by western blot (right panel, Welch's t-test). **E** Although some small effects on amplitude were observed, these effects were inconsistent, with the exception of G6PDH knockdown, which produced a small but significant decrease in amplitude (Dunnett's multiple comparisons test)

points in to the PPP and glycolysis respectively, 6-phosphogluconate dehydrogenase (PGD), the second NADPH-producing enzyme in the PPP and glyceraldehyde 3-phosphate dehydrogenase (GAPDH) (Figure 4.9A,B,C,D). Although knockdown was approximately 50% for all enzymes, the only consistent effect observed was that knockdown of G6PDH produced a small but significant decrease in amplitude (Figure 4.9E). Knockdown of G6PDH and GAPDH also sometimes produced small decreases in period, but this effect was inconsistent between experiments and so is not quantified here.

As metabolic enzymes are generally appreciably more abundant than cellular demand requires, it is possible that the comparatively small effects observed above stem from the fact that there is still a sufficient quantity of these above stem from the fact that there is still a sufficient quantity of these enzymes available for normal cell function. However, glucose 6-phosphate dehydrogenase is generally thought to be the rate-limiting enzyme in the PPP (Stanton 2012), which may explain why the only consistent effect is observed

when this enzyme is targeted. However, transient over-expression of bacterial isoforms of glucose 6-phosphate dehydrogenase (ZWF) and 6-phosphogluconate dehydrogenase (GND) did not produce significant effects on the cellular oscillation (Figure 4.10A,B). This, combined with the minimal effects seen following enzymatic knockdown, suggest that these enzymes are able to support normal cellular function within a wide range of expression. This is further supported by the fact that humans that are genetically deficient in these enzymes display relatively few symptoms when not experiencing unusual oxidative stress, generally brought about by certain foods, drugs or infection (Beutler 2008).

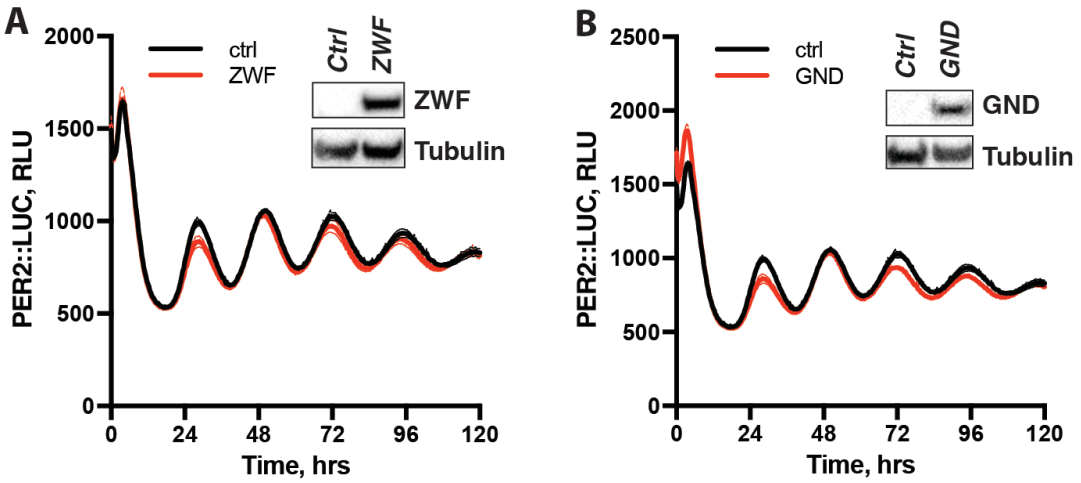

Figure 4.10

Overexpression of bacterial PPP enzymes

A Transient overexpression of ZWF, the bacterial isoform of glucose 6-phosphate dehydrogenase and **B** GND, the bacterial isoform of 6-phosphogluconate, shows inconsistent effects on PER2::LUC rhythms (n=4, mean±SEM). Overexpression was determined by western blot.

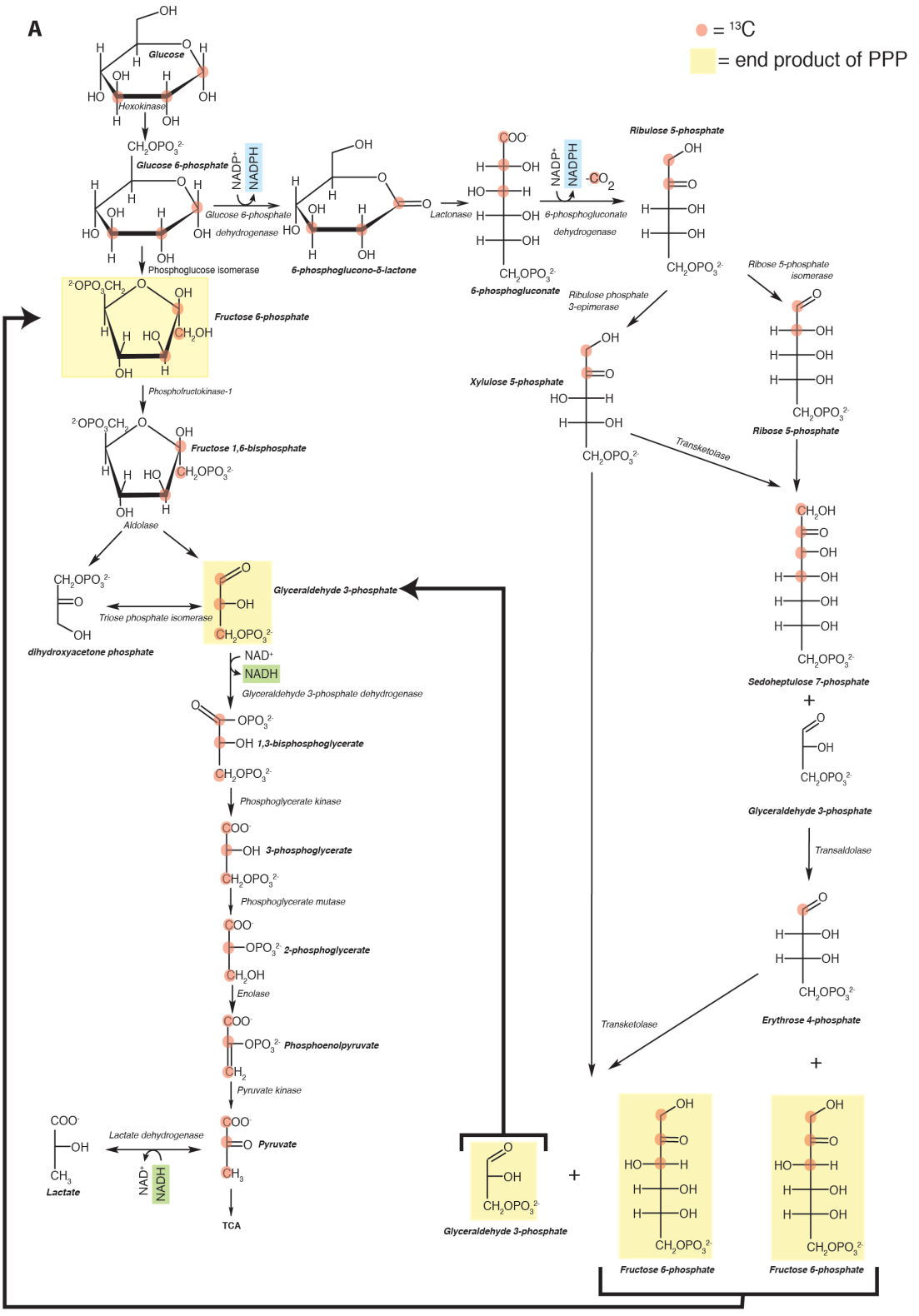

Figure 4.11

Schematic describing metabolic labelling strategy

A Schematic explaining the metabolism of 1,2,3-^{13}C labelled glucose. See text for full explanation.

4.1.6 Metabolic labelling

If the PPP is the source of the rhythm in cellular redox state, then it must follow that flux through the PPP is rhythmic. To test this hypothesis, a metabolic labelling approach in was used in continuously perfused cells.

Classically, either singly or doubly ^{13}C labelled glucose has been used to investigate flux through the PPP (Dusick et al. 2007; Brekke et al. 2012).

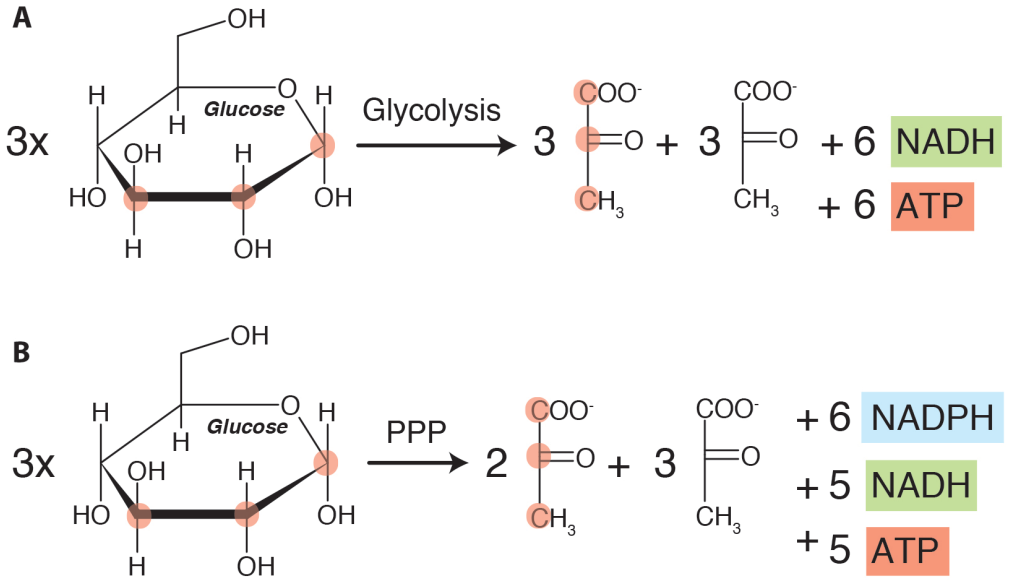

Figure 4.12

End products of labelled glucose metabolism

A Catabolism of 1,2,3-^{13}C labelled glucose results in different products depending on the pathways through which it has been metabolised. If glucose is only metabolised through glycolysis, the products are 3 fully labelled pyruvate molecules and 3 fully unlabelled pyruvate molecules for every 3 glucose molecules metabolised. 6 NADH molecules are also formed. **B** If instead, the glucose passes through the PPP before glycolysis, each three glucose molecules produces 2 fully labelled and 3 fully unlabelled pyruvate molecules, in addition to 6 NADPH and 5 NADH molecules.

Glucose passing though the PPP loses its first carbon molecule as CO_2 during the oxidative phase, following which, rearrangements in the non-oxidative PPP produce differently labelled metabolites to those from glucose that has passed solely through glycolysis, allowing for calculation of PPP flux. However, ^{13}C may also be present at additional glucose carbons due to its natural abundance (~1 %) or due to impurities from the enrichment process. This has the potential to introduce error into calculations of the relative fluxes between glycolysis and the PPP using either the singly or doubly labelled method. To avoid this problem, 1,2,3-^{13}C labelled glucose was utilized as a labelled substrate (Figure 4.10A). Metabolism of 1,2,3-^{13}C glucose through either glycolysis or the PPP produces fully ^{13}C labelled or completely unlabelled (^{12}C) 3-carbon metabolites, which either serve as substrates for mitochondrial respiration or are exported into the cell culture media. ^{13}C and ^{12}C lactate/pyruvate are produced in different ratios depending on which metabolic pathways they have passed through: flux through glycolysis produces a 1:1 ratio of ^{13}C-labeled to ^{12}C-unlabeled product, whilst flux through the PPP produces a ratio of 2:3 (Figure 4.12A). Assuming no preference for PPP or glycolytic products for further mitochondrial metabolism, analysis of the ratios of these two metabolites in the extracellular media allows for accurate determination of the relative metabolic fluxes between the two pathways. This method is not affected by 3-carbon metabolites produced by other pathways or as a result of impurities in the labelled glucose, as these will be singly or doubly labelled, allowing for more accurate determination of primary metabolic flux.

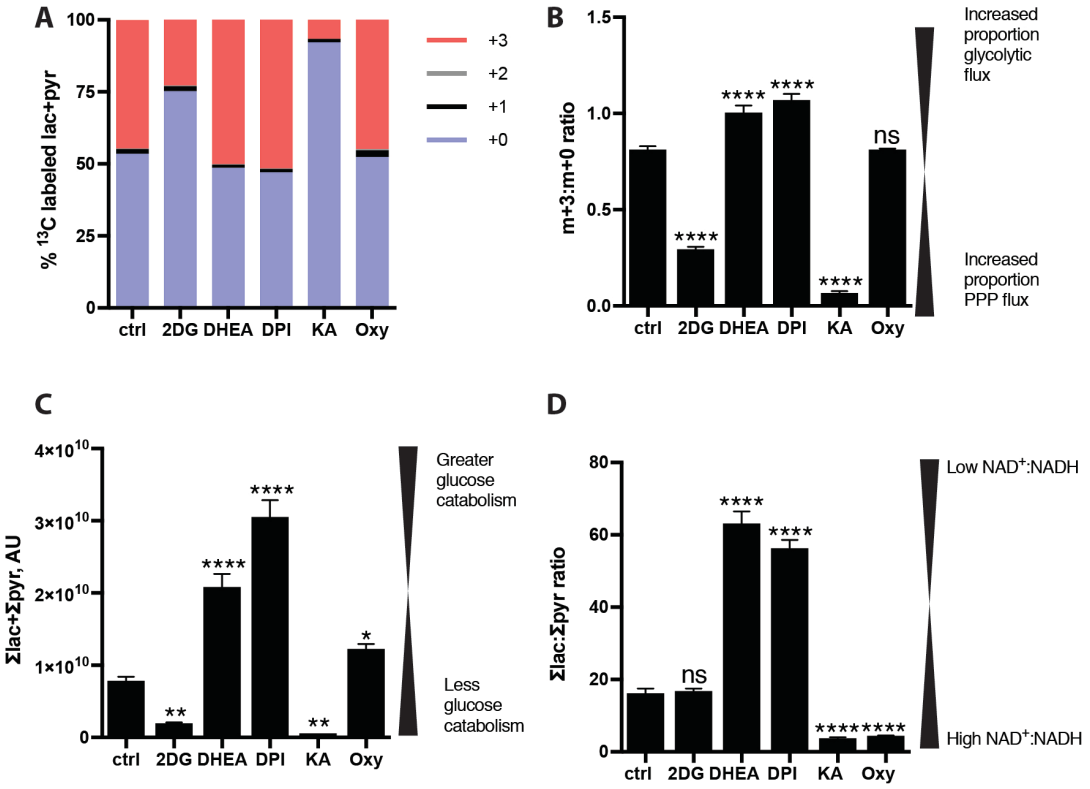

Figure 4.13

Validation of labelling strategy

A Inhibition of glycolysis and/or the PPP shifts the proportions of ^{13}C labelled and unlabelled 3-carbon products produced by PER2::LUC fibroblasts (n=4). **B** This can also be represented as a ratio (n=4, mean±SEM, Holm-Sidak's multiple comparisons test). **C** Analysis of lactate and pyruvate in these same samples shows that inhibition of glycolysis or the PPP also impacts upon total lactate and pyruvate production, a measure of glycolytic flux and **D** lactate:pyruvate ratio, which is a good proxy for NAD+:NADH ratio (Holm-Sidak's multiple comparisons test).

In order to validate this method, cells were treated with a number of known glycolytic and PPP inhibitors and the effects on the ratio of products in the extracellular media analysed by LC-MS (Figure 4.13 A,B). As predicted, those drugs that inhibited the PPP, thereby ensuring that flux passed entirely

through glycolysis alone, produced ratios of labelled to unlabelled products of close to 1. Following from this, inhibitors of glycolysis would be predicted to produce ratios of 0.6. However, the actual ratio in the presence of GAPDH inhibitor KA is lower than this. This can be accounted for if there is repeated cycling of products through the PPP – a likely occurrence in the event of GAPDH inhibition. 2DG also produced a ratio substantially below 0.6, suggesting that 2DG might preferentially inhibit glycolysis over the PPP. However, 2DG is clearly still a major inhibitor of both pathways, as the total flux through either pathway is very small, as evidenced by the total sum of 3-carbon products produced in the presence of this drug (Figure 4.13C), suggesting that very little glucose catabolism of any kind occurs in the presence of 2DG. In contrast, inhibition of both the oxidative and non-oxidative arms of the PPP significantly increased total glucose catabolism.

Overall, we take these results as validation, both that this method of labelling is a reliable and sensitive way of determining relative glycolytic and PPP flux and also of the function of the inhibitors that we have previously used to investigate glycolysis and the PPP.

4.1.7 Perfused cell culture

When seeking to investigate longitudinal changes in metabolism, one is required to take samples at multiple time points. If one is using classic static tissue culture techniques for such an assay, two major issues arise. Firstly, extracting the extracellular media for mass spectrometry analysis (as

described in the labelling section above) is generally an end-point procedure. This means that it is not possible to repeatedly test the same population of cells. Instead, one has to have a large number of identically-treated dishes of cells running in parallel, a number of which can be sampled and then disposed of at each time point. Although extremely similar, there are some subtle variations between different dishes of otherwise identically treated cells, arising from a number of uncontrollable factors, such as dish microenvironment, heterogeneity in the cell population or stochastic variation in seeding density. This adds an extra degree of variability to data collected in this way, which can make it difficult to detect more subtle changes in metabolite levels with confidence. Previous attempts in our group to study PPP flux using static methods have found this to be the case.

Secondly, when using labelled substrates to study primary metabolism, these substrates are generally pulsed in to the cellular media for a short period of time before those cells are sampled. This provides a snapshot of the metabolic activity of those cells in the few hours prior to sample collection. However, there is some evidence that glucose pulses are capable of resetting the circadian phase of cells in culture (Hirota et al. 2002). This makes a pulsed approach inappropriate for studying circadian changes in metabolism, as cells would not be in true free-run when sampled.

The problems described above make traditional static tissue culture inappropriate for the study of metabolic flux longitudinally. In order to

overcome this, a novel system of continuously perfused tissue culture was used. The design and optimisation of this is fully described in chapter 3. Briefly, cells are grown in a microfluidics slide and modified cell culture media is then driven across the slide at a low rate by a syringe pump. Media that has passed across the cells can then be collected on ice and snap-frozen at regular intervals. Metabolites were extracted from these samples and analysed using mass spectrometry. This technique overcomes both of the problems described above: there is no variability between different dishes at different time points as sequential measurements are being taken from the same population of cells and there is also no need to acutely pulse the cells with labelled glucose, so there is no potential for circadian resetting.

4.1.8 Rhythms in total glycolytic flux drive oscillations in cellular NAD(P)H

Having validated the technique for metabolic labelling under constant perfusion, cells were entrained using temperature cycles and then allowed to free-run under perfused conditions with 5.5 mM 1,2,3^{13}C-labelled glucose. After an initial 17 hour period, where cells were left to equilibrate intracellular stores with extracellular labelled glucose, the perfusate was collected every 3 hours for 3 days. Mass spectrometry analysis of this perfusate revealed significant variation in the total quantity of lactate and pyruvate produced by cells; this being a measure for total glycolytic flux (Figure 4.14A). The abundance of pyruvate and lactate peaked at a comparable time to PER2::LUC, which was simultaneously recorded.

In contrast, a significant circadian variation was not observed in ratio of labelled to unlabelled lactate and pyruvate produced by these same cells

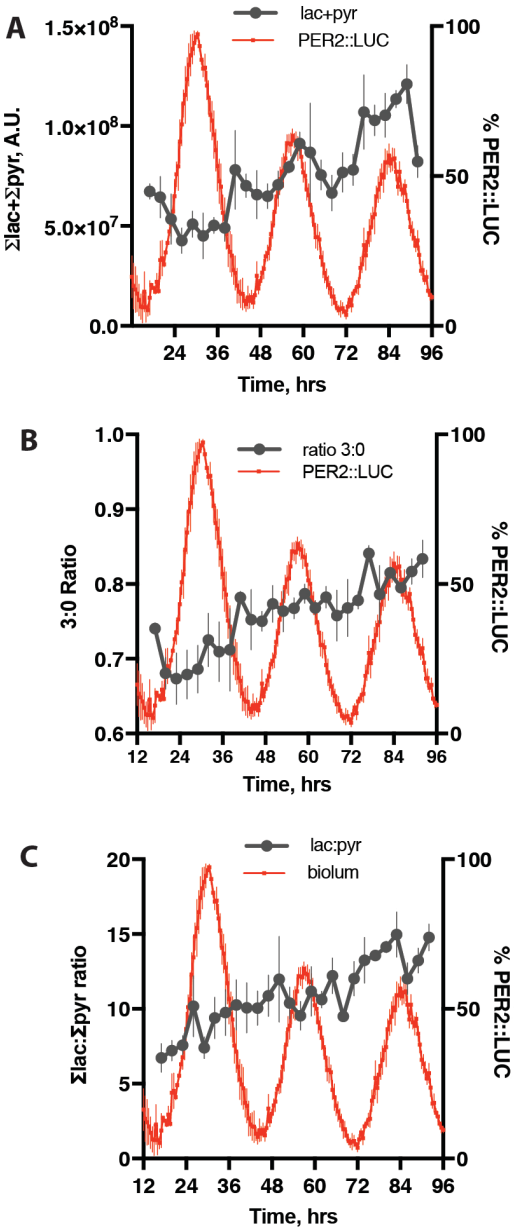

Figure 4.14

Longitudinal measurement of glycolytic and PPP flux

A Mass spectrometry on samples of extracellular media taken from PER2::LUC fibroblasts in perfused with 1,2,3-^{13}C labelled glucose shows a significant variation (cosinor analysis, $p<0.0001$) in total pyruvate and lactate production across the circadian cycle, (n=4, mean±SEM). **B** Analysis of the ratio of ^{13}C to ^{12}C labelled pyruvate and lactate in these same samples does not show a significant variation in the relative ratios. **C** Analysis of the total lactate:pyruvate ratios of these samples also showed no clear circadian variation. PER2::LUC bioluminescence is reproduced in all graphs to aid interpretation.

(Figure 4.13B). We also did not detect a rhythm in lactate:pyruvate ratio (Figure 4.13C), this ratio being a good report of the free NAD$^+$:NADH ratio within cells (Christensen et al. 2014). From this, it is possible to conclude that any oscillation in these two measurements is below the detection threshold of this assay. As such, it is likely that previously observed rhythms in NADH and

NADPH are the result of changes in total flux through both glycolysis and the PPP, rather than regulated changes in the proportion of flux shared between these two pathways.

4.2 Discussion

4.2.1 Summary

In this chapter, I have investigated the relationship between primary carbohydrate metabolism and circadian gene expression in cultured cells. It has been demonstrated using a novel labelling technique that there is circadian variation in the total flux passing through glycolysis and the PPP, but no evidence was found for circadian variation in the proportion of flux shared between these two pathways. This suggests that any oscillation observed in cellular NAD(P)H levels is most likely the result of changes in total flux through glycolysis and the PPP combined.

Furthermore, I have shown that although flux through total glycolysis is rhythmic, inhibition of either glycolysis or the TCA does not prevent observation of cellular rhythmicity. In contrast, pharmacological inhibition of the oxidative pentose phosphate pathway, a major source of cellular reducing equivalents, results in rapid loss of amplitude of circadian gene expression but with no major effect on the period of the oscillation was observed.

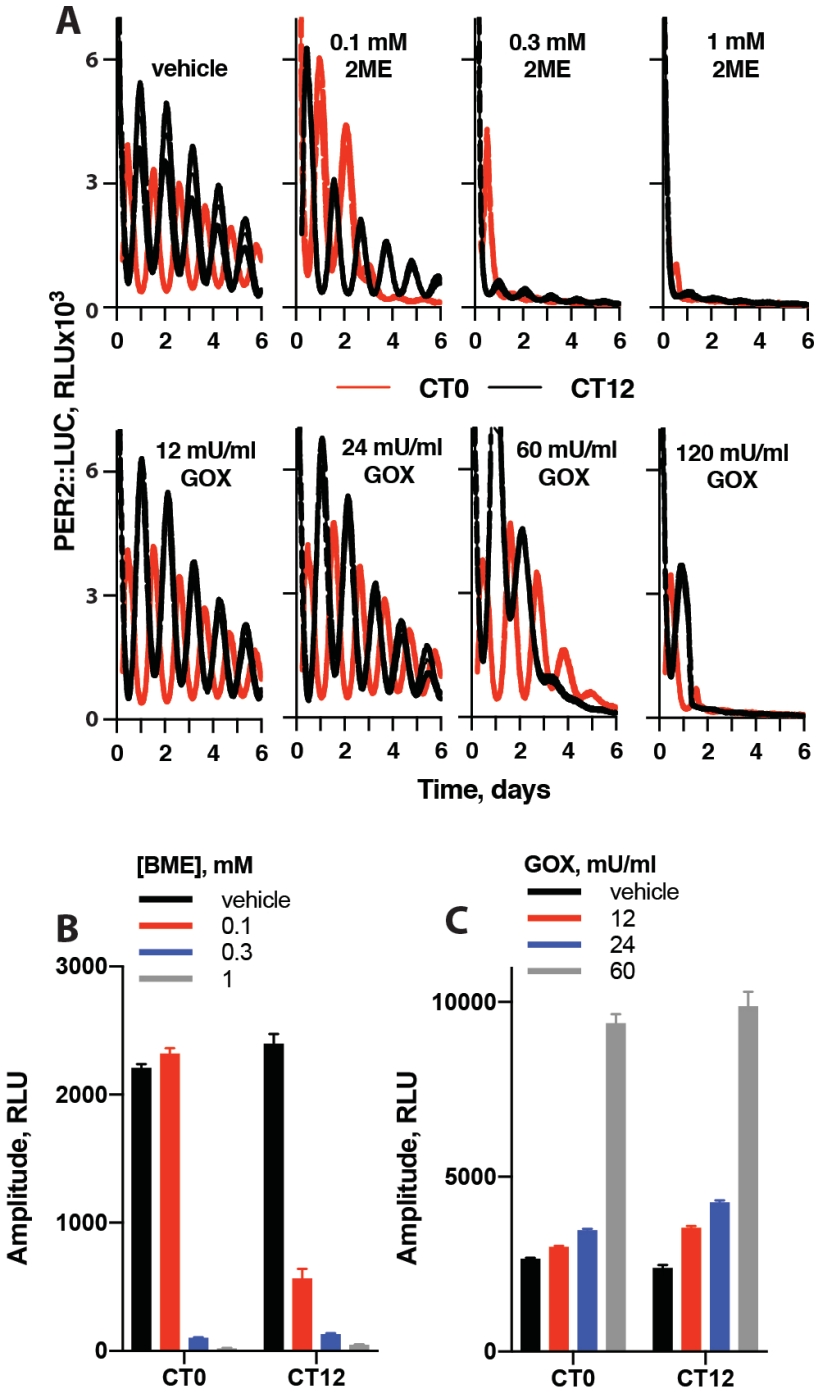

Figure 4.15

Redox balance regulates the amplitude of circadian rhythms in mouse fibroblasts.

A. Effect of chronic glucose oxidase (GOX) and 2-mercaptoethanol (2ME) treatment on PER2::LUC rhythms, with treatment beginning at two opposite circadian phases (circadian time, CT0 or CT12) (representative mean±SEM (n=4)).

Continued on next page

Small period effects were observed here, but they were highly variable and therefore not considered significant **B** Both BME and **C** GOX have effects on the amplitude PER2 expression, as measured at the first circadian peak. This experiment was performed by John O'Neill.

4.2.2 Redox state as a modulator of the cellular clock

As one of the major effects of pharmacological PPP inhibition is a shift towards a more oxidised cellular redox state (Figure 4.12D), it is possible that the effects on circadian gene expression observed under these conditions is as a result of changes in cellular redox state. In line with this prediction, in collaborative work with Marrit Putker, the effect of application of either reducing reagent 2-mercaptoethanol (2ME) or glucose oxidase (GOX), an enzyme that catalyses glucose to D-glucono-1,5-lactone whilst continuously producing H_2O_2, was investigated (Figure 4.14). Here, the two perturbations were applied at a range of concentrations at two circadian phases. We observed that the application of 2ME reduced the amplitude of the PER2::LUC oscillations, whilst application of GOX produced an initial increase and then a subsequent reduction in in amplitude. Most importantly, as with PPP inhibition, only very minimal effects were observed on the period of the oscillation, with by far the greatest effect of redox perturbation being to reduce the amplitude of PER2 expression. The similarity in the effect of these two treatments suggests that redox perturbation is likely to be the cause of the loss in amplitude of PER2 expression observed during PPP inhibition.

4.2.3 Redox oscillations do not constitute a conserved clock mechanism

Wide-spread observation of circadian rhythms in the abundance of hyperoxidised peroxiredoxins has led to speculation about the presence of a universal “redox oscillator” within cells that might represent an evolutionarily conserved mechanism for circadian timekeeping (Rey & Reddy 2015; Reddy & Rey 2014; Bass & Takahashi 2011). As the primary, although admittedly not the sole, source of both reactive oxygen species (ROS) and cellular reducing equivalents is primary metabolism, the thinking has been that oscillations in metabolic function might be responsible for the circadian variation in redox. The data shown here demonstrates that flux through multiple branches of primary metabolism varies on a circadian basis and therefore could be capable of producing rhythms in both ROS and cellular reducing equivalents although, unlike previous studies in other cell types (O’Neill & Reddy 2011; Wang et al. 2012), this was not sufficiently high amplitude to be directly detected by the methods used here. Furthermore, we demonstrate that changes in cellular redox state, either through metabolic perturbation or direct manipulation is capable of influencing the amplitude of expression of cellular clock proteins.

Both 2ME and GOX treatments and metabolic inhibition provide reducing and oxidative stresses far beyond the physiological range. Despite this, we were unable to observe any major effects of redox perturbation and metabolic inhibition on circadian period; in fact, the period of the oscillation was remarkably robust against large changes in both intracellular and extracellular

redox state. This, and the results of manipulation of primary metabolism, is difficult to reconcile with the hypothesis of a conserved cellular 'redox oscillator' capable of setting and maintaining cellular circadian period. In such a case, one would expect to observe much larger effects of metabolic or redox perturbation on cellular period. Instead, it appears that a certain redox range is permissive for the observation of cellular rhythms, and that cellular redox state is both rhythmically regulated and capable of modulating some aspects of cellular timekeeping, but that rhythmicity in cellular redox state is not essential for the timekeeping mechanism itself.

Chapter 5: Insulin regulates the circadian clock *via* PER2

5.0.1 Introduction

In mammals, time of feeding and light exposure are the two major factors that entrain the phase of the biological circadian clock to the 24 hour cycle of day and night (Damiola et al. 2000). In natural environments, this allows variations in food availability and day length to adjust the phase of an animal's innate circadian rhythm in behaviour and physiology, so that it resonates with and anticipates daily environmental cycles.

The mechanism by which humans, and other mammals, entrain to temporal lighting cues is well established: photic information is detected by photoreceptive cells in the retina, processed by associated retinal ganglion cells, and then relayed to the hypothalamic suprachiasmatic nucleus (SCN) – the mammalian master pacemaker (Berson et al. 2002; Jagannath et al. 2013). The SCN integrates external photic timing cues into its molecular and electrophysiological rhythms, and subsequently synchronises cells across the rest of the brain and body *via* local synaptic and distal humoral communication (Buijs et al., 1999).

Daily feeding cycles are also sufficient to entrain the phase of both cellular and behavioural circadian rhythms (Saini et al., 2013). This is not always immediately apparent when studying animal behaviour, both in the wild and in the laboratory, as animals generally feed during their most active phase, which is primarily determined by the light-dark cycle. It is only when animals

cease to be fed *ad libitum*, either as a result of natural shortage or experimental intervention that it is possible to dissociate entrainment to feeding from entrainment due to light. This is often referred to as a restricted feeding (RF) schedule, where food is only available within a certain time window. If this window is sufficiently out of phase with lighting cues, then animals can be seen to shift their behaviour over time such that their most active phase is in line with the time of food availability, even if this is out of phase with the normal phase of activity with respect to the light-dark cycle (Stokkan et al., 2001). This shift in behaviour is accompanied by a shift in the phase of expression of clock genes within the cells of a wide range of tissue (Saini et al., 2013). This effect is also observed in circadian mutants, which are capable of entraining to feeding cues even if incapable of maintaining a behavioural rhythm in constant conditions (Storch & Weitz 2009).

In contrast to light entrainment, the underlying mechanism by which food entrainment occurs is not understood (Stephan 2002). It is certain that, unlike entrainment to daily light-dark cycles, entrainment to daily feed-fast cycles does not require SCN input, as food entrainment persists following SCN ablation (Marchant & Mistlberger 1997). Furthermore, the SCN itself, unlike the rest of the body, does not show clear changes in phase of clock gene expression in response to feeding cues (Damiola et al., 2000). There must therefore exist alternative, potent and SCN-independent pathways that facilitate entrainment of circadian phase of clock gene expression in peripheral tissues and cells to feeding time (Dattolo et al. 2016).

The nature of these SCN-independent pathways continues to be the subject of some dispute, particularly with regard to two main points. Firstly, the preferred hypothesis for many years has been that there must exist an anatomical locus at which time of feeding information is co-ordinated and relayed to the rest of the body. This would parallel our existing understanding of how the SCN co-ordinates light information. Appreciable effort has been expended by a number of groups in the search for just such a central locus, both within the brain and at other anatomical sites (Stephan, 2002, Gooley et al., 2006, LeSauter et al., 2009). However, to date, no such locus has been identified.

The second major unresolved question with regards to food entrainment concerns the nature of the signal (or signals) that trigger entrainment to feeding cycles. Previous studies have suggested roles for metabolic signals such as post-prandial glucose surge (Stephan & Davidson 1998), as well as more complex hormonal signals, including insulin (Yamajuku et al. 2012; Sato et al. 2014), glucagon (Mukherji, Kobiita, Damara, et al. 2015; Mukherji, Kobiita & Chambon 2015), ghrelin (Verhagen et al. 2011) and oxyntomodulin (Landgraf et al. 2015). However, these studies have mostly focused on cell types that are highly metabolically sensitive, such as liver and adipose tissue, and have been unable to show shifts in behavior or peripheral tissues that are comparable to that seen with food entrainment. As such, work published thus far has not addressed the universal mechanisms of cellular clock entrainment

that would be required for rapid, systemic, SCN-independent synchronisation of peripheral cellular clocks and behaviour to feeding.

This chapter goes some way towards resolving both of the issues described above. These data suggest that the metabolic hormone insulin is sufficient to determine key parameters of the circadian rhythm in multiple cell types in a manner comparable to that observed with food entrainment. Furthermore, I demonstrate that this effect does not require any central co-ordination. Given that biological timekeeping is cell-autonomous, and the failure to identify any dominant neuroanatomical locus for entrainment to feeding cycles, I propose that circadian entrainment to feeding cycles occurs directly in every cell individually, without central co-ordination of a feeding signal.

Insulin and insulin-like growth factor are particularly pertinent candidates for the role of a universal feeding signal, as the insulin receptor (IR) and related insulin-like growth factor receptor (IGFR) are expressed in almost every mammalian cell, and are activated upon feeding by increased circulating levels of insulin and free IGF-1 (Bailyes et al. 1997). Moreover IR and IGFR have overlapping functions and communicate via the same, ubiquitous intracellular signal transduction network. In addition, components of these pathways are highly represented in assays for circadian expression of transcripts (Zhang et al. 2014).

Here, I demonstrate the effects of insulin on mammalian circadian rhythmicity *ex vivo* and *in vitro* and identify a molecular mechanism for its action on the cellular clockwork. Furthermore, I propose a mechanism for this by recapitulating the effect of insulin using a combination of pharmacological and genetic approaches.

5.1 Results

5.1.1 Cell culture supplement B-27® modulates rhythms in PER2

B-27® is a common cell culture supplement, initially devised as a serum-replacement to provide greater consistency for neuronal cell culture, due to its well-defined composition (Brewer et al. 1993). For historical reasons, B-27® is also included as a component in “Air Medium” in addition to serum (Hastings et al 2005). Although this medium was originally designed for the bioluminescent recording of SCN organotypic slices under ambient oxygen and carbon dioxide levels, it has subsequently been widely used for the bioluminescent recording of a variety of cell types in culture. The effect of B-27® on circadian activity in non-neuronal cells has not been investigated, however, any observation of such effects would also have been confounded by the fact that the serum in “Air Medium” is well established to produce effects on subsequent circadian rhythmicity, although the specific factor or factors which stimulates this are unknown (Balsalobre et al., 2000). It is only when cells are changed in a modified “Air Medium”, where serum has been removed, that any effects of B-27® become clear (Fig 5.1A). Under these conditions, cells that are changed into media containing B-27® show a much

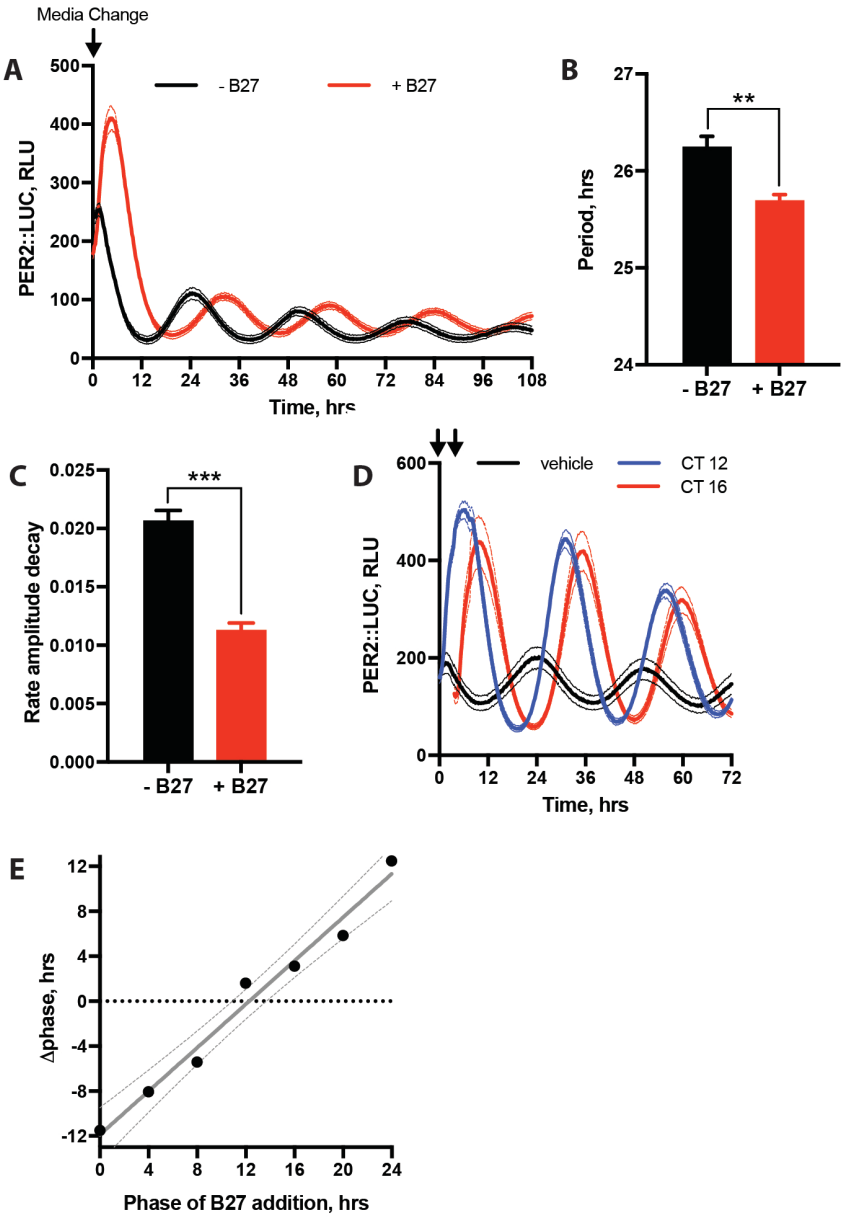

Figure 5.1

B-27® supplement affects rhythms in PER2::LUC fibroblasts

A Media change from standard serum-containing culture media to serum-free media containing media supplement B-27® results in an acute induction of PER2 expression, followed by a shift in phase of PER2 expression (n=4, mean±SEM) **B** The presence of B-27® in serum-free cell medium decreases the period of the oscillation by around 30 minutes (-B-27® = 26.25±0.11 hrs, + B-27® = 25.70±0.06 hrs, Welch's t –test). **C** The rate of dampening of the oscillation was also reduced in the presence of B-27® (-B-27® = 0.02±0.001, + B-27® = 0.01±0.001 , Welch's t –test, not including first 24 hours). **D,E** Phase response curve of insulin addition (n=4±SEM, R^2=0.978).

larger initial increase in PER2::LUC bioluminescence than those cells in the absence of B-27®. B-27® also affects cellular oscillations in the longer term, with cells in the presence of B-27® exhibiting a circadian period approximately 30 minutes shorter than cells in the absence of B-27® (Fig 5.1B). Cells in the

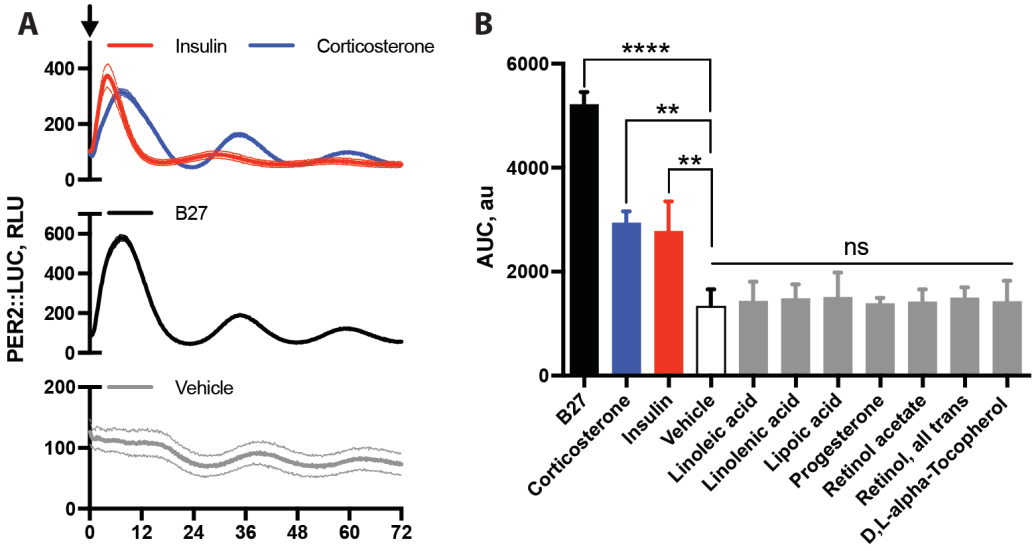

Figure 5.2

Insulin and corticosterone have distinct effects on cellular rhythmicity

A Addition of insulin or corticosterone to PER2::LUC fibroblasts induces PER2 expression (n=3, mean±SEM). Arrow indicates time of addition. Insulin was added at 600nM, corticosterone at 58nM. **B** Of the components of 27® tested, only insulin and corticosterone resulted in a significantly increase level of PER2 expression compared to vehicle within the first 12 hours following addition, as measured by the AUC for this time period (n≥3, mean±SEM, one-way ANOVA, Tukey's multiple comparisons test). **C** The shift in phase produced by insulin is significantly different to that brought about by B27 or corticosterone alone (n=3, mean±SEM, one-way ANOVA, Tukey's multiple comparisons test).

presence of B-27® also show a reduced rate of amplitude damping when fitted to a damped cos wave (constant k, Fig 5.1C). However, most striking is the fact that addition of B-27® to produces strong type 1 resetting of the cellular oscillation (Fig 5.1D).

As described above, B-27® was originally designed as a serum replacement and as such, it contains a number of different components. In order to determine which of these might be responsible for the effect of B-27® on PER2 expression, components were added to cells in serum and B-27®-free media in isolation and the effect on the subsequent PER2 oscillation recorded (Fig 5.2A). As an induction in initial PER2 expression was a key feature of the effect of complete B-27® PER2 expression, the effect of B-27® components was quantified using the area under the curve in the first 12 hours following B-27® addition, this being a measure for PER2 expression (Fig 5.2B). Using this criterion, only two factors had a significant effect of PER2: corticosterone and insulin. The capacity of corticosterone and other glucocorticoids to influence cellular rhythmicity has been previously described by a number of groups to selectively induce PER expression through activation of glucocorticoid response elements and was thus not particularly surprising (Balsalobre, Brown, et al. 2000; Cheon et al. 2013). In contrast, effects of insulin on cellular rhythms in fibroblasts have not previously been reported, and so this phenomenon was investigated further.

5.1.2 Insulin administration induces PER2 to modulate phase, period and amplitude of cellular rhythms.

Administration of insulin to PER2::LUC fibroblasts resulted in an acute induction of PER2 expression (Fig 5.3A), a sustained increase in the

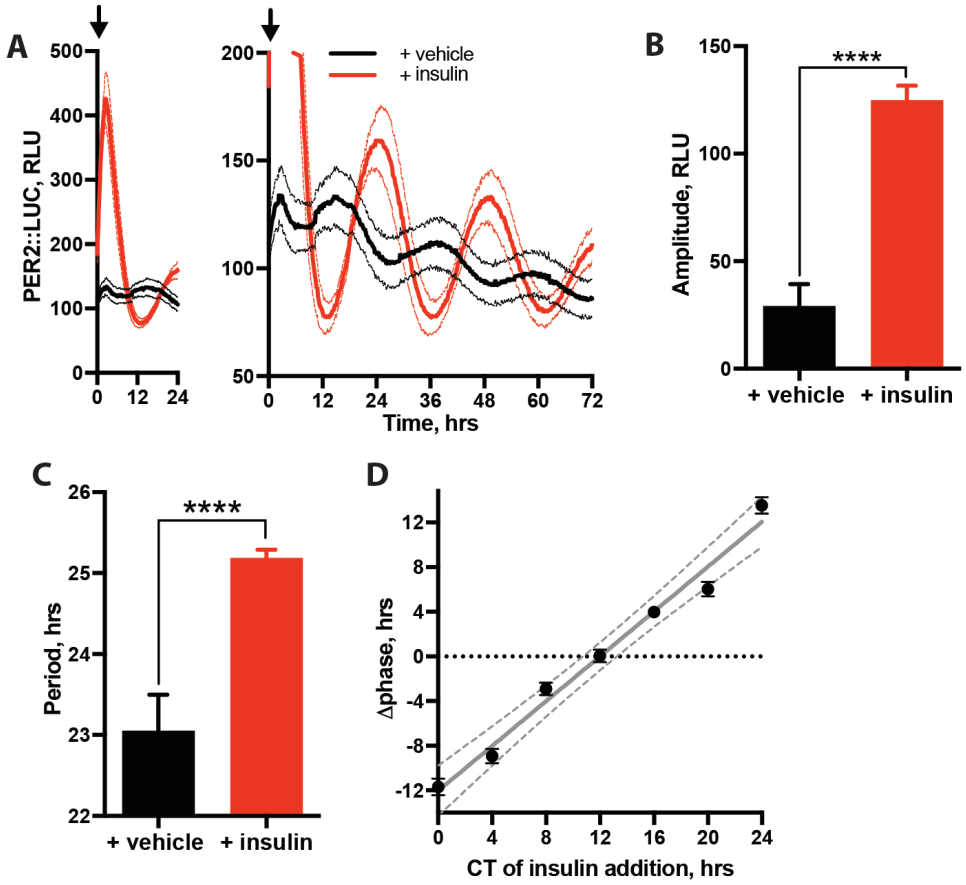

Figure 5.3

Insulin alone influences all aspects of cellular rhythms

A (Left panel) Addition of insulin stimulates a rapid increase in PER2 expression, (Right panel) followed by a shift in the phase of the PER2 oscillation (n=4, mean±SEM). **B** Insulin also significantly increases the amplitude of the resultant oscillation, as measured at the first circadian peak (n=4, mean±SEM). **C** Addition of insulin results in an increase in circadian period from 23.05±0.44 without insulin to 25.19±0.10 with insulin (n≥8, mean±SEM). **D** Phase-response curve of time of insulin addition against resultant circadian phase shows type 0 resetting, with a first order polynomial as the preferred fit (extra sum-of-squares F-test, n=4, mean±SEM).

amplitude of circadian gene expression (Fig 5.3B) and an approximately 2-hour increase in the period of the oscillation (Fig 5.3C). These effects were observed independent of the circadian phase at which insulin was applied. Moreover, insulin significantly affected the subsequent phase of cellular PER2::LUC rhythms, resetting the cellular clock to the same circadian phase (CT12) regardless of the biological time of insulin addition (Fig 5.3D). Importantly, insulin concentrations as low as 1nM were sufficient to affect cellular rhythms, well within the physiological range (0.5-50nM) (Fig 5.4A).

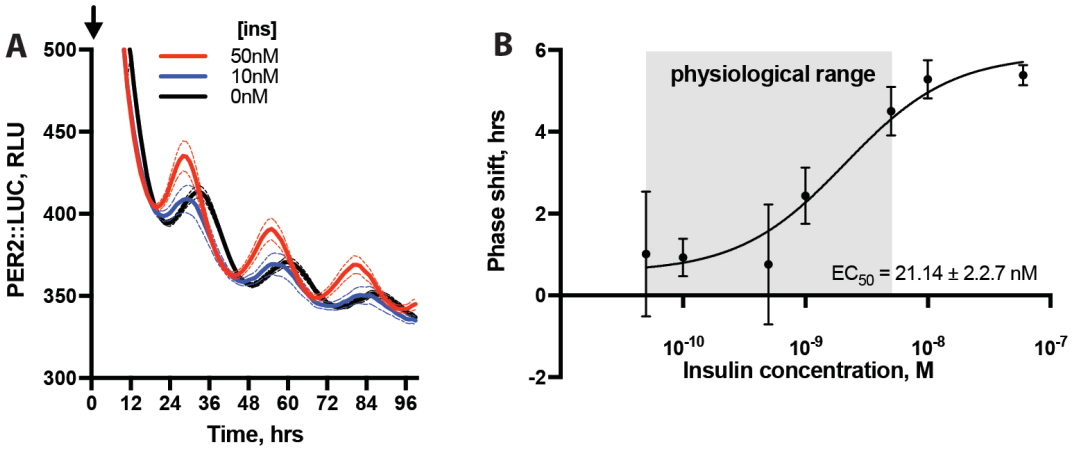

Figure 5.4

Insulin dose-response curve

A Representative traces from insulin dose-response curve. Cells were treated at CT 0 (n=4, mean±SEM). **B** Dose response curve for insulin concentration against subsequent phase shift. Insulin was added at CT 0. EC_{50}= 21.14±2.27 nM (n=6, mean±SEM).

However, as with most experiments performed *in vitro,* the kinetics of drug exposure in static culture differ greatly from conditions encountered *in vivo*, due to a number of factors such as lack of clearing mechanisms. We therefore assessed the impact of transient exposure to insulin, which we assume to be

more reflective of the natural post-prandial insulin surge. Cells exposed to a single 3-hour bolus of insulin under perfusion (Fig 5.5A) exhibited the same acute induction of PER2 that we observed in static cultures (Fig 5.5B).

Thus, insulin is sufficient to determine the phase, period and amplitude of circadian gene expression rhythms as reported by PER2::LUC, the essential parameters of the cellular circadian clock, in cultured mammalian cells. These observations are of particular interest when considered in the context of mammalian circadian entrainment to feeding cycles, as described in the introduction to this chapter, as one could consider insulin as a potential coordinating signal in response to feeding. However, as entrainment to food influences circadian gene expression in a large number of different tissues (Damiola, Le Minli, et al. 2000), for insulin to be a possible candidate for

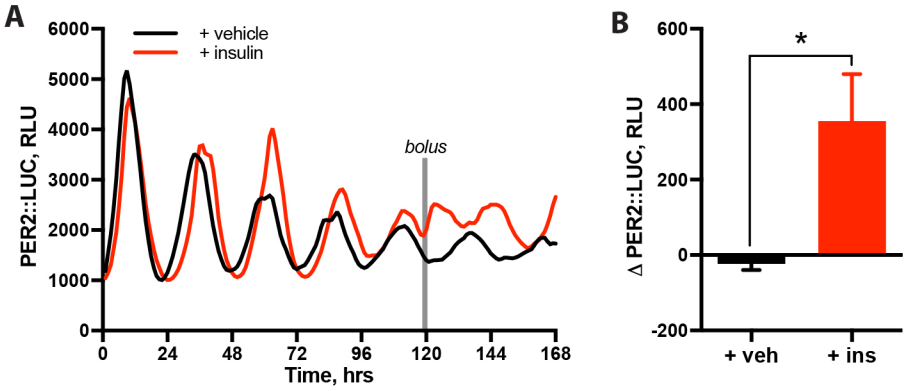

Figure 5.5

Rhythms in perfused cultures are affected by transient insulin treatment

A Application of insulin as a 3-hour bolus to cells in perfused culture also induces an acute increase in PER2 expression (representative, n≥3±SEM).

B Quantification of the acute increase in PER2 following insulin application under perfused culture (n≥3±SEM, Welch's t-test).

signaling entrainment to food, it must show the capacity to influence rhythms in a similar manner in most, if not all, mammalian tissues.

5.1.3 Insulin is chronoactive in primary cells and tissues

To explore the relevance of these observations in immortalised fibroblasts to other mammalian tissues, insulin addition experiments were repeated using primary dissociated cortical neurons (Fig 5.6A,B) and organotypic lung and kidney slices (Fig 5.6C) isolated from PER2::LUC mice. These experiments were also repeated using primary fibroblast cultures (Fig 5.6DE). In all cases, a rapid induction of PER2 expression, increased amplitude of reporter rhythms and shifts in phase following insulin addition were observed. Since acute changes in PER protein levels are a ubiquitous mechanism by which cellular clocks adjust to external timing cues across all tissues (Chen et al. 2009), the rapid response of PER2 to insulin supports the role of insulin as a potential entraining factor. One can therefore hypothesize a general mechanism by which time-of-feeding is communicated by insulin and adjusts the phase of clock gene expression in every cell of the body *in vivo* to resonate with any external cycles of food availability.

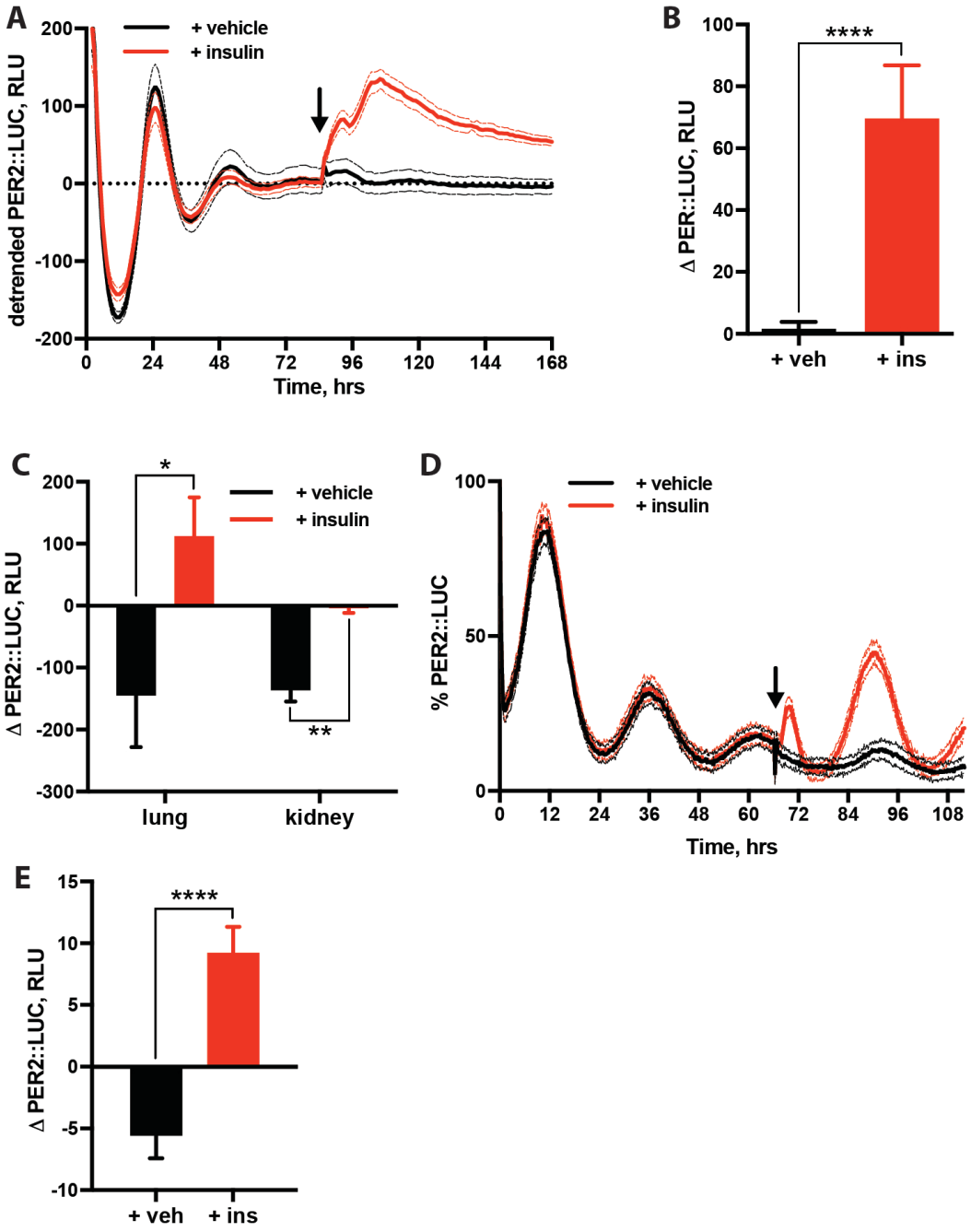

Figure 5.6

Insulin affects circadian gene expression in a wide range of tissues

A,B Addition of insulin to dissociated cortical neurons induces PER2 expression (n=8±, meanSEM, Welch's t-test). **C** Insulin also induces PER2 expression in organotypic slices of lung and kidney (n≥4, mean±SEM, Welch's t-test). **D,E** The induction following insulin is also observable in primary PER2::LUC fibroblasts (n=4, mean±SEM, Welch's t-test).

5.1.4 Insulin also affects clock gene expression in the SCN

The suprachiasmatic nucleus of the hypothalamus (SCN) is the central circadian pacemaker in mammals, coordinating circadian organization of behaviour and physiology with the 24 h light:dark cycle of the natural world. Unlike the rest of the body, the SCN does not respond to temporal shifts in feeding schedule (Damiola, Le Minh, et al. 2000). However, as SCN neurons express insulin receptors (Anhê et al. 2004) and both insulin and IGF-1 are capable of crossing the blood-brain barrier (Reinhardt & Bondy 1994), the SCN should therefore be capable of responding to feeding-related insulin signals. It was therefore hypothesized that strong interneuronal circadian coupling within the SCN might account for this apparent contradiction, rendering the SCN robust against feeding cues, as it is to temperature (Buhr et al. 2010). To test this, organotypic SCN slices from PER2::LUC mice were treated with insulin in the presence or absence of tetrodotoxin (TTX, 1µM), a Na^+-channel blocker (this experiment was performed by Ryan Hamnett). This revealed that insulin profoundly affects the SCN clock, but only in the absence of action potential generation (Fig 5.7A,B). Interestingly, the resultant waveform had two distinct peaks, suggesting that there might exist both insulin-sensitive and insulin-insensitive populations within the SCN, revealed by the uncoupling effect of TTX (Yamaguchi et al. 2003). Further analysis of TTX and insulin-treated SCN slices imaged using an EMCCD camera showed a lateral region of the SCN to be particularly responsive to insulin and to display this splitting pattern, which dorsal and ventral regions did not (Fig 5.E,F). In control SCN slices, insulin had no significant effect on the phase or

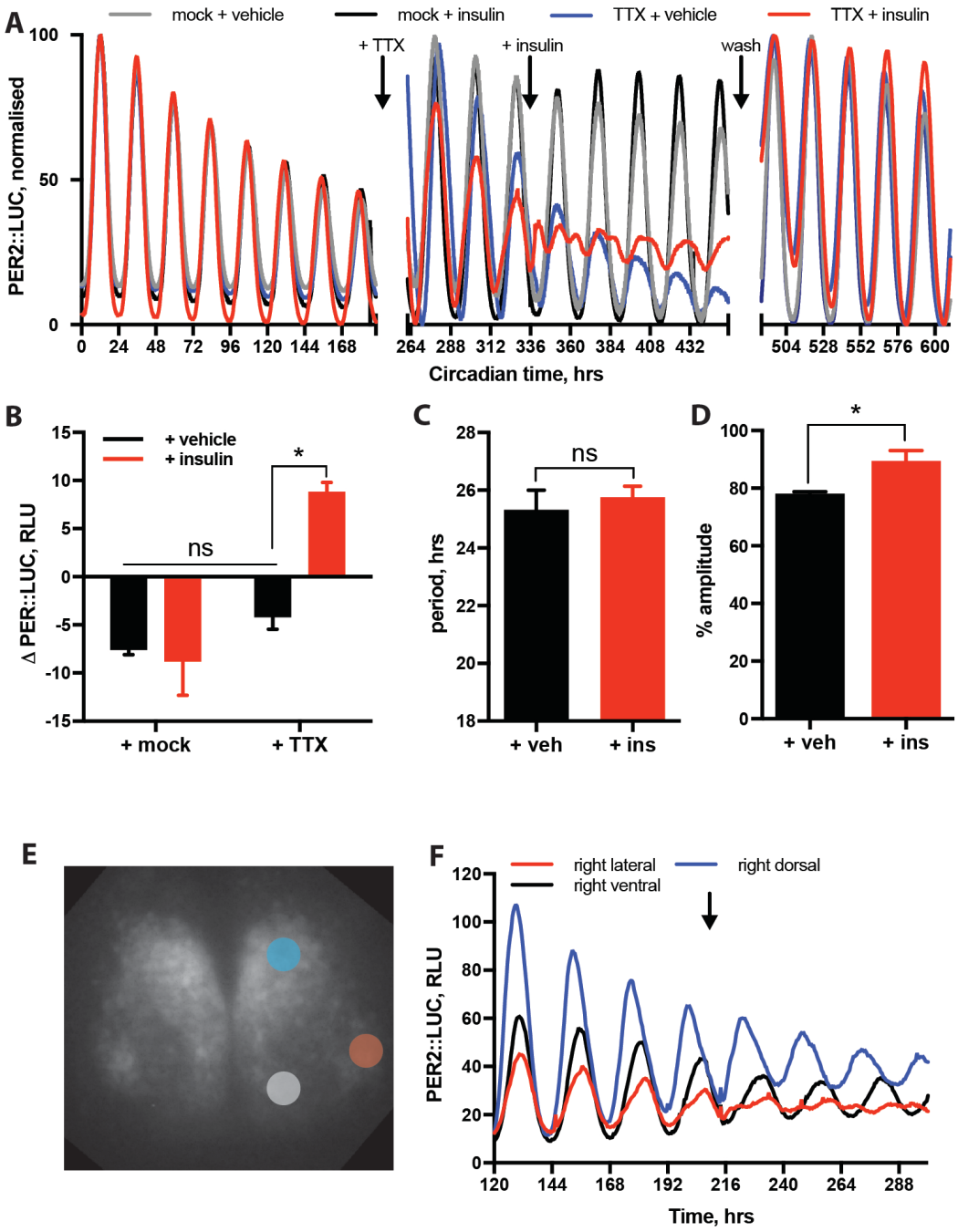

Figure 5.7

SCN network properties provide robustness to insulin

A Addition of insulin to intact organotypic slices of the SCN does not induce PER2 expression, nor does it affect the phase or period of the oscillation. In contrast, slices pre-treated with TTX show both an acute induction in PER2 expression and a change in the waveform following addition of insulin (n≥3, representative). **B** Quantification of the PER2 induction following insulin treatment in intact and TTX-treated SCN slices (n≥3±SEM, Welch's t-test).

Continued on next page

C Addition of insulin to intact SCN slices has no significant effect on the period of the oscillation (n≥3, mean±SEM, Welch's t-test). **D** Addition of insulin to intact SCN slices does result in a modest increase in the subsequent amplitude, as measured over the 3 successive cycles (n≥3, mean±SEM, Welch's t-test). **E** Schematic showing representative sub-regions of the SCN sampled. **F** Lateral regions of the SCN showed an ability to respond to insulin not observed in ventral or lateral regions (n=3, representative). SCN slices were taken and treated by Ryan Hamnett.

period of PER2 rhythms (Fig 5.7C), although we did observe a small but significant increase in PER2::LUC amplitude (Fig 5.7D) when insulin was applied during the falling limb of expression (CT20) but not during the rising limb (data not shown), suggesting that insulin might act phase-dependently to amplify SCN rhythms when feeding cues are received at the appropriate biological time.

5.1.5 The increase in bioluminescent signal following insulin is specific to PER2

To examine the selectivity of insulin action upon PER2::LUC, we compared the bioluminescent response in PER2::LUC fibroblasts with control fibroblasts stably expressing firefly luciferase under the SV40 promoter. In contrast with PER2::LUC, insulin administration did not affect bioluminescence from mouse fibroblasts expressing luciferase constitutively, demonstrating that insulin induction of PER2::LUC does not reflect an increase in luciferase activity or global translation but results from the targeted up-regulation of certain proteins, including PER2 (Fig 5.8A). Supporting this, administration of insulin to fibroblast cultures expressing cry1:LUC, (CRY1 being a repressive partner

to PER2) did not result in an acute induction of *Cry1* promoter activity but did shift the phase of gene expression (Fig 5.8B). Western blotting for CRY1, as well as CRY2 and PER1 did not show a significant increase in the abundance of these proteins following insulin treatment (Fig 5.8C,D,E,F). This suggests that, given the pivotal role of PER proteins in circadian gene expression rhythms, insulin elicits an acute and selective induction of PERIOD protein expression.

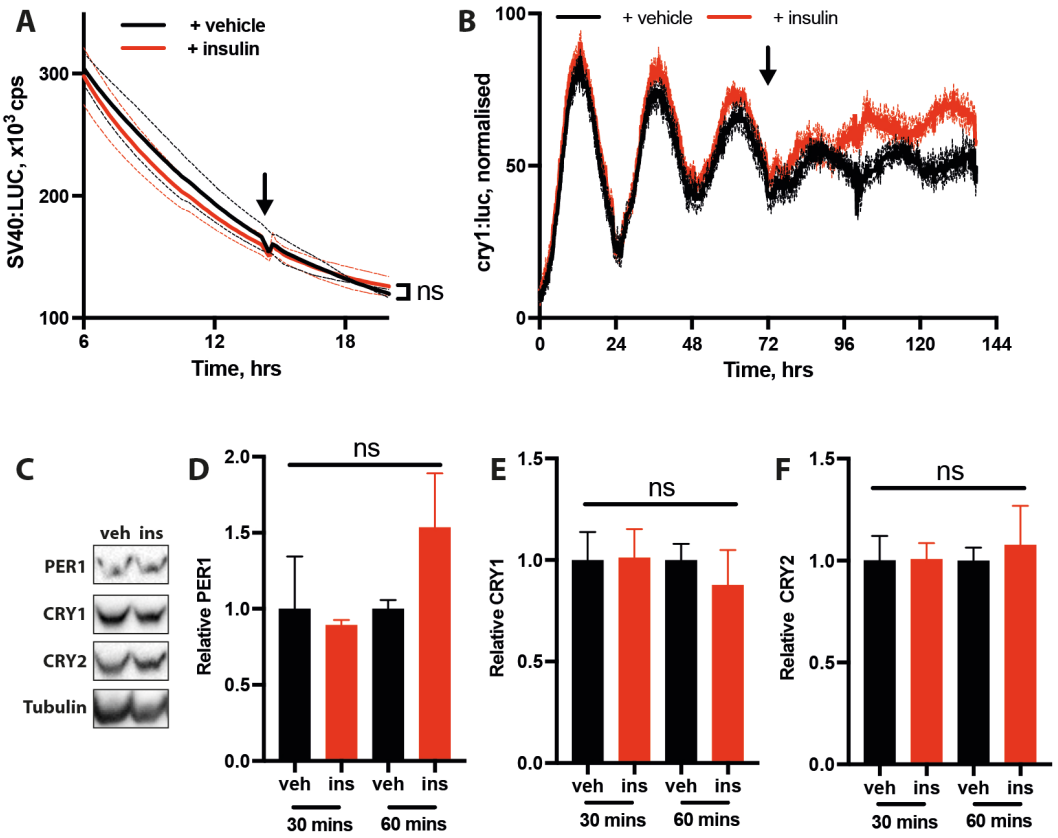

Figure 5.8

Increase in protein expression has specificity for PER2

A Addition of insulin to fibroblasts expressing SV40:Luc does not affect luciferase activity (n=3, mean±SEM, two-way ANOVA). **B** Addition of insulin to cry1:Luc fibroblasts does not produce an acute induction in cry1:Luc signal, but does produce a subsequent change in phase of expression (n=4, mean±SEM). **C** Representative western blot following insulin treatment. Samples shown were treated for 60 minutes. **D,E,F** Quantification of western blots (n=3, mean±SEM).

5.1.6 Increase in PER2::LUC signal does not require the TTFL

Another pertinent question when looking at the circadian response to insulin is whether this response requires a functioning canonical timekeeping mechanism. A significant body of literature shows that animals that lack essential timekeeping genes still show the capacity to entrain their behaviour to times of food availability (Pitts et al., 2003, Storch and Weitz 2009). The exception to this is PER2, where animals carrying $PER2^{bdrm1}$ have been shown have an impaired ability to entrain to food (Feillet et al., 2006). As such, for insulin to be a good candidate for a major entraining stimulus in response to feeding, one would expect to see effects on PER2 persist in the absence of these timekeeping genes. The effect of insulin on cells lacking either *Bmal1* or cells lacking both *Cry1* and *Cry2* was therefore investigated (Fig 5.9A,B). Both cells lines showed a significant increase in PER2::LUC bioluminescence following insulin addition, although the magnitude of this effect was small in $Bmal^{-/-}$ cells compared to their $Cry1^{-/-}/Cry2^{-/-}$ counterparts. It was hypothesized that this was a result of the low activity at the PER2 promoter in the absence of BMAL1. This was confirmed by the observation that the relative magnitude of the PER2 induction by insulin could be greatly increased if cells were treated with forskolin and IBMX for at least 24 hours prior to insulin addition (Fig5.9C,D). As forskolin is documented to increase *Per2* mRNA abundance in this timeframe (Yagita and Okamura, 1999), it appears that increased availability of the PER2 transcript may be implicated in this increased response. This observation is further addressed below.

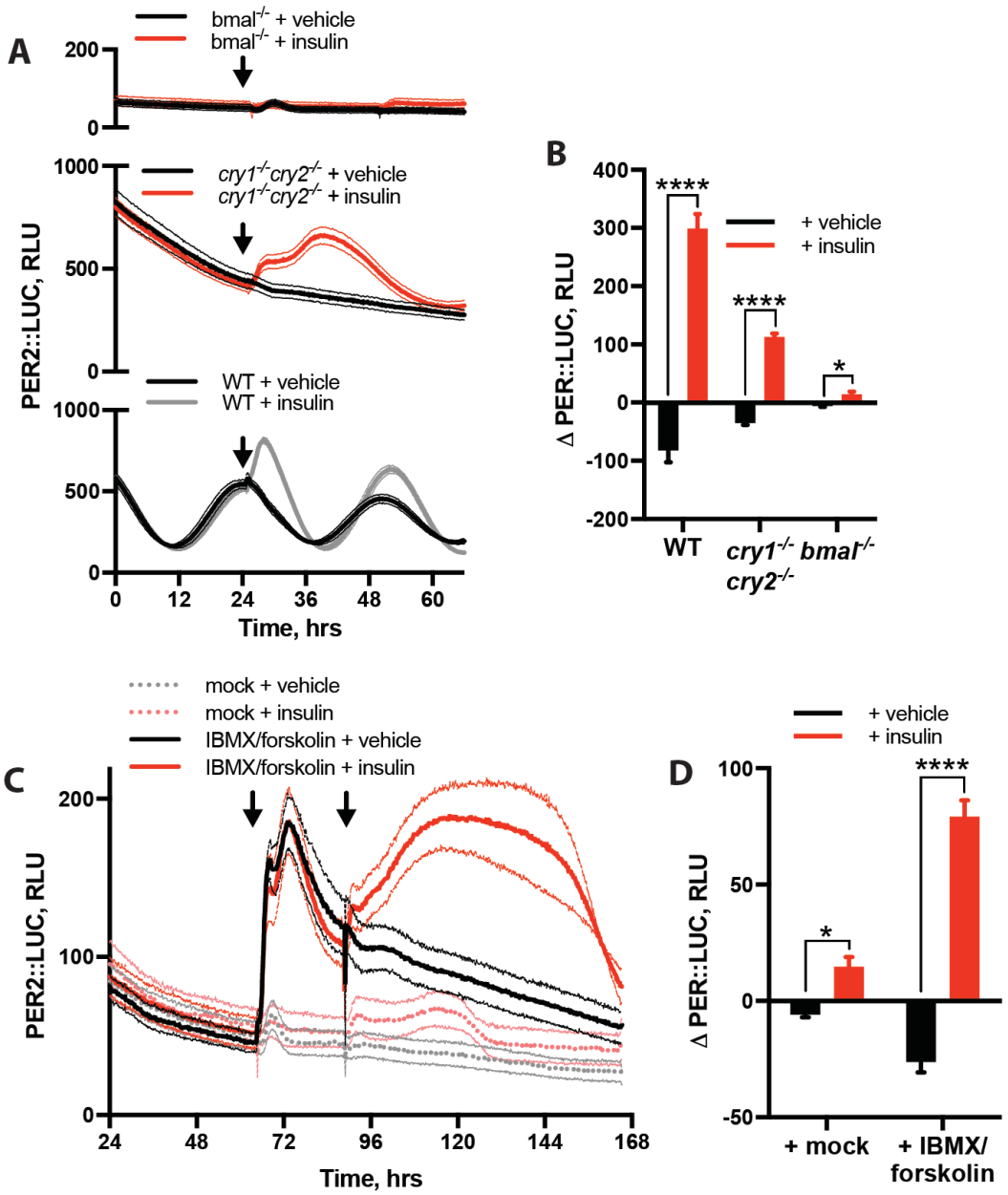

Figure 5.9

Insulin-induced increase in PER2 persists in the absence of the TTFL

A, B The acute increase in PER2 expression following insulin addition persists in cells lacking essential components of the canonical mammalian circadian clock, BMAL1 and CRY1/2 (n≥3, mean±SEM, Welch's t-test). **C,D** The acute response to insulin can be amplified in cells lacking BMAL1 by subjecting the cells to prior treatment with IBMX and forskolin (n≥3, mean±SEM, Welch's t-test).

5.1.7 Effects of insulin are modulated under specific kinase inhibition

Casein kinase 1 (CK1) and glycogen synthase kinase 3 (GSK3) are two well conserved kinase families which, in addition to a wide range of other roles within the cell, have been demonstrated to influence the period cellular rhythms across kingdoms, although their proposed targets differ (Meng et al., 2010, Hirota et al., 2008). Furthermore, GSK3 is a well-established part of the insulin signaling cascade. It is therefore plausible that either of these kinases might be involved in the PER2 response to insulin. To test this, insulin was added to PER2::LUC fibroblasts in the presence of either CK1 inhibitor PF-670462 (Fig 5.10A,B) or GSK3 inhibitor CHIR-99021 (Fig 5.10C,D). Whilst inhibition of GSK3 had no significant effect on the PER2 response, inhibition of CK1 resulted in a significant increase in the PER2 response following insulin. As phosphorylation by CK1 is required for nuclear translocation of PERIOD proteins (Lee et al. 2011), thereby allowing them to repress the activation of their own promoter, the increase in the PER2 induction seen in the presence of CK1 inhibition may either be the result of greater PER2 promoter activation or greater PER2 accumulation in the cytoplasm. In the context of mammalian entrainment to feeding, this lends further support to insulin as a major feeding signal, as mice lacking CK1ε show capacity to entrain to feeding faster than wild-type animals (Pers. Comm., David Bechtold).

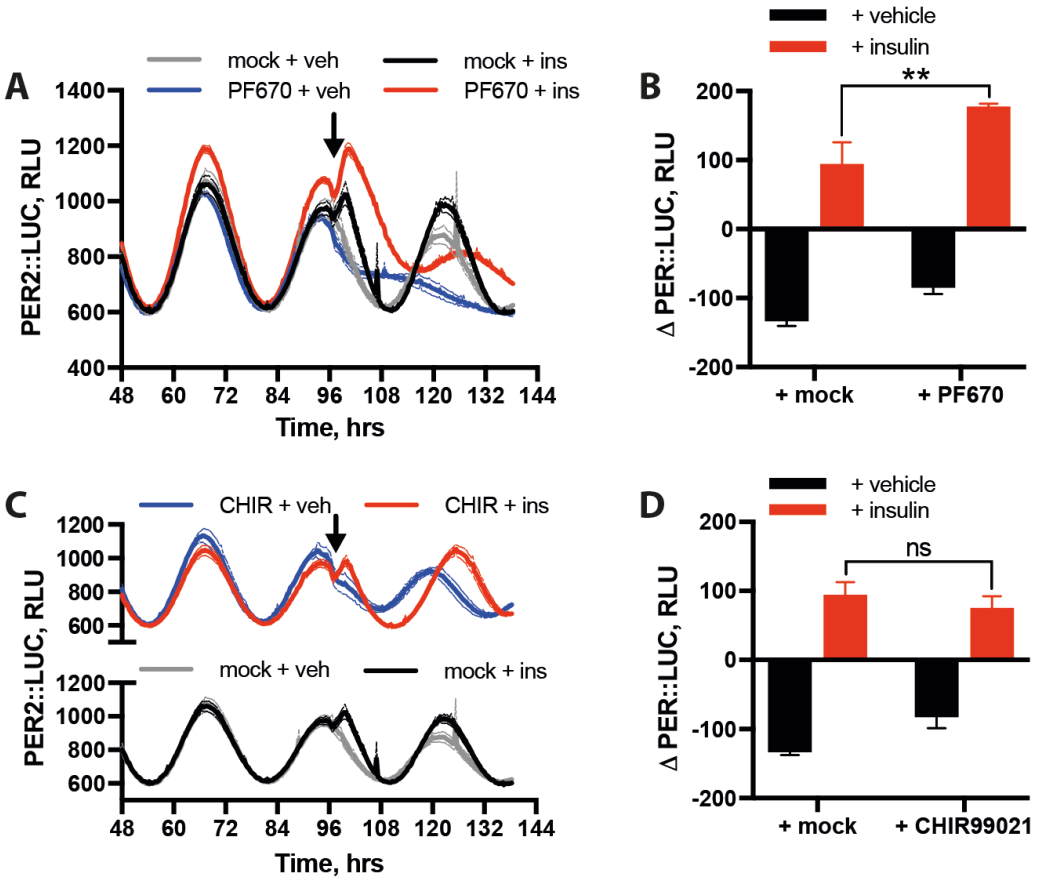

Figure 5.10

Effects of insulin are modulated by selective kinase inhibition

A The induction in PER2 following insulin is significantly increased in cells pre-treated with inhibitor of casein kinase 1 PF-670462 (n=4, mean±SEM). **B** Quantification of the acute increase in PER2 expression following insulin in the presence or absence of 3μM PF-670462 (two-way ANOVA, Tukey's multiple comparisons test). **C** Inhibition of glycogen synthase kinase 3 with CHIR-99021(3 μM) has no significant effect on the PER2 induction following insulin (n=4, mean±SEM). **D** Quantification of the acute increase in PER2 following insulin in the presence and absence of CHIR-99021 (two-way ANOVA, Tukey's multiple comparisons test).

5.1.8 Increased PER2::LUC bioluminescence indicates increased PER2 translation

Following the addition of insulin to PER2::LUC fibroblasts, a significant increase in the total bioluminescent signal from these cells is observed in under 1 hour (Fig 5.11A,B). This is reflective of an increase in the abundance of PER2 protein. Insulin is reported to increase ribosome association and so translation of certain transcripts, often through recognition of certain sequences in the 5' UTR of the transcript, such as TOP or TISU sequences (Gandin et al. 2016). Transcripts containing these elements have also been previously shown to be circadian regulated in response to feeding cycles (Atger et al. 2015). Although no such element could be clearly identified in the *Per2* transcript, it was nevertheless hypothesized that increased association of the *Per2* transcript with ribosomes might be observed following insulin addition. To test this, cells were lysed and polysome fractions (with simultaneous UV spectra) collected by average density after one hour of insulin treatment. qPCR was then performed on all fractions. This showed a significant difference in the distribution of Per2 mRNA across fractions in insulin-treated cells when compared to the vehicle-treated condition (Fig 5.11C), thereby suggesting altered recruitment of Per2 mRNA to translational machinery.

5.1.9 The acute PER2 response to insulin does not require transcription

For the abundance of a cellular protein to increase, one of three processes must occur: an increase in transcription and translation, an increase in

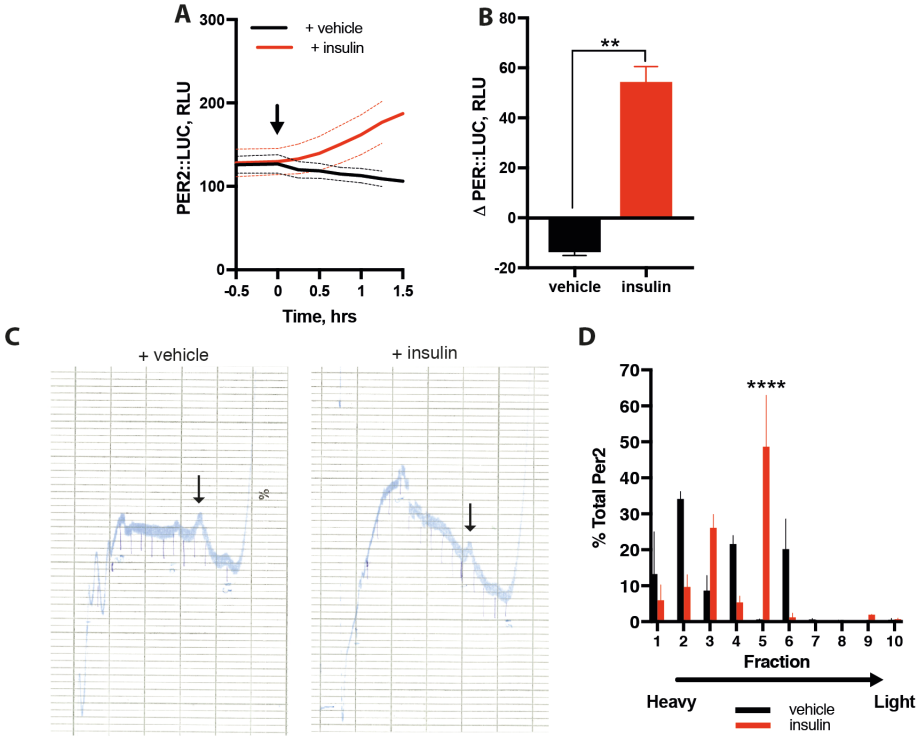

Figure 5.11

Increased PER2::LUC bioluminescence is the result of increased PER2 translation

A,B A significant increase in the bioluminescent signal produced by PER2::LUC cells can be observed within one hour of insulin application (n=4, mean±SEM, Welch's t-test). **C** Representative UV polysome trace of cells 1 hr after the addition of insulin or vehicle. Arrow indicate 80S peak. **D** Polysome fractionation of cells treated with insulin shows a significant shfift in the location of available Per2 transcript compared to the untreated condition (n=3, mean±SEM, Welch's t-test).

translation of existing mRNA or a decrease in protein degradation. When PER2 abundance increases during the cellular circadian oscillation, this increase is largely attributable to increased *Per2* mRNA levels and their ensuing translation (Lowrey and Takahashi 2004; Putker et al, submitted). As such, one might well assume the increase in PER2 protein abundance following insulin addition most likely to be the result of increased transcriptional activity.

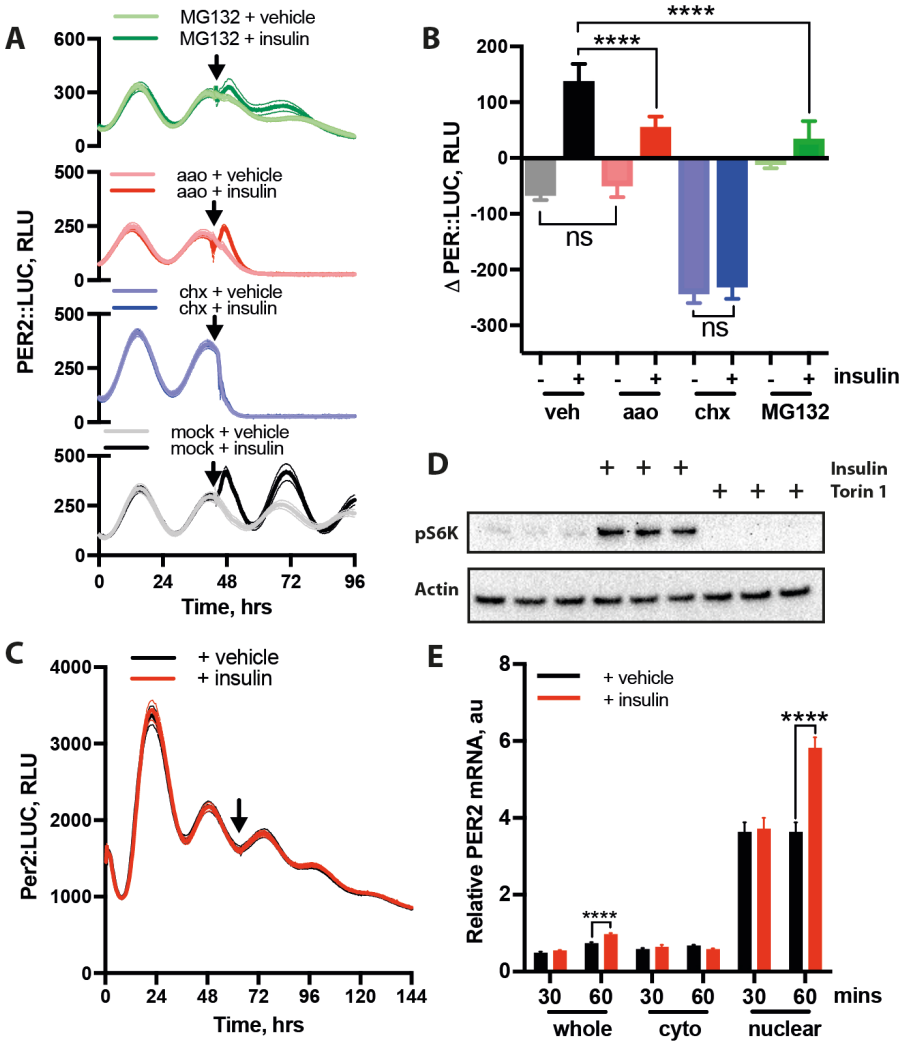

Figure 5.12

Initial increase in PER2 translation does not depend upon transcription

A Acute increase in PER2 expression following insulin is still observed in the presence of transcriptional inhibitor alpha-amanatin oleate (aao, 200μM), but not in the presence of translational inhibitor cycloheximide (chx, 17μM). Addition of inhibitor of proteosomal degradation MG132 (10μM) does not recapitulate the effect of insulin (n≥3, mean±SEM). **B** Quantification of the induction in PER2 expression in the presence of these inhibitors (two-way ANOVA). **C** Cells expressing reporter of Per2 transcription Per2:Luc do not show an acute induction in luciferase expression following insulin addition (n=4, mean±SEM).

Continued on the next page

D 3T3 fibroblasts expressing Per2:LUC still show robust phosphorylation of S6 kinase following insulin addition. All phosphorylation is abolished in the presence of mTOR inhibitor torin1 (n=3, all replicates shown). **E** qPCR at 30 and 60 minutes following insulin addition show no significant increase in PER2 transcript in any fractions after 30 minutes and still no increase in cytoplasmic transcript after 60 minutes (n=5, mean±SEM).

In order to confirm the basis of the increase in PER2 protein abundance, the persistence of the PER2 induction was investigated in the presence of pharmacological inhibitors of transcription (α-amanatin oleate, aao), translation (cycloheximide, CHX) and proteosomal degredation (MG132) (Fig 5.12A,B). Although a significant attenuation of the insulin response was observed, aao did not reduce the acute induction of PER2 to mock-treated levels, nor did addition of MG132 recapitulate the effect of insulin, suggesting that neither an increase in transcription nor a decrease in proteosomal degradation is sufficient to explain the increase in PER2 expression following insulin addition. Cycloheximide abolished the bioluminescent signal in both conditions, as did inhibitor of cap-dependent translation 4EGI-1 (Fig 5.13A,B).

This absence of increased *Per2* transcription despite increased PER2 protein abundance is supported by the observation that cells expressing the reporter of *Per2* transcription, Per2:LUC, despite retaining insulin sensitivity (Fig 5.12D), do not show an acute increase in bioluminescent signal following insulin addition (Fig 5.12C). This suggests that the change in bioluminescent signal observed in the PER2::LUC line is due to the use of a translational

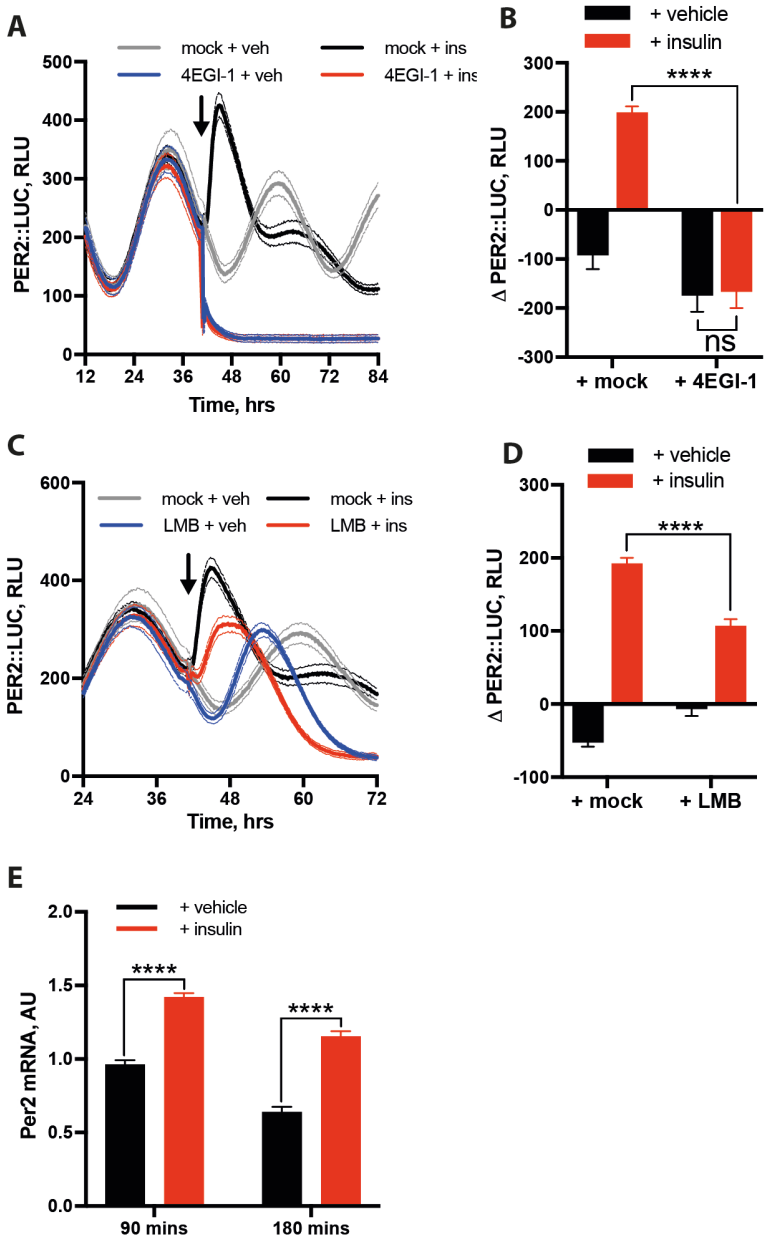

Figure 5.13

Inhibition of nuclear export attenuates the PER2 response to insulin

A 4EGI-1, an inhibitor of cap-dependent translation, completely abolishes the response of PER2 to insulin (n=4, mean±SEM). **B** Quantification of PER2 induction in the presence and absence of 4EGI-1 (two-way ANOVA). **C** Pre-treatment with leptomycin B (LMB), an inhibitor of nuclear export, attenuates the response of PER2 to insulin treatment (n=4, mean±SEM). **D** Quantification of the acute PER2 induction in the presence and absence of LMB (two-way ANOVA). **E** qPCR showing PER2 levels at 90 and 180 minutes following insulin addition (n=4, mean±SEM, two-way ANOVA).

shift due to insulin is expected. Furthermore, and perhaps most strikingly, qPCR analysis of insulin-treated cells at 30 and 60 min following insulin application showed no significant increase in *Per2* mRNA in any cellular fraction at 30 minutes following insulin addition and no increase in cytoplasmic *Per2* mRNA after 1 hr (Fig 5.12D), despite a significant increase in PER2::LUC protein levels occurring within this timeframe (Fig 5.11A,B).

It does appear however that some movement across the nuclear membrane is required for the full response to insulin to occur, as cells pre-treated with nuclear export inhibitor leptomycin B (LMB) show an attenuated, although still highly significant, response to insulin (Fig 5.13C,D). It is possible that this represents a later transcriptional component of the PER2 response to insulin. This concept of a secondary transcriptional component to the PER2 response is supported by the observation that although an increase in *Per2* mRNA is not observed at 30 minutes following insulin, and not in the cytoplasm at 60 minutes (Fig 5.12 D), a much greater abundance of the *Per2* transcript is observed at 90 and 180 minutes following insulin addition (Fig 5.13E).

From these data, it is reasonable to conclude that the initial increase in PER2 following insulin addition results from increased translation of pre-existing *Per2* mRNA. This conclusion is strengthened by the earlier observation that insulin produced only a small (but significant) increase in PER2 levels in cells that lack Bmal1, a transcription factor that is essential for E-box-mediated activation of Per2 transcription (Fig 5.9A,B). However, when we stimulated *Per2* mRNA production in these cells, *via* promoter Ca^{2+}/cAMP-response

elements using forskolin/IBMX (Fig 5.9C,D), we observed that insulin addition did elicit greatly increased PER2 levels. In light of the observation that insulin increases *Per2* mRNA association with single (non-polysomal) ribsosomes (Fig5.10D), we can infer that the greater increase in signal that we see in this condition is due to the increased pool of untranslated *Per2* in the cytoplasm which is available for translation following stimulation with insulin.

5.1.10 Glucose alone does not elicit the PER2 response to insulin

The experiments reported above reveal a pronounced effect of insulin on PER2 expression in *ex vivo* tissue culture and cell lines *in vitro*. We next sought to define the mechanism by which insulin selectively increases PER2 expression. We first confirmed that the effect of insulin is indeed due to IR/IGFR activation, by confirming that in the presence of the dual IR/IGFR antagonist, BMS-754807, the acute increase in PER2 expression was very significantly reduced (Figure 5.14A,B).

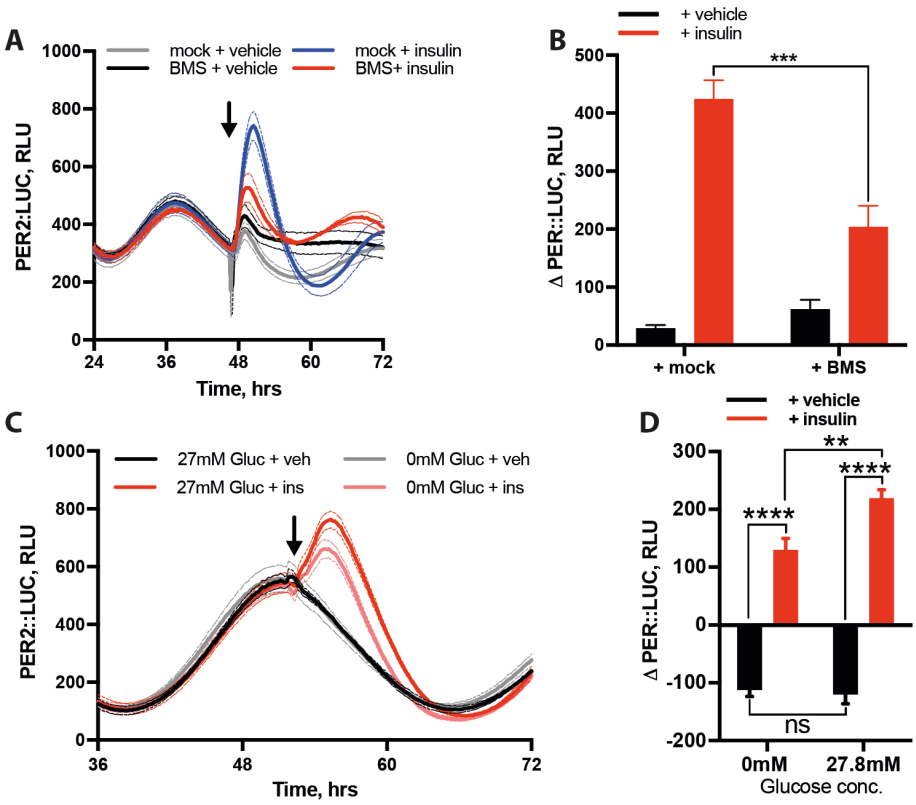

Figure 5.14

PER2 induction following insulin is not the result of increased glucose uptake

A,B Inhibition of IR and IGF-1R with 1μM BMS greatly attenuates the PER2 increase following insulin (n=4, mean±SEM, two-way ANOVA). **C** An acute induction in PER2 expression is observed in the absence of extracellular glucose (n=4, mean±SEM). **D** Quantification of the induction in PER2 luciferase following insulin addition in the presence and absence of extracellular glucose (two-way ANOVA, Tukey's multiple comparisons test).

One of the effects of insulin in many cell types is to increase cellular uptake of glucose, primarily through translocation of vesicles containing new GLUT3 or GLUT4 transporters to the membrane (Uemura and Greenlee, 2005, Lizunov et al., 2005). Previous work has suggested that changes in glucose have the capacity to modulate cellular rhythms (Hirota et al. 2002). To determine whether the effects on PER2 that we observe following insulin were simply the

result of increased intracellular glucose, insulin was added to cells in the presence and absence of extracellular glucose (Fig 5.14C,D). Although the absence of extracellular glucose did slightly attenuate the effect of insulin, a clear induction was still observed, suggesting that increased glucose uptake alone is not the primary event responsible for increased PER2 expression following insulin, although it does facilitate higher translation rates following the induction.

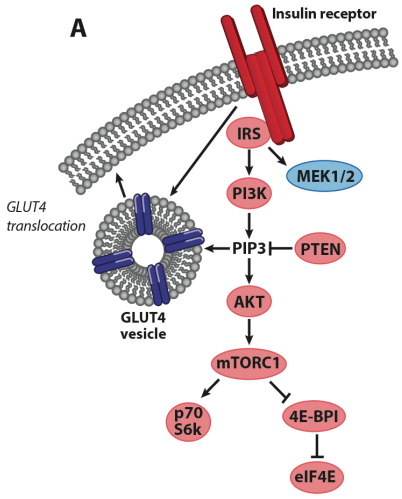

Figure 5.15
Schematic showing the major effectors in the insulin-signalling cascade

5.1.11 PER2 response to insulin is dependent on PI3K signaling

Ligand binding at the insulin receptor results in the activation of two signal transduction pathways: Mitogen-activated Protein Kinase (MAPK) and Phosphatidylinositol-3-Kinase (PI-3K, Fig 5.15), which then activate their respective downstream signaling cascades (Siddle 2011). To determine which arm of the insulin signaling pathway was responsible for PER2 induction, we targeted each of these enzyme families pharmacologically using MAPK inhibitor UO126 and PI-3K inhibitor LY294002 (Fig 5.16A,B). MAPK inhibition had no significant effect on the response to insulin in PER2::LUC cells, whilst

LY294 treatment abolished any PER2 response to insulin. This implicates PI-3K as the primary effector pathway from the insulin receptor to PER2 expression.

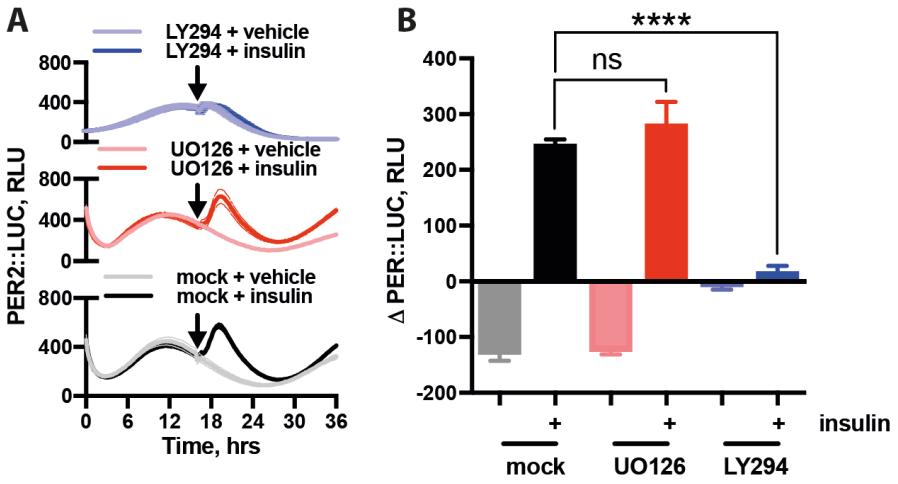

Figure 5.16

PI3K is required for PER2 response to insulin

A Inhibition of MEK1/2 with UO126 (4μM) has no significant effect on the insulin-induced change in PER2 expression, whilst PI3K inhibitor LY294002 (100 μM) abolishes the induction due to insulin (n=4, mean±SEM). **B** Quantification of the acute insulin-induced PER2 response under PI3K and MEK1/2 inhibition (two-way ANOVA, Tukey's multiple comparisons test).

5.1.12 Insulin-induced PER2 increase occurs through mTOR

Once activated, PI-3K phosphorylates protein kinase B (PKB/Akt), for which downstream targets include activation of mTOR. Pharmacological inhibition of mTOR (via rapamycin and torin 1) produced significant attenuation of PER2 expression induced by insulin, indicating an essential requirement for mTOR in the response (Fig 5.17A,B,C,D). However, activation of mTOR alone is not sufficient to phenocopy the effect of insulin on PER2 expression, as

pharmacological stimulation of mTOR (Fig 5.18A) does not induce PER2 expression. Thus, mTOR activation is necessary for insulin induction of PER2 expression, but is not sufficient to drive PER2 expression in isolation, implying other factors must be required.

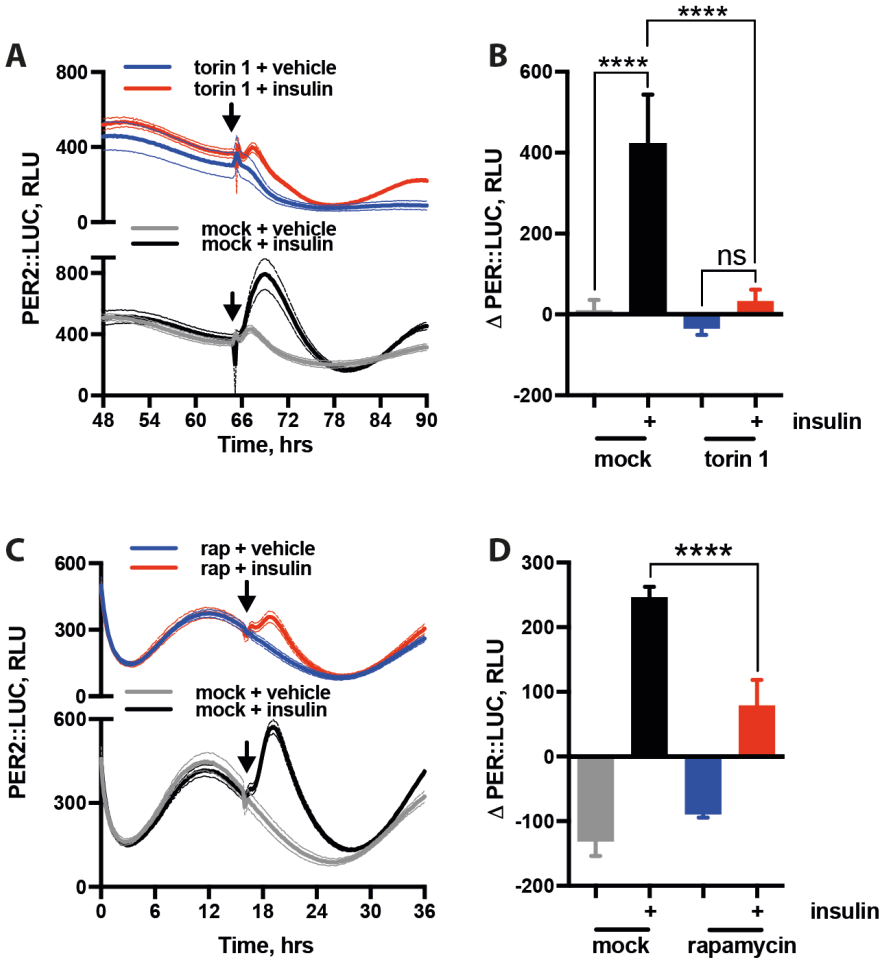

Figure 5.17

mTOR is required for PER2 response to insulin

A Pre-treating cells with mTOR inhibitor torin 1 (1 μM) inhibits the acute increase in PER2 (n=4, mean±SEM). **B** Quantification of effect of torin 1 on PER2 induction (two-way ANOVA, Tukey's multiple comparisons test). **C** Pre-treatment with classical mTOR inhibitor rapamycin (400nM) also significantly attenuates the effect of insulin on acute PER2 levels (n=4, mean±SEM). **D** Quantification of the effect of rapamycin on acute PER2 induction (two-way ANOVA, Tukey's multiple comparisons test).

It was therefore asked which additional effects of insulin on cell biology might act, in concert with activation of mTOR, to give facilitate increased PER2 translation. Another consequence of insulin receptor activation is the inactivation of Phosphatase and tensin homolog (PTEN): the phosphatase that dephosphorylates phosphatidylinositol-3,4,5-trisphosphate generated by PI3K, resulting in increased PIP3 abundance (Nakashima et al. 2000). It was hypothesized that a coincident increase in available PIP_3 might be required, in addition to mTOR activation, to replicate the PER2 response to insulin (Fig 5.18B). However, when cells were treated with both mTOR activator MHY1485 and PTEN inhibitor VO-OHpic, an acute increase in PER2 expression was not induced in a manner comparable to insulin treatment, although there was a clear change in the subsequent PER2 waveform.

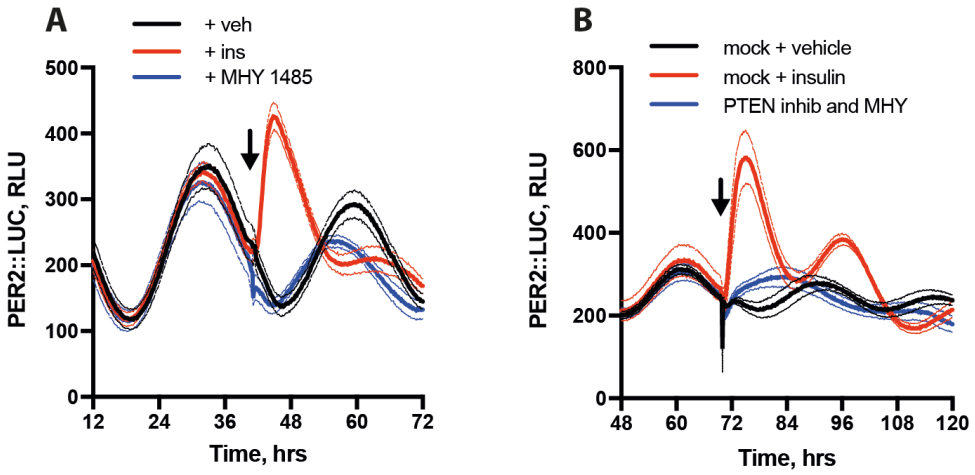

Figure 5.18

mTOR activation alone is insufficient to recapitulate the effect of insulin

A Treatment with mTOR activator MHY 1485 does not produce an acute increase in PER2 expression (n=4, mean±SEM). **B** Simultaneous pharmacological mTOR activation and PTEN inhibition is also insufficient to induce PER2 expression (n=4, mean±SEM).

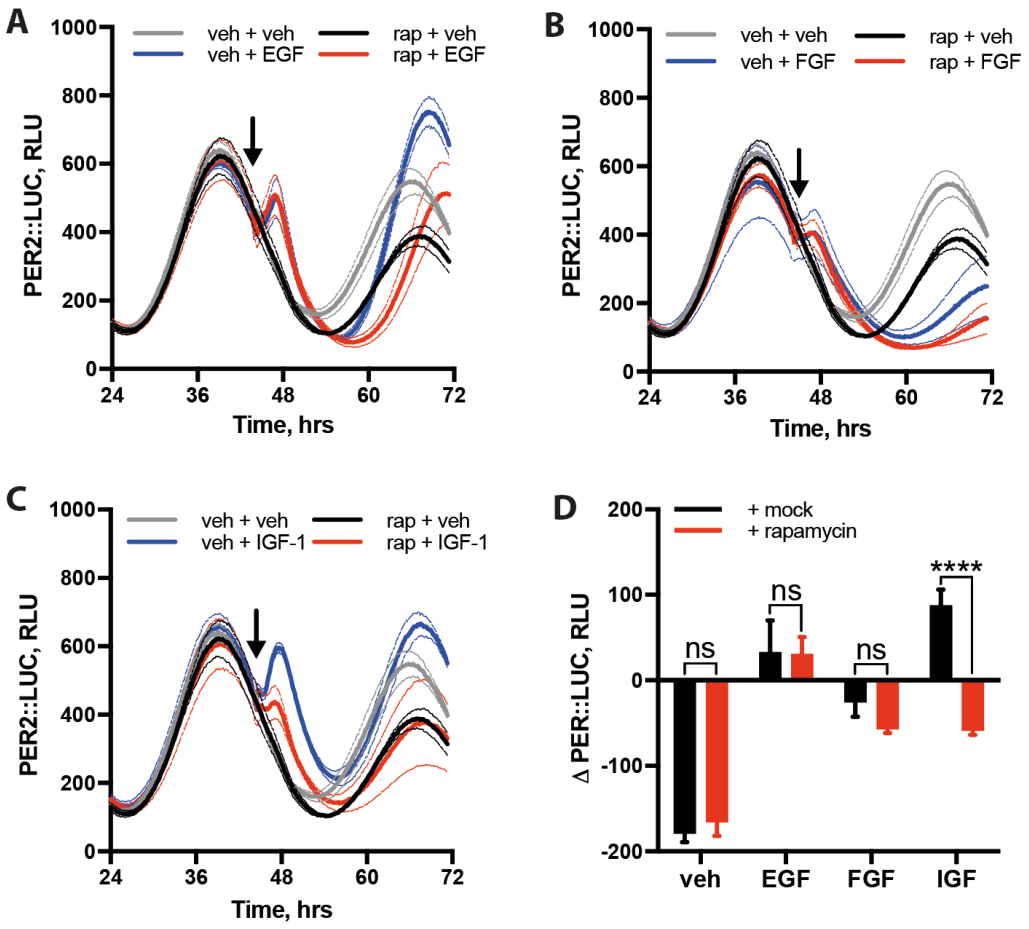

Figure 5.19

IGF-1 also acts on PER2 through mTOR

A,B,C Whilst growth factors EGF, FGF and IGF-1 all elicit some induction in PER2::LUC , only the effects of IGF-1 are attenuated in the presence of mTOR inhibitor rapamycin (n≥3, mean±SEM). **D** Quantification on the PER2 induction in the presence and absence of rapamycin (Welch's t-test).

5.1.13 IGF-1 also activates PER2 expression through mTOR

Following the observation that insulin can modulate cellular timekeeping, through PER2 it was posited that other growth factors with tyrosine kinase receptors might also produce this effect; in particular insulin-like growth factor 1 (IGF-1), which also has some affinity for the insulin receptor and *vice versa*. In order to test the selectivity of this PER2 induction, we tested the effects of

IGF-1, as well as fibroblast growth factor (FGF) and epidermal growth factor (EGF) on PER2::LUC fibroblasts. We found that all growth factors tested stimulated some induction in PER2 (Fig 5.19A,B,C), although inductions following EGF and FGF were modest in comparison to those following IGF-1 or insulin. Critically, the effect of IGF-1, but not EGF or FGF, was significantly attenuated by rapamycin inhibition of the mTOR signaling complex, which functions downstream of both the insulin and IGF-1 receptors (Fig 5.19D). This suggests that IGF-1 and insulin may stimulate an increase in PER2 expression through similar, if not the same, mechanism, whilst other growth factors do so through alternative pathways.

In the context of acute responses to feeding, insulin and IGF-1 are likely to be more physiologically relevant humoral cues than other growth factors, since

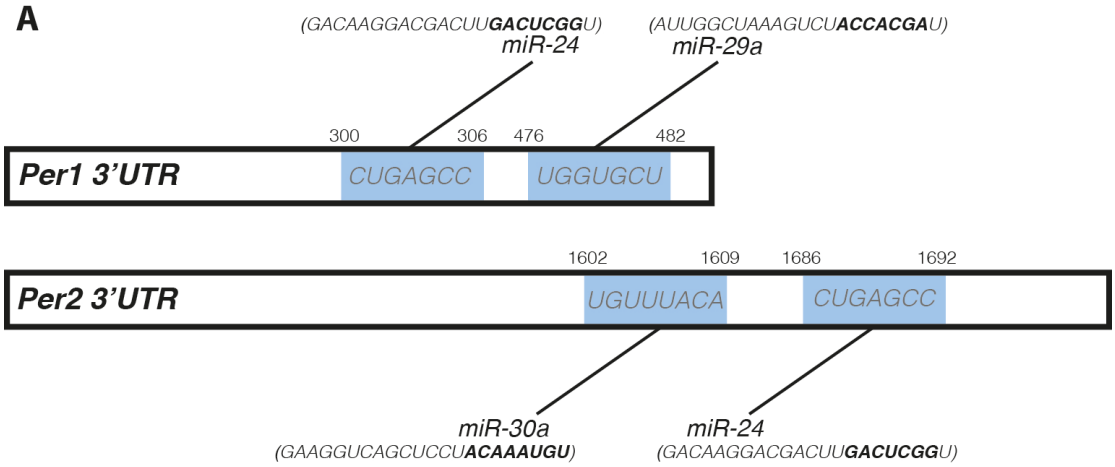

Figure 5.20

Insulin-regulated miRNAs bind to the 3'UTR of per1 and per2

A Schematic showing sites of miRNA binding in the 3'UTR of Per1 and Per2 mRNA.

both increase in response to certain dietary cues: insulin levels increase in response to dietary carbohydrates, whereas IGF-1 responds to dietary protein (Levine et al. 2002). As such, it is more likely that it is these cues that synergistically stimulate circadian responses to feeding *in vivo*.

5.1.14 miRNA down- regulation following insulin addition

Recent studies have shown that translation of *Per1* and *Per2* mRNA is regulated by three microRNAs, namely miR24, miR29a and miR30a (Fig 5.20A, Chen et al., 2013). These miRNA are complementary to sections of the 3'UTR of their target mRNAs, thereby reducing translation of these mRNA through the RNA-induced silencing complex (RISC). Furthermore, several miRNAs, including those that regulate PER expression, have been reported to be down-regulated in response to insulin (Granjon et al. 2009). qPCR was used to confirm that down-regulation of these specific miRNA also occurs in PER2::LUC fibroblasts after 60 minutes exposure to insulin (Fig 5.21A,B,C). It was thus hypothesized that a decrease in PER-regulating miRNA levels might be implicated in the increase in PER2 observed following insulin treatmen. It was therefore tested whether knockdown of these three miRNAs (confirmed by qPCR, Fig 5.21D,E,F) in combination with pharmacological activation of mTOR and/or inactivation of PTEN might be sufficient to recapitulate the. effect of insulin on PER expression (Fig 5.22A,B). Unlike mTOR activation alone, it was observed that mTOR activation in the presence of miRNA knockdown facilitated an acute induction of PER2 expression. However, this

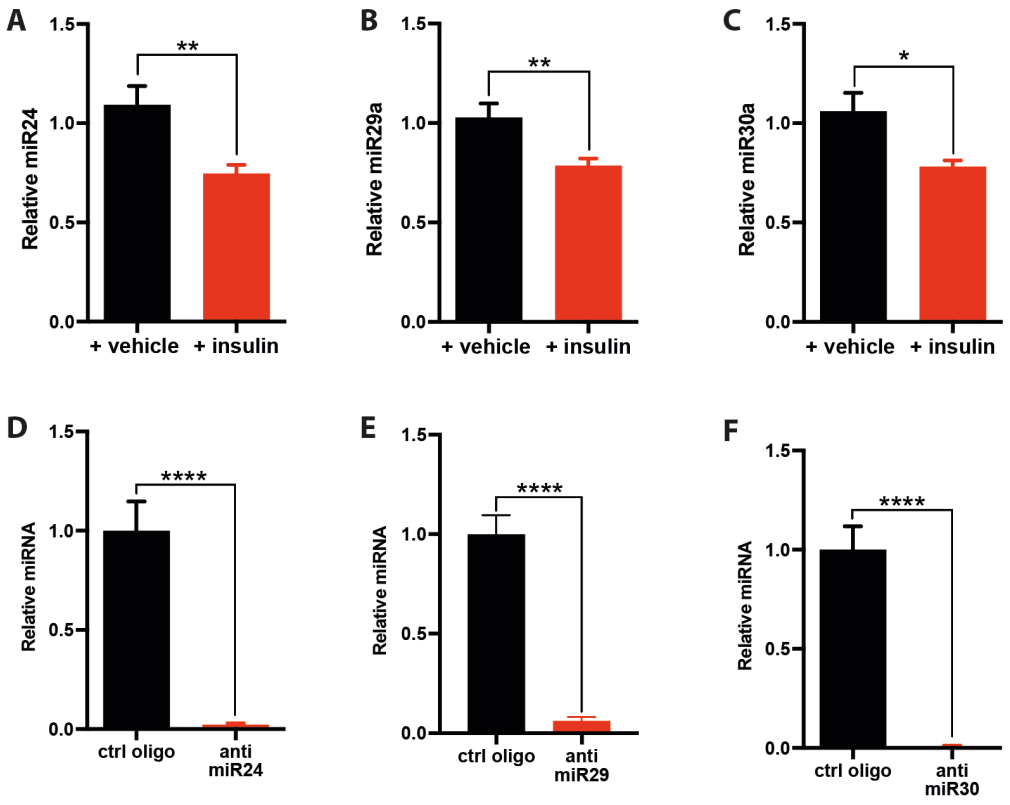

Figure 5.21

Per1/2-regulating miRNAs are down-regulated following insulin

A,B,C qPCR on samples taken 60 minutes after insulin addition shows a significant decrease in expression of miR24, miR29 and miR30 respectively following insulin treatment compared to vehicle controls (n=4, mean±SEM). **D,E,F** qPCR validating miRNA knockdown by antisense oligos compared to a control oligos (n=4, mean±SEM).

was significantly decreased in magnitude compared with the induction observed following insulin addition. Significantly, PTEN inhibition alone, or in combination with mTOR activation or microRNA knockdown had no significant effect upon PER2 levels. However, microRNA knockdown in combination with both mTOR activation and PTEN inhibition completely phenocopied the effect of insulin upon PER2 induction, producing an increase in PER2 expression that is statistically indistinguishable from that produced by insulin itself.

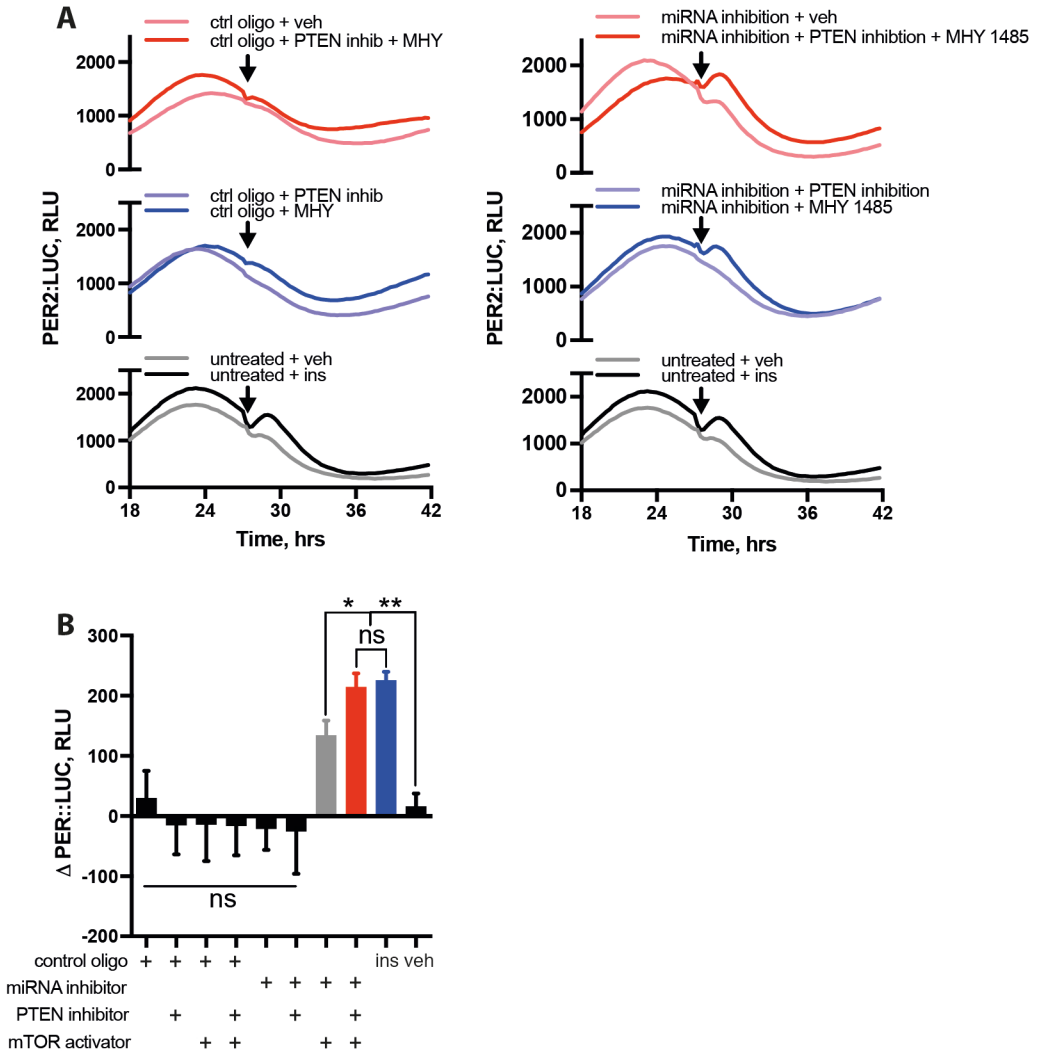

Figure 5.22

Combined RNAi and pharmacological interventions are required to recapitulate the effect of insulin on PER2

A (left panel) Neither mTOR activator MHY 1485, PTEN inhibitor VO-OHpic or a combination of these treatments is sufficient to induce an acute induction in PER2 levels in the presence of a control oligo. **(Right panel)** In the presence of antisense oligos, mTOR activation alone produces a significant increase in acute PER2 levels. Simultaneous activation of mTOR and inhibition of PTEN induces PER2 acutely in a manner not significantly different from insulin (n=4, mean±SEM). **B** Quantification of the effects of PTEN inhibition and mTOR activation in the presence and absence of antisense oligos (two-way ANOVA, Tukey's multiple comparisons test).

Together these studies reveal a universal action of insulin signaling to enhance PER protein translation via a three-way coincidence detection mechanism, which allows the cellular clock to respond appropriately to exogenous timing cues whilst remaining unperturbed by other cues that signal via PI3K/mTOR (Fig 15.23. It is plausible that this pathway serves *in vivo* to sculpt circadian responses to changes in food availability

5.2 Discussion

5.2.1 Overview

In this chapter, I have shown that the metabolic hormone insulin directly affects circadian rhythms *ex vivo* and *in vitro*. In particular, insulin is sufficient to modulate all of the key parameters of the circadian rhythm in a wide range of tissue and cell types. This is mediated by an acute induction of PER protein translation through an activation cascade involving specific coincident signaling within the insulin-signaling pathway (Figure 5.23A).

Previous work has shown insulin to be chronoactive, but its mechanism of action and possible role in entrainment to feeding cycles has not been firmly established. Evidence has been generally limited to cell types that are highly insulin sensitive, such as liver and adipose tissue (Balsalobre et al., 2000; Tahara et al., 2009; Sato et al., 2014; Yamajuku et al., 2012) . As such, insulin has been considered to be only one of a number of factors required to coordinate shifts in peripheral circadian gene expression during restricted feeding protocols. Here its is shown that the action of insulin upon the circadian clock is not restricted to any particular tissue and is observable

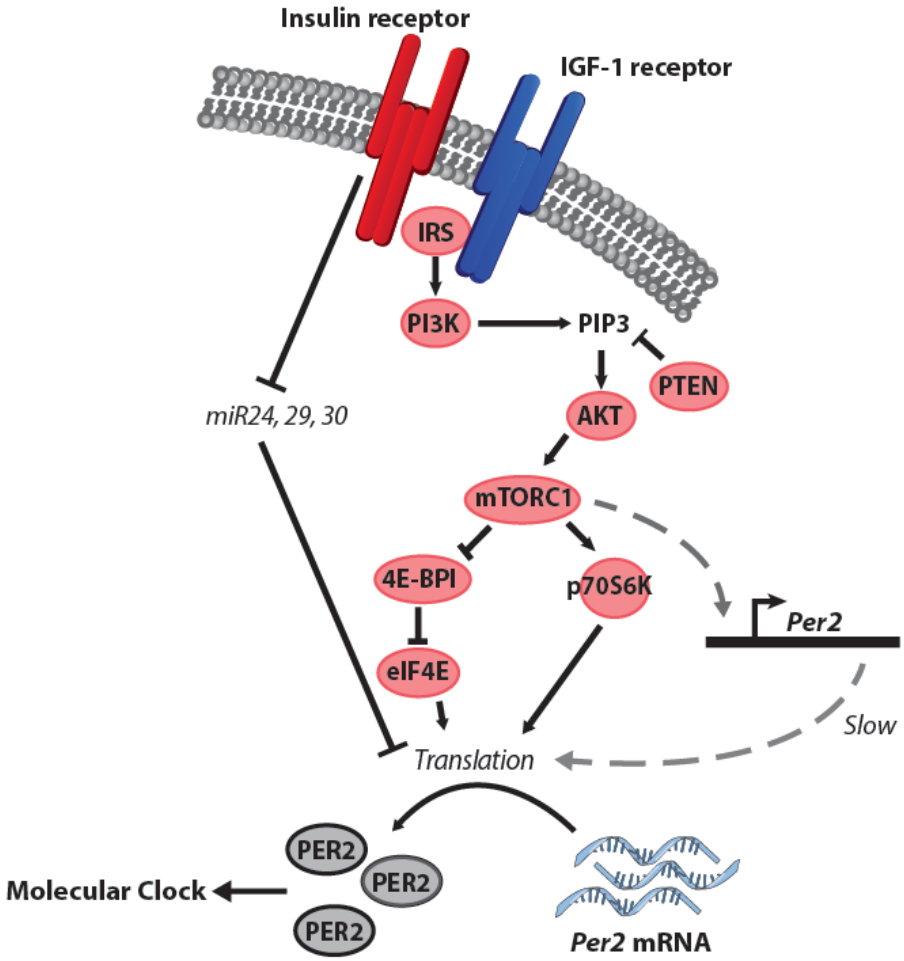

Figure 5.23

Proposed mechanism of insulin-induced PER2 expression

in tissue types that are typically considered less insulin-sensitive, including the suprachiasmatic nucleus. Our findings strongly suggest that insulin acts as an entraining stimulus (or zeitgeber) for all peripheral tissues through the ubiquitously expressed IR, with an overlapping and partially redundant role for IGF-1 and the IGFR, both of these receptors being very widely expressed. As such the insulin signaling pathway is likely to be a major synchronizer of the circadian clock in all peripheral tissues after fast-feeding, acting directly to

communicate timing cues to each cell individually, including those brain areas responsible for some aspects of animal behaviour.

Why previous studies have not observed the universal effect of insulin upon peripheral circadian rhythms we have identified is not entirely clear but, as serum and serum replacements often contain comparatively high concentrations of insulin, it is plausible that insulin receptors in less insulin-sensitive tissues become desensitized, preventing an acute increase in extracellular insulin from being communicated to the cellular clockwork. Moreover constitutive activation of the insulin signaling pathway is a common hallmark of cancer cell lines (Chang et al., 2002), highlighting the importance of using untransformed cells for investigation of circadian cellular function.

A role for insulin in adjusting the phase of the molecular clock to the timing of food intake is consistent with the current state of knowledge surrounding food entrainment. Recent work has shown that fluctuations in circulating glucose and insulin during imposed fasting/feeding cycles are permissive for the entrainment of circadian rhythms to restricted feeding *in vivo* (Mukherji, Kobiita & Chambon 2015; Mukherji, Kobiita, Damara, et al. 2015). Moreover, it has been demonstrated previously that the feeding-induced rise in hepatic PER2 expression typically observed in pre-fasted mice, is lost in streptozotocin (STZ)-induced diabetic mice (Tahara et al 2011), suggesting that insulin is essential for anticipation of and early circadian responses to feeding cues. Davidson and colleagues showed behavioural anticipation and

the restricted feeding-induced phase shift of Per1:luc in the liver to be attenuated but maintained in rats treated with a single bolus of STZ. It is noted however, that whilst STZ at a sufficient dose should ablate the insulin-producing β cells of the pancreas, it would not affect IGF-1-mediated responses to feed-fast cycles, providing redundancy within this system of entrainment. Moreover, liver slice cultures derived from STZ-treated rats do exhibit greatly increased dispersion of circadian phase reported by per1:luc bioluminescence (Davidson et al 2002; Tahara et al 2011) suggesting that insulin does indeed act to synchronize the phase of peripheral clocks under ad libitum feeding conditions.

5.2.2 A role for insulin *in vivo*

The ultimate proof of principle for the role of insulin in mammalian entrainment to food would be to show that the effects of insulin on cellular and tissue rhythms described in this chapter are also observed *in vivo*. As a result of collaboration with David Bechtold and Alex West at the University of Manchester, it was possible to test this. Initially, mice were singly house in constant conditions and wheel running behavior recorded. They were then fasted for 24 hours before receiving an intraperitoneal injection of either glucose or saline at the end of the active phase (Fig 5.24A). Those animals that received a glucose bolus (and so experienced an associated increase in circulating insulin) showed a significant delay in the onset of activity following the treatment (Fig 5.24B). Similarly, animals treated with either vehicle, glucose (3g/kg) or insulin (2.25U/kg), also showed significant increase in

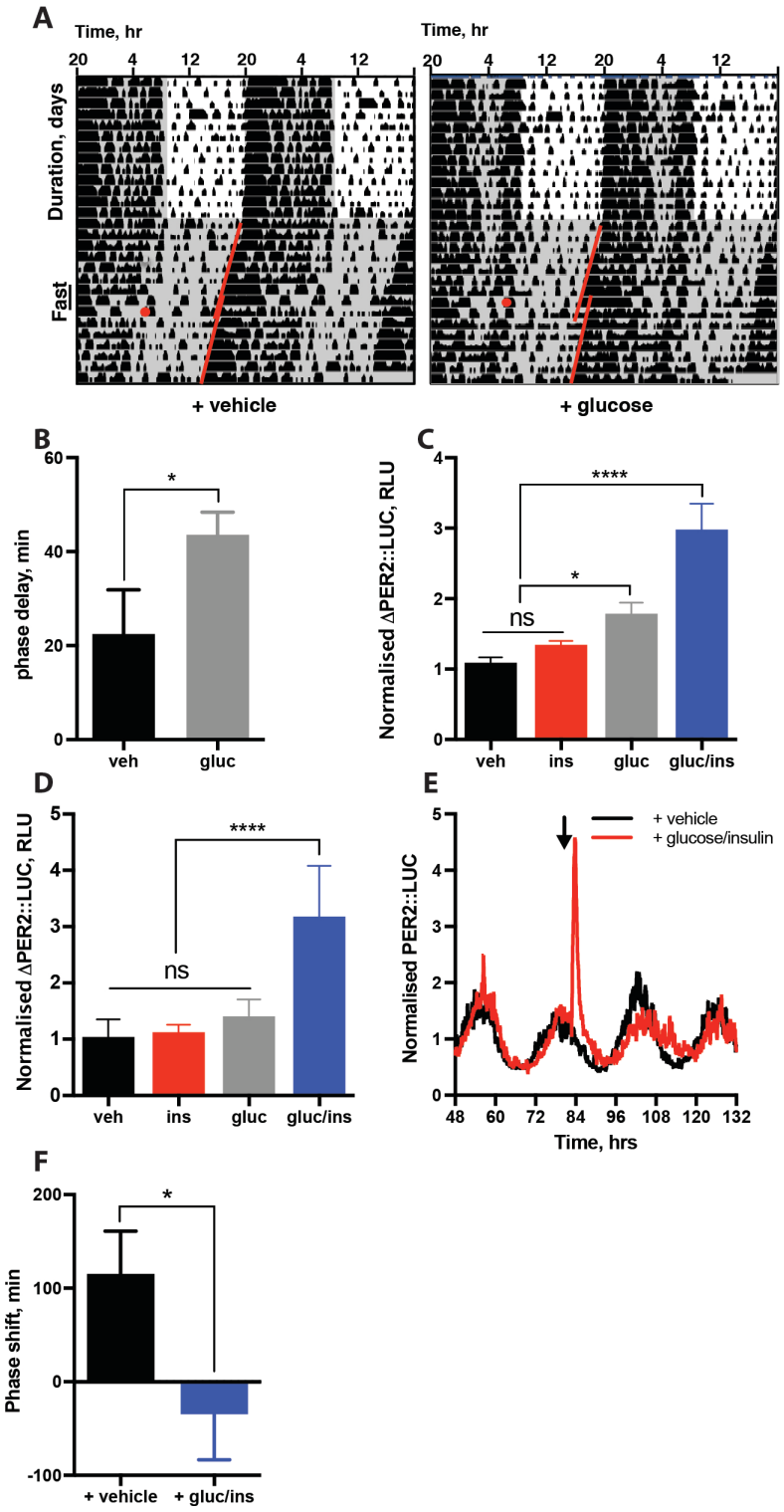

Figure 5.24

Insulin influences behaviour and gene expression in vivo

A,B Glucose administration was effective in causing a phase delay in wheel-running activity in fasted mice (3g/kg, ip at CT22; n=5-8/group, Students' t-test). **C** Peripheral administration of insulin (2.25U/kg, ip) or

Continued on next page

glucose (3g/kg, ip) caused a rapid, yet transient induction in PER2::LUC bioluminescence in pre-fasted mice after 1 hour, although **D** this was no longer significant after 2 hours. **E** In contrast, injection with insulin and glucose simultaneously produced a more prolonged induction in PER2 point in the untreated control. Arrow (**E)** and red dot (**A)** indicates injection timing.**F** Quantification of the change in phase of PER2 bioluminescence following insulin addition (n≥5, mean±SEM, Welch's t-test, p=0.5, 150 mins±68).. which was still significant after 2 hours (n=4-6/group, One-Way ANOVA, Dunnet's multiple comparisons test). Induction is quantified as the change in bioluminescent signal (ΔPER2::LUC) from time of insulin addition to the peak in bioluminescence following insulin addition, or the equivalent time point in the untreated control. Arrow (**E)** and red dot (**A)** indicates injection timing. **F** Quantification of the change in phase of PER2 bioluminescence following insulin addition (n≥5, mean±SEM, Welch's t-test, p=0.5, 150 mins±68). All experiments and analysis were performed by Alex West and David Bechtold

PER2::LUC signal when observed using LESA-biolumicorder cages (Yoo et al. 2004; Saini et al. 2013) after one hour (Fig 5.24C), although this was no longer significant after two hours (Fig 5.24D), in contrast to earlier observations *in vitro*, where the peak of the PER2::LUC response occurs approximately 3 hours after the addition of insulin. However, administration of insulin alone leads to hypoglycemia in the mice, which is likely to produce conflicted effects on gene expression. Furthermore, the transient pulse in insulin following intraperitoneal injection of insulin is likely to be much shorter than pulses of endogenous insulin release. When animals were instead injected with both glucose and insulin combined, a much more physiologically relevant cue than rapid increases in glucose or insulin alone as it mimics the

response to food, a rapid rise in PER2::LUC driven bioluminescence was observed, and this remained sustained for over 2 hours (Fig 5.24E). Furthermore, following the induction in PER2::LUC, it is possible to observe a shift in phase of bioluminesence of around 2 hours (Fig 5.24F). However, it is plausible that larger phase shifts might be seen if it were possible to apply such a stimulus in repeated circadian cycles in a manner equivalent to food entrainment. Thus, these data suggests that insulin is capable of influencing both behaviour and cellular rhythms *in vivo*, the two major effects of the mammalian circadian response to feeding. This confirms insulin as a relevant and primary cue involved in mammalian food entrainment.

5.2.3 A new model for mammalian entrainment to food

Based upon the observations described in this chapter, it is possible to propose a new model for mammalian food entrainment. Here there is no central 'food-entrainable oscillator' (Gooley et al., 2006, LeSauter et al., 2009, Stefan 2002), but instead insulin and IGF-1 released in response to food entrains each cell in the body individually, via induction of PER2.

Under normal 24 h light-dark cycles, animals feed during their active phase leading to increased plasma glucose levels which trigger insulin release from the pancreas, as well as IGF-1 from other tissues including the liver (Sjögren et al., 1999). Activation of the insulin-signaling pathway fine-tunes the timing of the expression of PER (and likely other clock-relevant) proteins in all tissues, including the brain, to resonate with and confer behavioural and

physiological anticipation of food availability. This surge in PER protein translation normally acts later than, and acts synergistically with, the earlier increase in plasma glucocorticoids stimulated by the SCN-dependent signals that elicit increased Per transcription towards the end of the rest phase (Balsalobre et al., 2000, Van Cauter et al., 1996). If this model is correct then corticosterone should reset the cellular clock to an earlier circadian phase than insulin does, concomitant with the approximately 4 h separation of peak glucocorticoid and insulin signaling following early feeding *in vivo* (Shamsi et al. 2014). This was observed to be the case (Fig 5.2A) in the initial experiments *in vitro* following the observation that both corticosterone and insulin can shift the phase of the PER2 oscillation. Here, the peaks of PER2 following insulin and corticosterone were approximately 3 hours apart, with insulin resetting to an earlier phase. We therefore predict that *in vivo*, animals experience a surge in circulating corticosterone before the start of the active phase, which is then followed 3 or 4 hours later by an increase in circulating insulin in response to feeding at the start of the active phase. These two signals will reinforce each other, producing an induction in PER2 greater than that achieved by either hormone alone.

We speculate that when instead, feeding occurs out-of-phase with the predicted active phase and so corticosterone release – such as in restricted feeding protocols - insulin directly simulates a feeding-induced PER-mediated phase shift in clock gene expression in peripheral tissues, resulting in

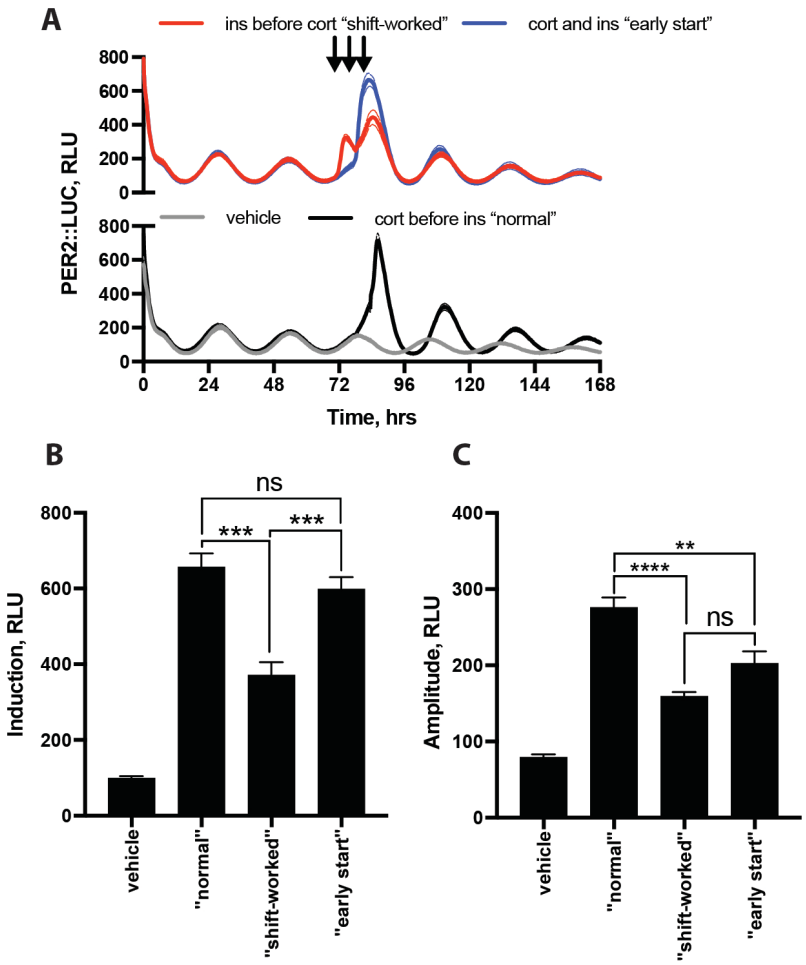

Figure 5.25

Conflicting entrainment signals influence amplitude of PER2 expression

A Addition of insulin before, after or at the same time as a corticosterone pulse (mimicking normal, shift-worked and early wake-up time conditions) has a significant effect on **B** the size of the PER2 induction and **C** the amplitude of the subsequent cycles, measured at the first circadian cycle after treatment (n≥3, mean±SEM, one-way ANOVA, Tukey's multiple comparisons test). Corticosterone was added at CT10, with insulin added at either CT 4, CT10 or CT16.

changes in the phase and amplitude of clock gene expression and possible internal desynchrony. Repeated events of this kind would lead to the uncoupling of circadian rhythms in peripheral tissues from those in the SCN, as has been previously described (Damiola et al. 2000). This speculation is

supported by observations in fibroblasts that have been treated with insulin either after, at the same time as or before a corticosterone pulse applied at a physiologically relevant time (Fig 5.25A). These conditions correlate with the signals that we expect to see in normal conditions, unusually early wake-up times (early start) and shift-workers respectively. It is clear here that application of insulin before corticosterone, analogous with food consumption during the night in humans, results in a significantly lower PER2 induction than the “normal” or “early-start” conditions, as well as lower amplitude of the next circadian cycle compared to the “normal” condition.

5.2.4 Clinical implications

The work described here has the potential to inform some medically relevant applications. Humans do not generally experience an enforced restricted-feeding protocol, but they do experience both shiftwork and jet-lag. In such situations, feeding occurs out-of-phase with the light-dark cycle, to which the SCN is primarily entrained. As such, individuals experiencing shift-work or jet-lag will likely show the same kind of internal desynchrony observed in mice under restricted feeding. These individuals show a higher propensity to develop hypertension, some cancers, metabolic syndrome and obesity (Karlsson et al. 2001), attributed to this uncoupling of central and peripheral clocks.

Knowledge of the possible mechanism by which feeding out-of-phase with photic cues might entrain peripheral tissues allows us to predict behaviours

that might reduce the detrimental effects of shift work or jet-lag. For example, individuals engaging in occasional shift might be best advised not to consume food during the dark if at all possible, and to instead eat their largest meal in the morning, as the time when the phase of the PER2 response following insulin reinforces the PER2 response to early-morning cortisol release from the adrenal glands. Similarly, it might be possible to minimise the severity of jet-lag by controlling the timing to food intake around the time of flight and ensuring consumption of a large meal at dawn at an individual's destination to promote synchrony with the new timing environment. Should the model of food entrainment described in this chapter be correct, implementation of such simple behaviours could have a significant impact on the long-term health of those engaging in shift work or those who frequently cross multiple time-zones.

Another potential application of the findings in this chapter concerns the treatment of certain cancerous tumors. With the increasing move towards personalized medicine, chronotherapeutic treatment of certain cancers is likely to become increasingly common. Both efficacy and side-effects of a number of cancer treatments vary across the circadian cycle and as such, varying the dose of these drugs in a circadian manner has a number of benefits for patient outcome (Dallman et al., 2016). However, it has been observed that a proportion of cancerous tumours have distinctly different circadian gene expression to the rest of the host tissues (Chen et al., 2005, Lin et al. 2008). It has also been noted that a significant proportion of

cancerous tumours are insulin-insensitive as a result of constitutive activation of the insulin-signaling pathway (Chang et al., 2002). It is plausible that these two observations are causative, and that tumours that have distinctly different expression of circadian genes to the host do so because their insulin-insensitivity prevents them from entraining to time-of feeding. As such, when considering when to administer anti-cancer drugs that are known to show a circadian variation in their efficacy and pharmacokinetics, it may be worthwhile considering the insulin sensitivity of the tumour itself when designing a circadian protocol of administration.

5.2.5 Conclusion

This chapter demonstrates that stimulation of the insulin signaling pathway is sufficient to reset the circadian clock in peripheral cells and the whole animal, but not the intact SCN master clock. A three-way coincidence detection mechanism downstream of the insulin receptor is proposed as the means by which insulin and IGF-1 produce this effect. This may explain the strong link between metabolic syndrome and shift work (Salgado-Delgado et al., 2013). Moreover these findings predict that appropriately timed schedules of fasting and feeding will reduce the time taken by the human biological clock to adjust during jet-lag and shift-work. Given that ~15% of the adult workforce engage in shift work, these findings have the potential to inform strategies to alleviate its associated long-term adverse health risks.

6.0 General Discussion

6.0.1 The relationship between circadian rhythms and metabolism

That links exists between circadian rhythmicity and metabolism has been appreciated for the majority of the history of the modern field. Early experiments showed that food intake (and so associated gross metabolism) in whole animals was rhythmic and furthermore that rhythms in food intake could be used to modulate the phase of circadian animal behaviour (Stephan et al. 1979). With the identification of the SCN as the central circadian pacemaker in mammals it was further noted that, whilst the SCN itself shows circadian rhythmicity in nutrient uptake (Cassone et al. 1988) the SCN itself, unlike peripheral tissues and animal behaviour, is not entrained by feeding cues (Damiola et al. 2000) and is not required for entrainment to feeding (Stephan et al. 1979). This discrepancy was an early indicator of the existence of biological pace-making outside of the SCN, a property that was later attributed to almost every cell (Balsalobre et al. 1998).

With the discovery that circadian timekeeping is cell autonomous and occurs in every cell of the body, there has been an increasing number of observations connected circadian timekeeping to metabolic processes. Both nutrient uptake and utilisation displays clear circadian rhythmicity (Peek et al. 2013; Paulose et al. 2012; Altman et al. 2015), as does the activity of a number of organs, particularly those with an endocrine function (Perelis et al. 2015). With the identification of TTFL mechanisms for cellular timekeeping, it has been possible to correlate and in many cases directly links between TTFL

events and metabolic processes (Shinohara et al. 1998). This has led to the hypothesis that, like many other processes in the cell, circadian rhythms in metabolism are driven by TTFL activity.

However, a number of observations are at odds with this idea. More recent work has shown that rhythms in nutrient uptake can persist in the absence of TTFL rhythmicity, as in embryonic stem cells (Paulose et al. 2012). Most strikingly, rhythms in PRX hyperoxidation persist in the absence of nascent transcription (O'Neill & Reddy 2011; O'Neill et al. 2011) and are observed across kingdoms (Edgar et al. 2012). These rhythms even persist in cells from what have been generally considered arrhythmic genetic backgrounds. It has also been noted that the TTFL in multiple organisms can be perturbed by alterations in metabolic events (Martinek et al. 2001). Observations such as these have given rise to the hypothesis that rhythms in metabolism might constitute an evolutionarily conserved mechanism of cellular timekeeping that feeds in to the TTFL, possibly to the extent that the two cannot be dissociated from each other (Asher & Schibler 2011).

6.0.2 Contributions of this thesis

The initial aim of this thesis was to attempt to elucidate the nature of the relationship between metabolism and the cellular circadian clock. Of particular interest was testing the second hypothesis above, that cellular metabolism might constitute an essential component of cellular timekeeping. Emphasis was placed on the pathways of carbohydrate metabolism, both because the

pathways of carbohydrate metabolism are amongst the most evolutionarily conserved and also because this is the sole source of ATP generation in erythrocytes, which display circadian rhythmicity in the absence of a functioning TTFL. Combined genetic, pharmacological and metabolomic investigation of these pathways indicated that, although capable of influencing both phase and amplitude of the cellular oscillation, flux through any constituent pathway of carbohydrate metabolism make only minimal contribution to the period of the TTFL circadian oscillation. There does, however, appear to be a permissive redox range within which it is possible to observe circadian TTFL activity, but this range far exceeds the range of redox states found under physiological conditions.

A comparable result was seen when considering the cellular response to changes in whole organism nutrient status. That time of feeding is capable of entraining both animal behaviour and cellular circadian phase has been known for some time, although any precise mechanism had not previously been elucidated. We see in the final experimental chapter of this thesis that the metabolic signalling hormone insulin is capable of recapitulating the effects of food entrainment and provide a mechanism by which this is communicated to the cellular TTFL. However, even this hormone, which signals major metabolic change within both a whole organism and the individual cell, although capable of influencing the amplitude and phase of cellular clock gene expression, again has minimal effects on the cellular period.

In light of this work, I propose that, contrary to prior hypothesis, cellular metabolism is unlikely to represent a fundamental component of cellular timekeeping. Whilst metabolism is of course required for cell viability, it does not appear to be a state variable of cellular rhythms. Instead, the experiments shown here support a third hypothesis: that metabolism is capable of contributing to cellular timekeeping and is permissive for it, but is not an essential component of the timekeeping mechanism itself.

6.0.3 Features of a conserved oscillator

If the pathways of cellular metabolism do not contain an essential component of cellular timekeeping then the natural question is: what else might such an oscillator?

Firstly, it is useful to consider what conditions this non-TTFL oscillator would have to satisfy. It would, most likely, have to conform to the basic definition of a circadian rhythm – that is to say, it must have a free-running period of around 24 hours, it must be capable of entrainment and it must be temperature compensated (Pittendrigh 1960). It addition, it must be capable of running in the absence of nascent transcription (O'Neill et al. 2011; O'Neill & Reddy 2011). Thirdly, it should be evolutionarily conserved (Edgar et al. 2012).

These criteria, although by no means capable of elucidating the identity of such a post-transcriptional oscillator, do enable us to pick out certain clues

from the existing literature. For example, the fact that both ck1 and GSK3-β have clear circadian effects in multiple organisms, despite the apparent differences in the canonical TTFL mechanisms within these organisms, suggests that these enzymes, or their some of their conserved targets, might be components of a non-TTFL oscillator (van Ooijen et al. 2013; Meng et al. 2010; Hirota et al. 2008; O'Neill et al. 2011). This might be suggestive of a phosphorylative oscillator, as in cyanobacteria.

Alternatively, it is also of potential utility to consider older models of circadian rhythmicity, prior to the dominance of the TTFL model. Proposed in 1974, the Njus-Sulzman-Hastings model of the circadian oscillator posits a mechanism for cellular timekeeping that is entirely post-transcriptional (Njus et al. 1974). Here, the model proposes a system of cellular timekeeping that is dependent upon flux of ions (most likely K^+ and Na^+) across the extracellular membrane and intra- and extracellular ion concentration, where the gating of transport proteins or channels in the membrane is determined by the relevant ion concentrations. Phase shifts can be effected by acute opening of channels than also transport these ions. Temperature compensation is provided by the lipid bilayer, which is established to have a well-regulated lipid content in order to maintain a constant fluidity. As movement of proteins within a membrane is dependent on the membrane viscosity, this regulation could provide temperature compensation.

Although by no means proven to act as an oscillator, let alone one of fundamental importance to cellular timekeeping, this model for a post-

transcriptional circadian oscillator cannot currently be excluded and makes a number of testable predictions (Nitabach et al. 2005). With regards to this thesis, it is of interest to note that inhibition of the PPP can result in the increased opening of voltage-gated potassium channels in a number of cell types, which might provide an alternative explanation for the effects seen with these drugs (Gupte et al. 2002).

6.0.4 Identification of a conserved oscillator

In addition to further investigation of the possible circadian mechanism models described above, it may be useful to take a less directed approach when attempting to identify components of a possible conserved post-transcriptional oscillator. As Pittendrigh described, one of the essential features of a circadian rhythm is the ability to entrain to external cues (Pittendrigh 1960). Any evolutionarily conserved oscillator should exhibit this ability. It is also interesting to note that relatively few external events are capable of entraining circadian oscillators, and a number of these appear to be common across organisms. Prominent amongst these is entrainment to light and temperature cycles, both of which are capable of entraining organisms as diverse as mammals, flies and the bread mould *Neurospora crassa* (Brown et al. 2002; Zimmerman et al. 1968; Liu 1998). Even entrainment to feeding has been suggested to be exhibited in both vertebrates and invertebrates (Stephan 2002; Frisch & Aschoff 1987). We currently have varied levels of knowledge as to the exact mechanisms by which these external events entrain the cellular oscillator. However, given the universal

nature of these entrainment pathways, it is plausible that they might act to entrain a conserved oscillator rather than, or in addition to, feeding directly in to the TTFL of each organism. As such, it may be of utility to consider similarities in the cellular effects of each of these entraining factors when looking for components of a conserved circadian oscillator, in addition to the other approaches described above.

6.0.5 Concluding remarks

It is clear that over the almost six decades since Pittendrigh defined the features of a circadian rhythm there has been an enormous expansion in our knowledge of this area, with crucial developments, such as the identification of central pacemakers and of cell autonomous oscillations. Despite this, we are still somewhat in the dark when it comes to the exact molecular mechanisms by which these essential characteristics – namely period, entrainability and temperature compensation – particularly in a mammalian context. It is my hope that this thesis has contributed in some way towards a greater understanding of at least two of these features and will assist in future investigation in to the mechanistic basis of circadian timekeeping.

7.0 Bibliography

Adimora, N.J., Jones, D.P. & Kemp, M.L., 2010. A Model of Redox Kinetics Implicates the Thiol Proteome in Cellular Hydrogen Peroxide Responses. *Antioxidants & Redox Signaling*

Alberts, B. et al., 2002. *Molecular Biology of the Cell*,

Altman, B.J. et al., 2015. MYC Disrupts the Circadian Clock and Metabolism in Cancer Cells. *Cell Metabolism*

Altman, B.J. et al., 2015. MYC Disrupts the Circadian Clock and Metabolism in Cancer Cells. *Cell Metabolism*

Andreyev, A. Y., Kushnareva, Y.E. & Starkov, A. A., 2005. Mitochondrial metabolism of reactive oxygen species. *Biochemistry*

Anhê, G.F. et al., 2004. In vivo activation of insulin receptor tyrosine kinase by melatonin in the rat hypothalamus. *Journal of Neurochemistry*

Aronson, B.D. et al., 1994. Negative feedback defining a circadian clock: autoregulation of the clock gene frequency. *Science*.

Asher, G. & Schibler, U., 2011. Crosstalk between components of circadian and metabolic cycles in mammals. *Cell Metabolism*

Atger, F. et al., 2015. Circadian and feeding rhythms differentially affect rhythmic mRNA transcription and translation in mouse liver. *Proceedings of the National Academy of Sciences of the United States of America*

Bailyes, E.M. et al., 1997. Insulin receptor/IGF-I receptor hybrids are widely distributed in mammalian tissues: quantification of individual receptor species by selective immunoprecipitation and immunoblotting. *The Biochemical Journal*

Balsalobre, A, Brown, S. A, et al., 2000. Resetting of circadian time in peripheral tissues by glucocorticoid signaling. *Science*

Balsalobre, A, Damiola, F. & Schibler, U., 1998. A serum shock induces circadian gene expression in mammalian tissue culture cells. *Cell*

Balsalobre, A, Marcacci, L. & Schibler, U., 2000. Multiple signaling pathways elicit circadian gene expression in cultured Rat-1 fibroblasts. *Current Biology*

Barban, S. & Schulze, H. 0, 1961. The Effects of 2-Deoxyglucose on the Growth and Metabolism of Cultured Human Cells. *The Journal of Biological Chemistry*

Barclay, J.L. et al., 2013. High-fat diet-induced hyperinsulinemia and tissue-specific insulin resistance in Cry-deficient mice. *Am J Physiol Endocrinol Metab*

Bass, J. & Takahashi, J.S., 2011. Circadian rhythms: Redox redux. *Nature*

Bell-Pedersen, D. et al., 2005. Circadian rhythms from multiple oscillators: lessons from diverse organisms. *Nature reviews. Genetics*,

Berson, D.M., Dunn, F.A. & Takao, M., 2002. Phototransduction by Retinal Ganglion Cells That Set the Circadian Clock. *Science*

Beutler, E., 2008. Glucose-6-phosphate dehydrogenase deficiency : a historical perspective Early history. *Blood*

Boros, L.G. et al., 1998. Inhibition of the oxidative and nonoxidative pentose phosphate pathways by somatostatin : a possible mechanism of antitumor action. *Medical Hypotheses*

Brekke, E.M.F. et al., 2012. Quantitative importance of the pentose phosphate pathway determined by incorporation of 13C from [2-13C]- and [3-13C]glucose into TCA cycle intermediates and neurotransmitter amino acids in functionally intact neurons. *Journal of cerebral blood flow and metabolism*

Brown, S.A. et al., 2002. Rhythms of mammalian body temperature can sustain peripheral circadian clocks. *Current Biology*

Buhr, E.D., Yoo, S.-H. & Takahashi, J.S., 2013. Temperature as a universal resetting cue for mammalian circadian oscillators. *Science*

Cassone, V.M., Roberts, M.H. & Moore, R.Y., 1988. Effects of melatonin on 2-deoxy-[1-14C]glucose uptake within rat suprachiasmatic nucleus.

Am.J.Physiol

Chen, R. et al., 2009. Rhythmic PER Abundance Defines a Critical Nodal Point for Negative Feedback within the Circadian Clock Mechanism. *Molecular Cell*

Chen, R., D'Alessandro, M. & Lee, C., 2013. MiRNAs are required for generating a time delay critical for the circadian oscillator. *Current Biology*,

Chen, Y. et al., 2008. NS21: re-defined and modified supplement B27 for neuronal cultures. *Journal of neuroscience methods*

Cheon, S. et al., 2013. Glucocorticoid-mediated Period2 induction delays the phase of circadian rhythm. *Nucleic Acids Research*,

Cho, C.-S. et al., 2014. Circadian rhythm of hyperoxidized peroxiredoxin II is determined by hemoglobin autoxidation and the 20S proteasome in red blood cells. *Proceedings of the National Academy of Sciences of the United States of America*

Christensen, C.E. et al., 2014. Non-invasive in-cell determination of free cytosolic [NAD+]/ [NADH] ratios using hyperpolarized glucose show large variations in metabolic phenotypes. *Journal of Biological Chemistry*

Cox, A.G. et al., 2009. Mitochondrial peroxiredoxin 3 is more resilient to hyperoxidation than cytoplasmic peroxiredoxins. *The Biochemical Journal*

Croushore, C.A. et al., 2012. Microfluidic device for the selective chemical stimulation of neurons and characterization of peptide release with mass spectrometry. *Analytical Chemistry*,

Damiola, F., Le Minh, N., et al., 2000. Restricted feeding uncouples circadian oscillators in peripheral tissues from the central pacemaker in the suprachiasmatic nucleus. *Genes & Development*

Damiola, F., Le Minli, N., et al., 2000. Restricted feeding uncouples circadian oscillators in peripheral tissues from the central pacemaker in the suprachiasmatic nucleus. *Genes and Development*,

Dattolo, T. et al., 2016. Neural activity in the suprachiasmatic circadian clock

of nocturnal mice anticipating a daytime meal. *Neuroscience*

Davidson, A.J. et al., 2003. Is the food-entrainable circadian oscillator in the digestive system? *Genes, brain, and behavior*

DeCoursey, P.J., Walker, J.K. & Smith, S. a, 2000. A circadian pacemaker in free-living chipmunks: essential for survival? *Journal of Comparative Physiology*

Drummond, G.R. et al., 2011. Combating oxidative stress in vascular disease: NADPH oxidases as therapeutic targets. *Nat Rev Drug Discov*,

Dulbecco, R. & Freeman, G., 1959. Plaque production by the polyoma virus. *Virology*

Dusick, J.R. et al., 2007. Increased pentose phosphate pathway flux after clinical traumatic brain injury: a [1,2-13C2]glucose labeling study in humans. *Journal of cerebral blood flow and metabolism*

Edgar, R.S. et al., 2012. Peroxiredoxins are conserved markers of circadian rhythms. *Nature*

Feneberg, R. & Lemmer, B., 2004. Circadian rhythm of glucose uptake in cultures of skeletal muscle cells and adipocytes in Wistar-Kyoto, Wistar, Goto-Kakizaki, and spontaneously hypertensive rats. *Chronobiology International*

Frezza, C. et al., 2011. Haem oxygenase is synthetically lethal with the tumour suppressor fumarate hydratase. *Nature*

Frisch, B. & Aschoff, J., 1987. Circadian rhythms in honeybees: entrainment by feeding cycles. *Physiological Entomology*

Fustin, J.M. et al., 2012. Rhythmic Nucleotide Synthesis in the Liver: Temporal Segregation of Metabolites. *Cell Reports*.

Gandin, V. et al., 2016. nanoCAGE reveals 5′ UTR features that define specific modes of translation of functionally related MTOR-sensitive mRNAs. *Genome Res*

Gerhart-Hines, Z. & Lazar, M.A., 2015. Circadian metabolism in the light of evolution. *Endocrine Reviews*

Ges, I.A. & Baudenbacher, F., 2010. Enzyme-coated microelectrodes to monitor lactate production in a nanoliter microfluidic cell culture device. *Biosensors and Bioelectronics*

Gibbs, J.E. et al., 2011. The nuclear receptor REV-ERBα mediates circadian regulation of innate immunity through selective regulation of inflammatory cytokines. *Proceedings of the National Academy of Sciences of the United States of America*

Grossmann, G. et al., 2011. The RootChip: an integrated microfluidic chip for plant science. *Plant Cell*,

Guillaumond, F. et al., 2005. Differential control of Bmal1 circadian transcription by REV-ERB and ROR nuclear receptors. *Journal of Biological Rhythms*, 20(5)

Gupte, S. a et al., 2002. Inhibitors of pentose phosphate pathway cause vasodilation: involvement of voltage-gated potassium channels. *The Journal of pharmacology and experimental therapeutics*

Halldorsson, S. et al., 2015. Advantages and challenges of microfluidic cell culture in polydimethylsiloxane devices. *Biosensors and Bioelectronics*

Han, D., Williams, E. & Cadenas, E., 2001. Mitochondrial respiratory chain-dependent generation of superoxide anion and its release into the intermembrane space. *The Biochemical Journal*

Hardin, P.E., Hall, J.C. & Rosbash, M., 1990. Feedback of the *Drosophila* period gene product on circadian cycling of its messenger RNA levels. *Nature*

Harmer, S.L. et al., 2000. Orchestrated transcription of key pathways in Arabidopsis by the circadian clock. *Science*

Harrison, R.G., 1912. The cultivation of tissues in extraneous media as a method of morpho-genetic study. *The Anatomical Record*

Hastings, M.H. et al., 2005. Analysis of circadian mechanisms in the

suprachiasmatic nucleus by transgenesis and biolistic transfection. *Methods in enzymology*

Haus, E.L. & Smolensky, M.H., 2013. Shift work and cancer risk: Potential mechanistic roles of circadian disruption, light at night, and sleep deprivation. *Sleep Medicine Reviews*

Haydon, M.J. et al., 2013. Metabolic regulation of circadian clocks. *Seminars in Cell and Developmental Biology*,

Hirota, T. et al., 2008. A chemical biology approach reveals period shortening of the mammalian circadian clock by specific inhibition of GSK-3beta. *Proceedings of the National Academy of Sciences of the United States of America*

Hirota, T. et al., 2002. Glucose down-regulates Per1 and Per2 mRNA levels and induces circadian gene expression in cultured Rat-1 fibroblasts. *The Journal of biological chemistry*

Ishida, A. et al., 2005. Light activates the adrenal gland: Timing of gene expression and glucocorticoid release. *Cell Metabolism*

Jacobi, D. et al., 2015. Hepatic Bmal1 Regulates Rhythmic Mitochondrial Dynamics and Promotes Metabolic Fitness. *Cell Metabolism*

Jagannath et al. 2013 The CRTC1-SIK1 Pathway Regulates Entrainment of the Circadian Clock. *Cell.*

Jang, C. et al., 2015. Ribosome profiling reveals an important role for translational control in circadian gene expression. *Genome Research*

Johnson, C.H., 2010. Circadian clocks and cell division: What's the pacemaker? *Cell Cycle*

Kalsbeek, A. et al., 2012. Circadian Disruption and Scn Control of Energy. *FEBS Lett.*

Kalsbeek, A. et al., 2012. Circadian rhythms in the hypothalamo-pituitary-adrenal (HPA) axis. *Molecular and Cellular Endocrinology*

Karlsson, B., Knutsson, A. & Lindahl, B., 2001. Is there an association

between shift work and having a metabolic syndrome? Results from a population based study of 27,485 people. *Occupational and environmental medicine*

Keller, M. a., Turchyn, A. V. & Ralser, M., 2014. Non-enzymatic glycolysis and pentose phosphate pathway-like reactions in a plausible Archean ocean. *Molecular Systems Biology*

Kojima, S., Shingle, D.L. & Green, C.B., 2011. Post-transcriptional control of circadian rhythms. *J Cell Sci*

Konopka, R.J. & Benzer, S., 1971. Clock mutants of Drosophila melanogaster. *Proceedings of the National Academy of Sciences of the United States of America*

Koike et al., 2012 Transcriptional Architecture and Chromatin Landscape of the Core Circadian Clock in Mammals. *Science*

Kurabayashi, N. et al., 2010. DYRK1A and glycogen synthase kinase 3beta, a dual-kinase mechanism directing proteasomal degradation of CRY2 for circadian timekeeping. *Molecular and cellular biology*

Lakin-Thomas, P.L., 2000. Circadian rhythms. *Trends in Genetics*,

Landgraf, D. et al., 2015. Oxyntomodulin regulates resetting of the liver circadian clock by food. *eLife.*

Lazar, A.S., Lazar, Z.I. & Dijk, D.J., 2015. Circadian regulation of slow waves in human sleep: Topographical aspects. *NeuroImage*.

Lee, J. et al., 2011. Loss of Bmal1 leads to uncoupling and impaired glucose-stimulated insulin secretion in β-cells. *Islets*

Lee, K.K., Ahn, C.H. & Hong, C.I., 2013. Circadian rhythms in neurospora crassa on a microfluidic device for real-time gas perturbations. *2013 Transducers and Eurosensors XXVII: The 17th International Conference on Solid-State Sensors, Actuators and Microsystems, Transducers and Eurosensors*

Lin, J.-M. et al., 2002. A role for casein kinase 2a in the Drosophila circadian clock. *Nature*

Lipton, J.O. et al., 2015. The Circadian Protein BMAL1 Regulates Translation in Response to S6K1-Mediated Phosphorylation. *Cell*

Liu, G. et al., 2010. Optimisation of conoidin A, a peroxiredoxin inhibitor. *ChemMedChem*

Liu, Y., 1998. How Temperature Changes Reset a Circadian Oscillator. *Science*

Luka, G. et al., 2015. Microfluidics integrated biosensors: A leading technology towards lab-on-A-chip and sensing applications. *Sensors*

Mahesh, G. et al., 2014. Phosphorylation of the transcription activator CLOCK regulates progression through a 24-h feedback loop to influence the circadian period in drosophila. *Journal of Biological Chemistry*

De Mairan, J.J., 1729. Observation Botanique. *Histoire de l'Academie Royale des Sciences*

Marchant, E.G. & Mistlberger, R.E., 1997. Anticipation and entrainment to feeding time in intact and SCN-ablated C57BL/6j mice. *Brain Research*

Marcheva, B. et al., 2010. Disruption of the clock components CLOCK and BMAL1 leads to hypoinsulinaemia and diabetes. *Nature*

Margulis, L. et al., 2006. The last eukaryotic common ancestor (LECA): acquisition of cytoskeletal motility from aerotolerant spirochetes in the Proterozoic Eon. *Proceedings of the National Academy of Sciences of the United States of America*

Martinek, S. et al., 2001. A role for the segment polarity gene shaggy/GSK-3 in the Drosophila circadian clock. *Cell*

Matsuo, T. et al., 2003. Control mechanism of the circadian clock for timing of cell division in vivo. *Science*

Mattis, J. & Sehgal, A., 2016. Circadian Rhythms, Sleep, and Disorders of Aging. *Trends in Endocrinology and Metabolism*

Maywood, E.S. et al., 2014. The Tau mutation of casein kinase 1ε sets the

period of the mammalian pacemaker via regulation of Period1 or Period2 clock proteins. *Journal of biological rhythms*

Meng, Q. et al., 2010. Entrainment of disrupted circadian behavior through inhibition of casein kinase 1 (CK1) enzymes. *Proceedings of the National Academy of Sciences of the United States of America*

Meng, Q.J. et al., 2008. Setting Clock Speed in Mammals: The CK1ε tau Mutation in Mice Accelerates Circadian Pacemakers by Selectively Destabilizing PERIOD Proteins. *Neuron*

Mistlberger, R.E., 2006. Circadian Rhythms: Perturbing a Food-Entrained Clock. *Current Biology*

Mukherji, a., Kobiita, a., Damara, M., et al., 2015. Shifting eating to the circadian rest phase misaligns the peripheral clocks with the master SCN clock and leads to a metabolic syndrome. *Proceedings of the National Academy of Sciences*

Mukherji, a., Kobiita, a. & Chambon, P., 2015. Shifting the feeding of mice to the rest phase creates metabolic alterations, which, on their own, shift the peripheral circadian clocks by 12 hours. *Proceedings of the National Academy of Sciences*

Musiek, E.S. et al., 2013. Circadian clock proteins regulate neuronal redox homeostasis and neurodegeneration. *Journal of Clinical Investigation*

Nagoshi, E. et al., 2004. Circadian Gene Expression in Individual Fibroblasts : Oscillators Pass Time to Daughter Cells. *Cell*

Nakajima, M. et al., 2005. Reconstitution of circadian oscillation of cyanobacterial KaiC phosphorylation in vitro. *Science*

Nakashima, N. et al., 2000. The Tumor Suppressor PTEN Negatively Regulates Insulin Signaling in 3T3-L1 Adipocytes. *The Journal of biological chemistry*

Nitabach, M.N., Holmes, T.C. & Blau, J., 2005. Membranes, ions, and clocks: Testing the Njus-Sulzman-Hastings model of the circadian oscillator. *Methods in Enzymology*

Njus, D., Sulzman, F.M. & Hastings, J.W., 1974. Membrane model for the circadian clock. *Nature*

Nohales, M.A. & Kay, S.A., 2016. Molecular mechanisms at the core of the plant circadian oscillator. *Nature Structural & Molecular Biology*

O'Neill, J.S. et al., 2011. Circadian rhythms persist without transcription in a eukaryote. *Nature*.

O'Neill, J.S. & Reddy, A.B., 2011. Circadian clocks in human red blood cells. *Nature*

van Ooijen, G., Hindle, M., et al., 2013. Functional Analysis of Casein Kinase 1 in a Minimal Circadian System. *PLoS ONE*

van Ooijen, G., Martin, S.F., et al., 2013. Functional analysis of the rodent CK1tau mutation in the circadian clock of a marine unicellular alga. *BMC cell biology*

Oster, H. et al., 2006. The circadian rhythm of glucocorticoids is regulated by a gating mechanism residing in the adrenal cortical clock. *Cell Metabolism*

Pan, A. et al., 2011. Rotating night shift work and risk of type 2 diabetes: Two prospective cohort studies in women. *PLoS Medicine*

Partch, C.L., Green, C.B. & Takahashi, J.S., 2014. Molecular architecture of the mammalian circadian clock. *Trends in Cell Biology*

Paulose, J.K., Rucker, E.B. & Cassone, V.M., 2012. Toward the Beginning of Time: Circadian Rhythms in Metabolism Precede Rhythms in Clock Gene Expression in Mouse Embryonic Stem Cells. *PLoS ONE*

Peek, C.B. et al., 2013. Circadian clock NAD+ cycle drives mitochondrial oxidative metabolism in mice. *Science*

Perelis, M. et al., 2015. Pancreatic cell enhancers regulate rhythmic transcription of genes controlling insulin secretion. *Science*

Perkins, A. et al., 2015. Peroxiredoxins: guardians against oxidative stress

and modulators of peroxide signaling. *Trends in biochemical sciences*,

Pittendrigh, C.S., 1960. Circadian rhythms and the circadian organization of living systems. *Cold Spring Harbor Symposia on Quantitative Biology*

Pittendrigh, C.S., 1993. Temporal organization: reflections of a Darwinian clock-watcher. *Annual Review of Physiology*

Putker, M. & O'Neill, J.S., 2016. Reciprocal Control of the Circadian Clock and Cellular Redox State - a Critical Appraisal. *Molecules and cells*

Qin, X. et al., 2010. Coupling of a core post-translational pacemaker to a slave transcription/translation feedback loop in a circadian system. *PLoS Biology*

Rajah, R. et al., 1999. Insulin-like growth factor-binding protein-3 is partially responsible for high-serum-induced apoptosis in PC-3 prostate cancer cells. *Journal of endocrinology*

Ralph, M.R. & Menaker, M., 1988. A Mutation of the Circadian System in Golden Hamsters. *Science*

Reddy, A.B. et al., 2006. Circadian Orchestration of the Hepatic Proteome. *Current Biology*

Reddy, A.B. & Rey, G., 2014. Metabolic and nontranscriptional circadian clocks: eukaryotes. *Annual Review of Biochemistry*

Refinetti, R. & Menaker, M., 1991. The circadian rhythm of body temperature. *Frontiers in Bioscience*

Reinhardt, R.R. & Bondy, C.A., 1994. Insulin-Like Growth-Factors Cross the Blood-Brain-Barrier. *Endocrinology*

Rey, G. et al., 2012. The Pentose Phosphate Pathway Regulates the Circadian Clock. *Cell Metabolism*

Rey, G. & Reddy, A.B., 2015. Interplay between cellular redox oscillations and circadian clocks. *Diabetes, Obesity and Metabolism*

Riganti, C. et al., 2004. Diphenyleneiodonium inhibits the cell redox metabolism and induces oxidative stress. *Journal of Biological Chemistry*

Risso, A. et al., 2001. Intermittent high glucose enhances apoptosis in human umbilical vein endothelial cells in culture. *American journal of Physiology. Endocrinology and Metabolism*.

Rosbash, M., 2009. The implications of multiple circadian clock origins. *PLoS Biology*

Rudic, R.D. et al., 2004. BMAL1 and CLOCK, two essential components of the circadian clock, are involved in glucose homeostasis. *PLoS biology*

Rusak, B., 1979. Neural mechanisms for entrainment and generation of mammalian circadian rhythms. *Federation Proceedings*

Rutter, J. et al., 2001. Regulation of clock and NPAS2 DNA binding by the redox state of NAD cofactors. *Science*

Sahar, S. et al., 2010. Regulation of BMAL1 protein stability and circadian function by GSK3β-mediated phosphorylation. *PLoS ONE*

Saini, C. et al., 2013. Real-time recording of circadian liver gene expression in freely moving mice reveals the phase-setting behavior of hepatocyte clocks. *Genes & development*

Sato, M. et al., 2014. The Role of the Endocrine System in Feeding-Induced Tissue-Specific Circadian Entrainment. *Cell Reports*

Schmalen, I. et al., 2014. Interaction of circadian clock proteins CRY1 and PER2 is modulated by zinc binding and disulfide bond formation. *Cell*

Shamsi, N.A. et al., 2014. Metabolic consequences of timed feeding in mice. *Physiology and Behavior*

Shinohara, M.L., Loros, J.J. & Dunlap, J.C., 1998. Glyceraldehyde-3-phosphate dehydrogenase is regulated on a daily basis by the circadian clock. *Journal of Biological Chemistr*y

Shrirao, A.B. et al., 2012. Adhesive-tape soft lithography for patterning

mammalian cells: application to wound-healing assays. *BioTechniques*

Siddle, K., 2011. Signalling by insulin and IGF receptors: Supporting acts and new players. *Journal of Molecular Endocrinology*

Stanton, R.C., 2012. Glucose-6-phosphate dehydrogenase, NADPH, and cell survival. *IUBMB Life*

Stephan, F.K., 2002. The “other” circadian system: Food as a zeitgeber. *Journal of Biological Rhythms*

Stephan, F.K. & Davidson, A.J., 1998. Glucose, but not fat, phase shifts the feeding-entrained circadian clock. *Physiology and Behavior*

Stephan, F.K., Swann, J.M. & Sisk, C.L., 1979. Entrainment of circadian rhythms by feeding schedules in rats with suprachiasmatic lesions. *Behavioral and Neural Biology*

Stokes, G.G., 1922. On the Effect of the Internal Friction of Fluids on the Motion of Pendulums. *Math. and Phys. Papers*, 3

Stokkan, K. et al., 2001. Entrainment of the Circadian Clock in the Liver by Feeding. *Science*

Storch, K.-F. & Weitz, C.J., 2009. Daily rhythms of food-anticipatory behavioral activity do not require the known circadian clock. *Proceedings of the National Academy of Sciences of the United States of America*

Sumbilla, C.M. et al., 1983. Gluconeogenic enzymes in fibroblasts from infants dying of the sudden infant death syndrome (SIDS). *European Journal of Pediatrics*

Sun, Z.S. et al., 1997. RIGUI, a putative mammalian ortholog of the Drosophila period gene. *Cell*

Takahashi, J.S., 1993. Circadian-clock regulation of gene expression. *Current Opinion in Genetics and Development*

Takeda, K. et al., 2004. Distribution of Prx-linked hydroperoxide reductase activity among microorganisms. *Bioscience, biotechnology, and*

biochemistry.

Tataroğlu, Ö. et al., 2012. Glycogen synthase kinase is a regulator of the circadian clock of Neurospora crassa. *The Journal of biological chemistry*

Tataroglu, O. & Emery, P., 2015. The molecular ticks of the Drosophila circadian clock. *Current Opinion in Insect Science*

Tei, H. et al., 1997. Circadian oscillation of a mammalian homologue of the Drosophila period gene. *Nature*

Teng, S.-W. et al., 2013. Robust circadian oscillations in growing cyanobacteria require transcriptional feedback. *Science*

Tilles, A.W. et al., 2001. Effects of oxygenation and flow on the viability and function of rat hepatocytes cocultured in a microchannel flat-plate bioreactor. *Biotechnology and Bioengineering*

Tu, B.P. & McKnight, S.L., 2006. Metabolic cycles as an underlying basis of biological oscillations. *Nature Reviews Molecular Cell Biology*

Untergasser, A. et al., 2012. Primer3-new capabilities and interfaces. *Nucleic Acids Research*

Verhagen, L.A.W. et al., 2011. Acute and chronic suppression of the central ghrelin signaling system reveals a role in food anticipatory activity. *European Neuropsychopharmacology*

Wang, T.A. et al., 2012. Circadian Rhythm of Redox State Regulates Excitability in Supraciasmatic Nucleus Neurons. *Science*

Welsh, D.K. et al., 1995. Individual Neurons Dissociated From Rat Suprachiasmatic Nucleus Express Independently Phased Circadian Firing Rhythms. *Neuron*

Winterbourn, C.C., 2008. Reconciling the chemistry and biology of reactive oxygen species. *Nat Chem Biol*

Woelfle, M.A. et al., 2004. The adaptive value of circadian clocks: An experimental assessment in cyanobacteria. *Current Biology*

Xu, K. et al., 2011. The circadian clock interacts with metabolic physiology to influence reproductive fitness. *Cell Metabolism*

Yamaguchi, S. et al., 2003. Synchronization of cellular clocks in the suprachiasmatic nucleus. *Science*

Yamajuku, D. et al., 2012. Real-time monitoring in three-dimensional hepatocytes reveals that insulin acts as a synchronizer for liver clock. *Scientific reports*

Yang, Y. et al., 2003. Phosphorylation of FREQUENCY protein by casein kinase II is necessary for the function of the Neurospora circadian clock. *Molecular and cellular biology*

Yang, Z. & Sehgal, A., 2001. Role of molecular oscillations in generating behavioral rhythms in Drosophila. *Neuron*

Yin, L. et al., 2006. Nuclear receptor Rev-erbalpha is a critical lithium-sensitive component of the circadian clock. *Science*

Ying, W., 2008. NAD+/NADH and NADP+/NADPH in cellular functions and cell death: regulation and biological consequences. *Antioxidants & redox signaling*

Yoo, S.-H. et al., 2004. PERIOD2::LUCIFERASE real-time reporting of circadian dynamics reveals persistent circadian oscillations in mouse peripheral tissues. *Proceedings of the National Academy of Sciences of the United States of America*

Yoshii, K. et al., 2014. Changes in pH and NADPH regulate the DNA-binding activity of NPAS2, a mammalian circadian transcription factor. *Biochemistry*.

Zhang, R. et al., 2014. A circadian gene expression atlas in mammals: Implications for biology and medicine. *Proceedings of the National Academy of Sciences*

Zielinski, T. et al., 2011. The Biodare Data Repository.

Zimmerman, W.F., Pittendrigh, C.S. & Pavlidis, T., 1968. Temperature compensation of the circadian oscillation in drosophila pseudoobscura

and its entrainment by temperature cycles. *Journal of insect physiology*